



HAL
open science

From Enzyme Stability to Enzymatic Bioelectrode Stabilization Processes

Charlène Beaufils, Hiu-Mun Man, Anne de Poulpiquet, Ievgen Mazurenko,
Elisabeth Lojou

► **To cite this version:**

Charlène Beaufils, Hiu-Mun Man, Anne de Poulpiquet, Ievgen Mazurenko, Elisabeth Lojou. From Enzyme Stability to Enzymatic Bioelectrode Stabilization Processes. *Catalysts*, 2021, 11 (4), pp.497. 10.3390/catal11040497 . hal-03199106

HAL Id: hal-03199106

<https://hal.science/hal-03199106v1>

Submitted on 15 Apr 2021

HAL is a multi-disciplinary open access archive for the deposit and dissemination of scientific research documents, whether they are published or not. The documents may come from teaching and research institutions in France or abroad, or from public or private research centers.



L'archive ouverte pluridisciplinaire **HAL**, est destinée au dépôt et à la diffusion de documents scientifiques de niveau recherche, publiés ou non, émanant des établissements d'enseignement et de recherche français ou étrangers, des laboratoires publics ou privés.



Distributed under a Creative Commons Attribution 4.0 International License

Review

From Enzyme Stability to Enzymatic Bioelectrode Stabilization Processes

Charlène Beaufils, Hiu-Mun Man, Anne de Poulpiquet, Ievgen Mazurenko  and Elisabeth Lojou * 

Aix Marseille University, CNRS, BIP, Bioénergétique et Ingénierie des Protéines, UMR 7281, 31, Chemin Joseph Aiguier, CS 70071 13402 Marseille CEDEX 09, France; cbeaufils@imm.cnrs.fr (C.B.); hman@imm.cnrs.fr (H.-M.M.); adepoulpiquet@imm.cnrs.fr (A.d.P.); imazurenko@imm.cnrs.fr (I.M.)

* Correspondence: lojou@imm.cnrs.fr; Tel.: +33-(0)491-164-144

Abstract: Bioelectrocatalysis using redox enzymes appears as a sustainable way for biosensing, electricity production, or biosynthesis of fine products. Despite advances in the knowledge of parameters that drive the efficiency of enzymatic electrocatalysis, the weak stability of bioelectrodes prevents large scale development of bioelectrocatalysis. In this review, starting from the understanding of the parameters that drive protein instability, we will discuss the main strategies available to improve all enzyme stability, including use of chemicals, protein engineering and immobilization. Considering in a second step the additional requirements for use of redox enzymes, we will evaluate how far these general strategies can be applied to bioelectrocatalysis.

Keywords: enzyme; metalloenzyme; catalysis; stability; electrochemistry; bioelectrochemistry



Citation: Beaufils, C.; Man, H.-M.; de Poulpiquet, A.; Mazurenko, I.; Lojou, E. From Enzyme Stability to Enzymatic Bioelectrode Stabilization Processes. *Catalysts* **2021**, *11*, 497. <https://doi.org/10.3390/catal11040497>

Academic Editor: Giovanni Gadda

Received: 17 March 2021

Accepted: 10 April 2021

Published: 14 April 2021

Publisher's Note: MDPI stays neutral with regard to jurisdictional claims in published maps and institutional affiliations.



Copyright: © 2021 by the authors. Licensee MDPI, Basel, Switzerland. This article is an open access article distributed under the terms and conditions of the Creative Commons Attribution (CC BY) license (<https://creativecommons.org/licenses/by/4.0/>).

1. Introduction

In the search for a more sustainable way of life, our society must adapt nowadays to reduce the use of harmful products or high carbon energy sources deleterious for our planet, hence for our lives. Many industrial sectors are concerned by this revolution, from fine product synthesis to environmental monitoring, clinical diagnosis or energy production. Catalysis of the involved chemical reactions is a key process towards sustainability by accelerating kinetics, or increasing selectivity. However, chemical catalysts themselves are very often not produced and used in eco-friendly manner, requiring organic solvents for their synthesis or being based on metals rare on earth. In that sense, enzymes can be regarded as sustainable alternatives with great advantages directly linked to their intrinsic properties required to sustain life [1]. In particular, many different enzymes are involved in a variety of reactions in microorganisms where they operate in mild conditions, developing high catalytic activity and specificity for their substrate. Their amazing functional diversity directly originates from the chemistry and polarity of amino acids that fold in a diversity of structures. In addition, they are produced in mild aqueous conditions and are totally biodegradable. However, their weak stability and ability to maintain biological activity during storage and operation, freeze-thaw steps, and in non-physiological environments lower their attractiveness. Development of strategies to enhance enzyme shelf life while maintaining catalytic activity have been the subject of many researches during the last decades [2–4].

Redox enzymes belong to a class of enzymes containing redox cofactors that are necessary for their activity. These oxidoreductases transform their substrate by exchanging electrons with their physiological partners in the metabolic chain. Intra-enzyme redox components can be organic cofactors such as flavin adenine dinucleotide (FAD) for sugar oxidation [5]. They can be metal centers, including copper for oxygen reduction [6], iron and nickel for hydrogen evolution and uptake or CO₂ reduction [7–9], manganese for water oxidation in photosynthesis [10], etc. Some others are dependent on nicotinamide adenine dinucleotide phosphate (NADPH) to realize enzymatic transformations [11]. Such enzymes

have been envisioned as biocatalysts in biosensors [12–14], biosynthesis reactors [15,16], or biofuel cells [17,18]. This domain is referred as Bioelectrochemistry. As for non-redox enzymes, one of the main limitations in the large-scale development of these biotechnologies is the weak stability of bioelectrodes based on redox enzymes. In particular, in the different biotechnological devices listed just before, enzymes may face high temperatures or high salt concentrations. They may have to operate at gas-liquid interfaces or even at the three phase boundaries. In addition, to exploit the catalytic properties of these redox enzymes in biotechnology, a further step is to ensure electron exchange between the protein and a conductive surface [19–21]. This prerequisite imposes the enzyme adopts certain configurations once immobilized, so that not only the structural conformation and dynamic remains for substrate accessibility and activity, but also enzyme positioning and orientation on the solid interface allows electron transfer.

The purpose of this review is to discuss whether general strategies available for all enzyme stabilization can be applied for the special case of redox enzymes used in bioelectrochemistry. To reach this objective, the fundamental bases for all enzyme stabilization by general reported strategies will be first detailed, with a focus on the immobilization procedure as an important way for stabilization. In a second step, we will emphasize the particular features of redox enzymes that must be considered before applying any available stabilization strategies. Ultimately, we will discuss which additional specific strategies must be set up for redox protein, and by extension for bioelectrode, stabilization. Because the topic is very large, this review will not provide an exhaustive list of references but will instead aim to highlight major issues related to enzyme and redox enzyme stability with illustrations taken from papers published during the last few years.

2. Intrinsic (in)Stability of Enzymes

The metabolisms essential for life are catalyzed by enzymes. Over time, these proteins may have undergone different changes resulting from mutations, which cause enzymes to evolve to function in a particular cellular environment and will be very sensitive to exogenous conditions. In addition, in the cell, enzymes can be subjected to various stresses, which can lead to their denaturation or the formation of aggregates. Thanks to a perfectly designed proteolysis machine, new fresh proteins are produced to replace the deactivated proteins. These two fundamental concepts mean that using enzymes outside a cell is expected to induce some loss of activity and eventually progressive denaturation, which can be irreversible. The will to exploit enzymes for other works than predicted by evolution, although highly attractive, imposes finding out strategies to preserve activity within durations compatible with fundamental laboratory studies and with applications [3]. Before reaching that objective, the prerequisite is to know which factors affect enzyme activity and stability. A subtle balance between stability and flexibility is required to maintain activity, so that stability can be the price to pay against activity. Each enzyme is composed of a linear chain of amino acids that fold to produce a unique three-dimensional structure which confers specific and unique enzymatic properties. The overall structure of an enzyme is described according to four levels which contribute to its specific function and stability (Figure 1). The secondary structure refers to the arrangement of the polypeptide chain (the primary structure) as random coil, α -helix, β -sheet and turn stabilized by hydrogen bonds between amino acid residues. While the primary structure is stable thanks to the strength of the peptide bonds which are unlikely to be broken upon changes in the environmental conditions, the secondary structure can be altered even during protein storage. The tertiary structure is the three-dimensional arrangement of the amino acid residues, giving the overall conformation of the polypeptidic chain. Hydrophobic interactions between nonpolar chains as well as disulfide bonds and ionic interactions between charged residues are involved in the stabilization of the tertiary structure. To fulfill the requirement of enzyme localization in the cell, hydrophobic and hydrophilic groups are arranged within the protein. For soluble proteins, hydrophobic side groups tend to be hidden in the protein core while hydrophilic groups are exposed to the surrounding environment. These amino

acid residues on the surface of the enzyme are more likely to be sensitive to the external environment than the core amino acids.

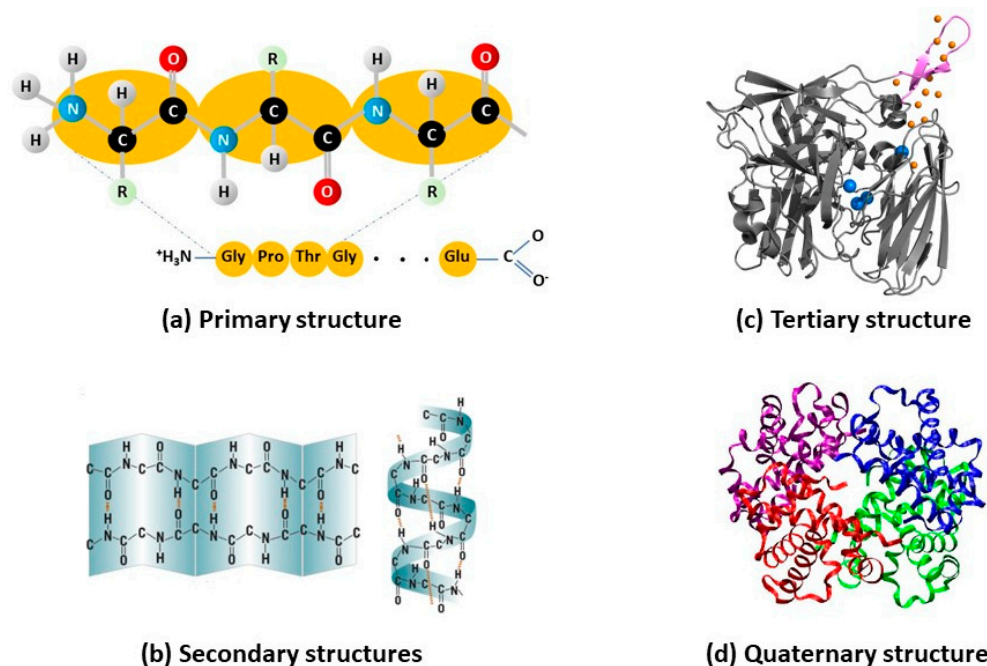


Figure 1. The four levels of protein structures determine the enzyme function.

Denaturation occurs upon unfolding of the tertiary structure to a disordered polypeptide where residues are no longer arranged for functional or structural stabilizing interactions [22]. This process may be reversible. Irreversible loss of activity may also occur upon external stresses. This leads to two different concepts to evaluate in vitro stability of a protein. The thermodynamic stability refers to the ability for a protein to unfold/refold after being subjected to stresses (elevated temperature, extreme pH, or high organic solvent concentration). Methods to evaluate this stability range from scanning calorimetry to circular dichroism (CD) and fluorimetry. Kinetic stability represents the duration of enzyme activity before irreversible denaturation and is measured by activity assays. Actually, the native active state of an enzyme is in equilibrium with the partially denatured, enzymatically inactive state, and the folded/unfolded transition involves mainly intramolecular hydrogen bonds and hydrophobic interactions. This scheme is most certainly more complicated since it was shown that a protein can oscillate between many different folded/unfolded configurations. Each oscillation is governed by the second thermodynamic law, the entropy decreasing as the protein folds, and hydrogen bond formation contributing to the enthalpy. Each strategy that tends to increase rigidity in the enzyme architecture decreases entropy and enhances stability [23]. Thermodynamic instability of enzymes can be partly attributed to the lack of rigidity within the tertiary structure, caused by flexible random coils in contrast to stable β -sheets [24]. In addition to higher rigidity and compact packing, the presence of α -helices with antiparallel arrangement contributes to stability. Water is the natural environment in which protein molecules do exist and operate, and water molecules play a key role in maintaining the entropic stability of the enzyme structure.

Any engineering towards enzyme structural rigidification must maintain the hydration shell and flexibility required for activity. Based on enzyme structural features, many different agents are potential enzyme “killers”. When temperature increases, the enzyme tends to unfold in a cooperative process. Disulfide bridges can be broken by reducing agents, extreme pHs are going to affect hydrogen bonding and salt bridges, high salt concentration may aggregate the protein, while charged components may form bonds with charged amino acids modifying the tertiary structure. Organic solvents or detergents will alter hydrophobic interactions, and stability of enzymes in organic solvents will be

dependent on the ability of the solvent to strip the essential hydration layer from the protein surface [25,26]. Last but not least, mechanical stress or radiation may disrupt the delicate balance of forces that maintain protein structure [27]. Stabilizing the enzyme means preventing these changes.

3. Strategies for All Enzyme Stabilization

Enzyme stability involves a balance between intramolecular interactions of functional groups and their interaction with the protein environment. Water, as many protein natural solvent, plays a key role in enzyme stability by controlling the hydration shell structure and dynamics and by providing required plasticity for activity [28]. As a direct consequence, many stabilization strategies target water activity in the environment of the enzyme or inside the protein moiety, with the main objective of decreasing the enzyme motion (Figure 2). However, this enhanced stability should not be achieved at the expense of activity, so a delicate balance must be maintained between rigidification and sufficient plasticity controlled by water. As another mere general rule, stabilization over one stress tends to enhance stability against another stress.

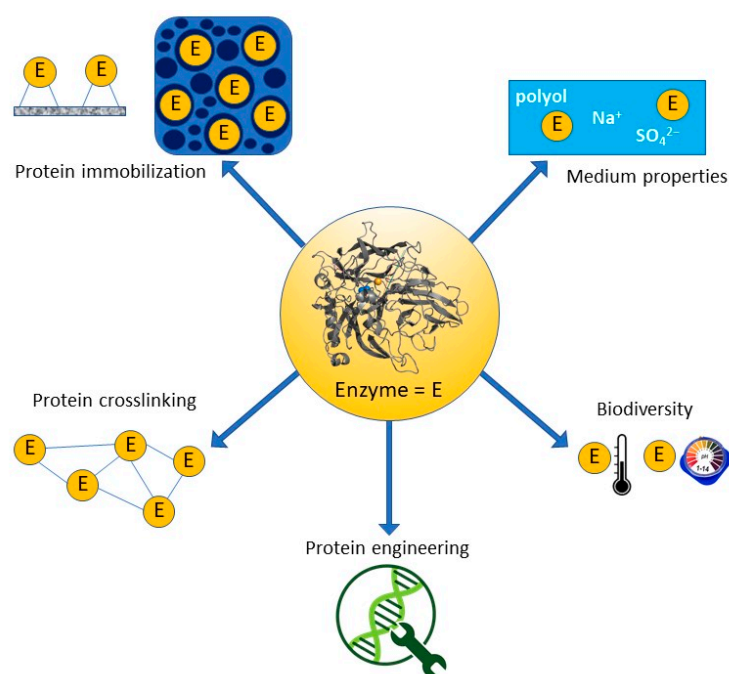


Figure 2. Strategies for all enzyme stabilization.

3.1. Addition of Stabilizers in the Medium

3.1.1. Chemical Stabilizer Addition

It has been known for long time that addition of polyols and polysaccharides such as trehalose, glycerol, dextran, etc. helps stabilizing enzymes [29–32]. Protective effect of polyols was reported in many recent studies in different experimental situations and exposition to stresses (high pressure or high temperature, presence of non-aqueous solvents) [33–37].

Generally speaking, polyols stabilize proteins either in the dried state by serving as water substitutes and preventing dehydration through hydrogen bonding, or in solution by altering protein-solvent interactions [38]. Several mechanisms are discussed to account for the effect of such chemical additives on the protein stabilization [23]. Hydrophilic polyols tend to strengthen hydrophobic interactions among nonpolar amino acid residues resulting in a more compact and spherical enzyme form with smaller surface area, preventing protein dynamics and enhancing stability. Compressibility of proteins, a crucial thermodynamic parameter that determines flexibility, is affected by polyol addition [39]. One accepted mechanism is based on the different sizes between water and stabilizing molecules that

preferentially exclude the latter from the protein surface. The preferential hydration of proteins causes an unfavorable free energy change that the proteins tend to minimize by favoring the more compact state over the structurally expanded state. Protective effect is also explained in terms of influence of additives on water activity that results in an increase of structural organization of water molecules contributing to the conservation of low energy interactions favoring native protein conformation [25].

Surfactants, maltodextrine, sodium azide, or special buffers have also been used as additives to maintain the native structure of proteins through purification steps [25]. Dimethyl sulfoxide (DMSO) acts as a stabilizer because it is preferentially excluded from the protein surface [22,40,41]. Addition of DMSO but also of glycerol or ethylene glycol serve as cryoprotectants preventing protein solutions from freezing at $-20\text{ }^{\circ}\text{C}$ and allowing multiple use of a unique sample without freeze-thaw cycles [38,42]. Adding polymers in solution such as poly(ethylene glycol) (PEG), alginate, or chitosan maintains a hydration shell around the protein according to the exclusion mechanism [38,43–45]. Addition of polymers also prevents protein aggregation by modifying protein-protein interactions and increasing medium viscosity, thus decreasing enzyme motion. Macromolecular crowding, which is the natural environment of enzymes *in vivo*, can explain the stabilizing effect of some additives [46–49]. It can be mimicked *in vitro* through the addition of high concentrations of macromolecules such as dextran or PEG [50] and would favor the folded state of proteins and compact conformation through the excluded volume effect [51–55]. However, the stabilizing effect of *in vitro* crowding would not be universal as the properties of all macromolecules *in vivo* are finely regulated under different physiological conditions [56]. Aggregation under crowded conditions can be enhanced because the activity of water is decreased, and the refolding rate of proteins as a consequence of increased viscosity is also decreased.

3.1.2. Salt Effect

Salt addition affects protein stability according to a combination of binding effect, screening of protein surface electrostatic potential, and effect on protein/water interface. Salts may contribute to hydrophobic interaction strengthening in proteins, hence to stabilization, but salt binding to amino acids on the protein surface decreases the repulsion between proteins and induces aggregation. The salting out process, or salt-induced precipitation, depends on the structure of the protein and in particular on the population of hydrophilic amino acid residues. It also largely depends on the salt concentration. The effect of salts on protein stabilization has been tentatively explained on the basis of the Frank Hofmeister series [4,57–59] (Figure 3A). This series early ordered anions and cations composing salts according at first to their ability to precipitate lysozyme, and later to their ability to stabilize protein secondary and tertiary structure. They were respectively classified at that time as water-structure formers (kosmotropes) or water-structure breakers (chaotropes). Kosmotropes and chaotropes would be nowadays more understood as a characterization of the degree of hydration, and different models are developed to consider the various effects observed experimentally [60]. Ionic liquids (IL) would follow the same tendency as salts where kosmotropic anions and chaotropic cations stabilize the enzyme, while chaotropic anions and kosmotropic cations destabilize it [61]. While they can be considered as eco-friendly solvents, many proteins are inherently inactive in ILs, requiring the addition of water for activity recovery. This suggests ILs could affect the internal water shell [61,62].

Recent examples in the literature illustrate the effect of salts on enzyme stability, and most of them agree with the Hofmeister series. Changes in the secondary structure of two proteins with helical and beta structural arrangement, respectively, were followed by Fourier Transform Infra-Red spectroscopy (FTIR) in the presence of various salts. It was shown that the stabilization effect of the salt follows the Hofmeister series of ions, although some exceptions were observed with formation of intermolecular β -sheets typical of amorphous aggregates [62]. Glucose oxidase (GOx) stability was studied using microcalorimetry

in the presence of various salts [63]. At high salt concentrations (over 1 M), it was shown that the Hofmeister effect on the temperature of inactivation was determined by the ion-specific effect on the protein/water interface. Correlation between stability and activity of lysozyme in the presence of various salts from the Hofmeister series suggested a role of local stability/flexibility in enzyme activity [64]. The thermal stability of *Aspergillus terreus* glucose dehydrogenase (GDH) was substantially improved by kosmotropic anions, retaining more than 90% activity after 60 min of heat treatment at 60 °C. The stabilizing effect followed the Hofmeister series and was anion concentration-dependent and strongly related to the structural stabilization of the enzyme, which involved enzyme compaction [65] (Figure 3B). It was further shown that salts can stabilize proteins not only in vitro but also in vivo or intracellularly, the stabilization level correlating with the Hofmeister series of ions [66].

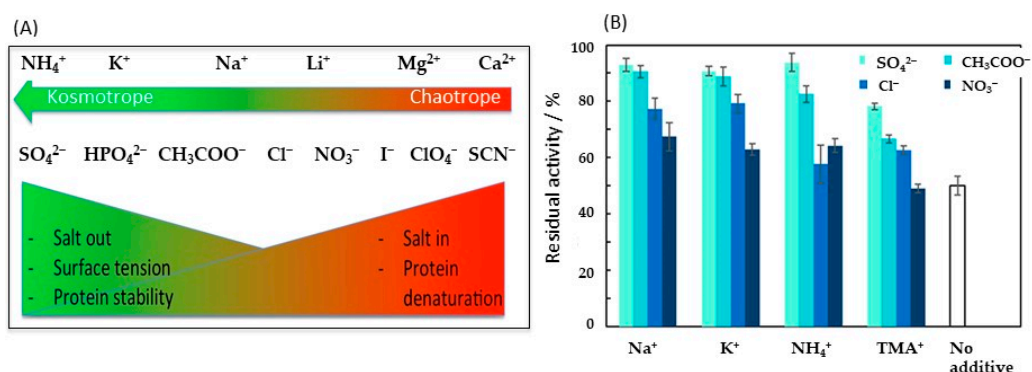


Figure 3. Salt effect on enzyme stability. (A) Hofmeister series and effect on protein properties. (B) Stabilization effect of kosmotropic anions and cations on *Aspergillus terreus* GDH. Residual activity after 1 h incubation at 50 °C as a function of added anions and cations. Reproduced with permission from [65].

3.2. Chemical Modification of Enzymes, Directed Evolution

More than 95% of all charged components are located on the surface of proteins, consisting mostly of hydrophilic moieties, while most of the hydrophobic ones are buried deep inside the core. As already discussed above, the physico-chemical microenvironment of the protein will be sensed intrinsically through those moieties, demonstrating the protein surface to be an attractive target for protein engineering to enhance protein stability. The efforts toward engineering enzyme catalysts with increased stability can be divided into two groups: (i) chemical protein modification and (ii) protein engineering, such as site-directed mutagenesis and directed evolution. The combination of these two approaches is appealing for improving the catalytic properties of enzymes.

3.2.1. Chemical Modification of Enzymes

Chemical protein modification can be achieved either by modification of one sort of amino acid on the protein surface or by polyfunctional modification using reticulating agents or by conjugation to water-soluble polymers. One widely used method consists in reticulation through cross linking via glutaraldehyde (GA) that increases the protein rigidity and mimics disulfide physiological bonds or salt bridges [25]. Activity is however very often affected. Stabilization of proteins through cross-linked-enzyme-aggregates (CLEAs) will be further discussed below in Section 4 [67,68]. Conjugation through water-soluble polymers such as PEG, chitosan, alginate, dextran, etc. has also been widely reported [38,69,70]. Those polymers present either one functionality or are bifunctional to enable reaction with N- or C-terminal or with one individual amino-acid residue on the protein. Increase in the half-life of proteins is frequently observed [71,72]. Other polymers responding to temperature stimuli can tailor the temperature dependence of enzyme stability [73]. Two different methods can be carried out to synthesize the bioconjugate. In

the “grafting to” strategy, the polymer is first synthesized; then, an end-group functionality is attached to one amino-acid on the protein surface. As an example, a mono-PEGylated arginase was constructed by linkage of PEG-maleimide to a cysteine residue on the enzyme surface [74]. The protein was protected against proteases thanks to the shielding effect of PEG, allowing the modified arginase to operate as a promising anticancer drug candidate. In the “grafting from” method, radical polymerization occurs at sites attached to the protein. A recent work describes the ligation of Atom Transfer Radical Polymerization (ATRP) initiators to lysine residues on the surface of a laccase [75]. The polymer-enzyme hybrid obtained by this “grafting-from” procedure showed enhanced solvent and thermal stability, as well as a clear enhancement of activity in a much wider pH range than the free enzyme. Combination of PEGylation and chemical modification by GA can also be efficient [76]. GOx was first PEGylated to provide steric protection; then, it was cross-linked with GA which stabilized the tertiary and quaternary structures. Intermolecular crosslinking-induced aggregation was prevented by the PEG shield. The GA-modified PEGylated GOx retained 73% of activity after 4 weeks at 37 °C against 8.2% for the control (Figure 4).

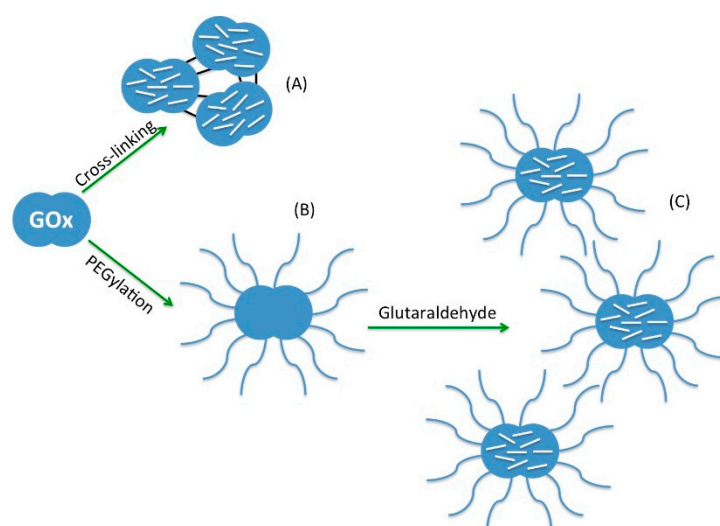


Figure 4. PEGylation of GOx (B) followed by chemical modification (C) enhances enzyme stability, while preventing intermolecular crosslinking contrary to direct cross-linking (A). Reprinted with authorization from [76].

3.2.2. Enzyme Engineering

Protein engineering is another relevant strategy to enhance stability [4,77,78] (Figure 5). Rational design takes benefit of structures and sequences of already known stable proteins. Through identification of amino acids which are assumed to participate in (de)stabilization, new variants of proteins of interest are created through site-directed mutagenesis [79]. As an example, asparagine is a thermolabile residue prone to deamination which can be mutated into threonine or isoleucine, with similar geometry but more thermostable. Replacement of lysines (or histidines) by arginine residues increases thermostability by increasing intramolecular or inter-subunit salt bridges. Otherwise, we will discuss further in this review the interest in the screening of biodiversity to search for more stable enzymes such as in extremophilic organisms. However, because the production of extremophile enzymes may be delicate, genes from hyperthermophiles can be implemented into suitable mesophilic hosts, coupling advantages of high productivity and high thermostability [22,80]. Use of directed evolution to design more stable enzymes is now common. With this method, mutant libraries are created by random changes, and the most promising variants are subjected to further rounds of evolution [81–85]. Rational approach based on molecular

dynamic (MD) and QM/MM simulations may help in identifying and redesigning variants with increased stability [86].

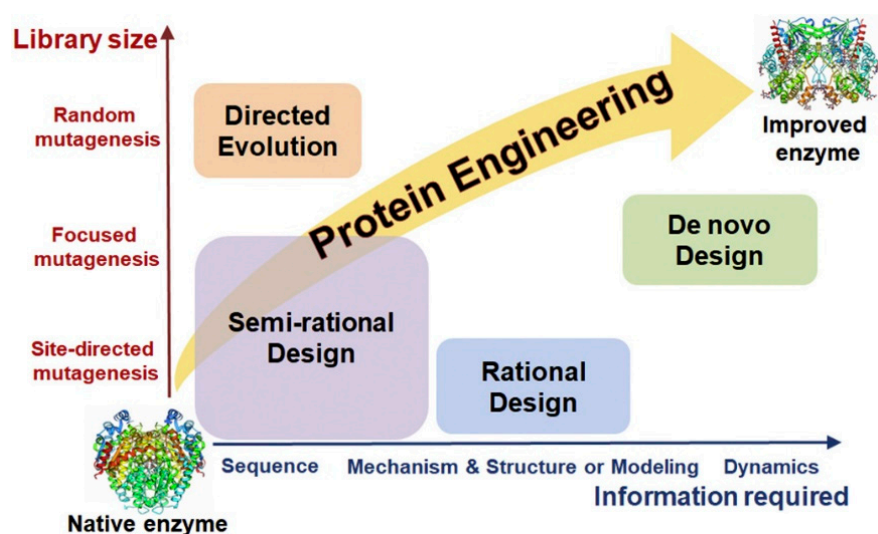


Figure 5. Protein engineering methods to improve enzyme stability. Reprinted with permission from [87].

3.3. Screening of the Biodiversity and Outstanding Properties of Extremophiles

Screening in the biodiversity for “exotic” enzymes such as extremophiles presenting unusual and/or outstanding properties is an attractive strategy to be considered. Although this research topic is increasingly growing, there is no doubt that Nature still retains many secrets that would allow new opportunities for stable biocatalysis. However, the harsh conditions required for the growth of extremophiles very often limit their laboratory studies. Extremophiles have evolved to survive in ecological niches presenting extreme temperatures (thermophiles and psychrophiles living at high (>80 °C) and low (<20 °C) temperatures, respectively), extreme pH (acidophiles and alkalophiles), high pressures (barophiles), high salt concentrations (halophiles), or in the presence of heavy metals (metallophiles)). These extreme environments are found in deep-sea hydrothermal vents, hot springs, volcanic areas, or mine drainage [88–90]. Ancestral microorganisms are another source of stable enzymes because distant ancestors of current organisms were thermophiles and would be composed of proteins that are more thermostable than their current homologues [91–93].

Extremophilic enzymes present specific structural characteristics that afford them to resist in extreme conditions. Interestingly, the same structural features often induce enhanced stability of such enzymes at normal conditions or in the presence of non-aqueous solvents. Moreover, “extremostable” enzymes, thermostable, halostable, acidostable, etc. isolated from extreme environments or obtained by protein engineering can support large number of mutations due to their robustness, leading to eventually even more stable enzymes.

3.3.1. Thermophiles

Thermostability refers to two different concepts: thermotolerance, which is the transient ability to maintain activity at high T° , and thermostability, which is the ability to resist irreversible inactivation at high T° [94]. In addition to the ability to resist to high temperatures, thermostable enzymes usually also present higher resistance to chemical denaturants and extreme pHs. Such cross-adaptations are highly interesting to get stable enzymes in many different extreme conditions. Furthermore, due to their stability at elevated temperatures, enzymatic reactions are faster and less susceptible to microbial contaminations. Many different structural characteristics have been demonstrated to be

involved in thermostability. Compared to mesophiles, protein packing, a high number of hydrophobic residues, increased helical fold content, a high number of disulfide bonds, density of internal hydrogen bonds and salt bridges, and distribution of charged residues on the surface are some of the features often shared by thermostable enzymes [95–97]. Proportion of certain amino acids is also significantly different between extremophiles and mesophiles. For instance, in thermostable enzymes, lysines are replaced by arginines; asparagine/glutamine content is lower while proline content is higher [22,98–100]. The most widespread explanation is that these structural features contribute to reducing the flexibility of the enzyme and to allowing optimal conformation at higher temperatures than mesophiles, with no denaturation [101]. MD simulations confirmed that hydrophobic packing and electrostatic interaction network provided by salt bridges explain enzyme thermostability [102]. Dimerization can also be a key factor for enhanced thermostability [103].

3.3.2. Halophiles

Halophiles grow in the presence of high concentrations of salts. In order to avoid osmotic shock, they accumulate inorganic salts or small organic molecules in the cytoplasm until the intracellular osmolarity equals the extracellular ion concentration [101]. They also require their proteins to operate under extreme ionic conditions. Actually, halophilic enzymes require high salt concentrations for activity and stability (1–4 M range) [104]. Stabilization of proteins in high salinity environments is linked to the interaction of hydrated ions with negatively charged surface residues. A highly ordered shell of water molecules is formed that protects the protein and prevents denaturation [105]. Compared to non-halophilic proteins, halophilic enzymes present less non-polar residues and more charged residues on the protein surface, a higher frequency of acidic (Asp and Glu) over basic residues (Lys), and low hydrophobicity [105] (Figure 6). This high surface charge is neutralized mainly by tightly bound water dipoles [22]. Such excess of acidic over basic amino acid residues makes them more flexible at high salt concentrations in conditions where non-halophilic proteins tend to aggregate [106,107]. Halophilic proteins seem to be specially adapted to have multiple crossover adaptations, especially to pH and temperature.

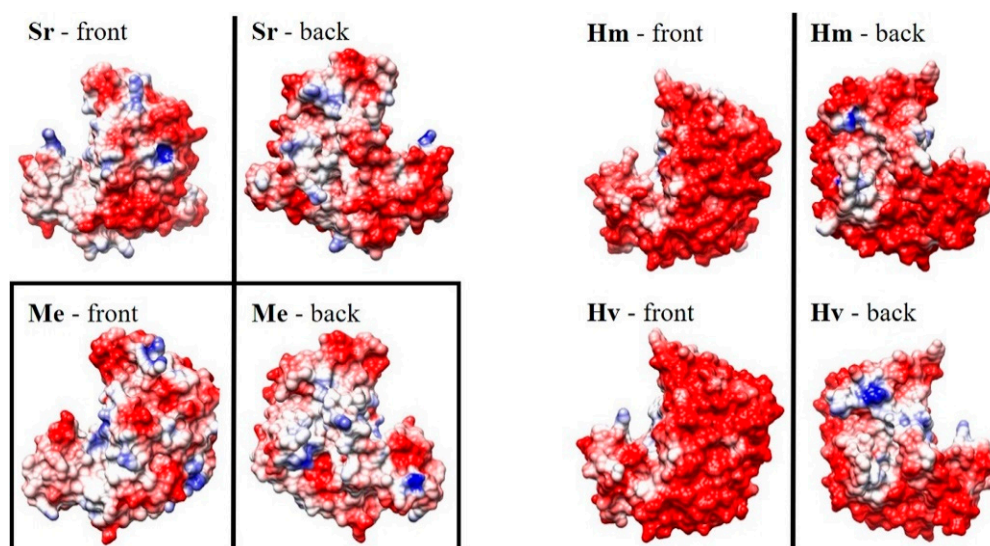


Figure 6. Coulombic surface maps for both sides of the *Salinibacter ruber* (Sr), *Haloarcula morimortui* (Hm), *Haloferax volcanii* (Hv) and *Methylobacterium extorquens* (Me) malate dehydrogenases. The halophilic structures display negative surface areas (in red), a common feature of halophilic proteins. Reprinted with permission from [101].

3.3.3. Cross-Stabilities of Extremophiles

Many examples are reported in the recent literature that highlight the enhanced and cross-stabilities of extremophilic enzymes. Thermostability can be accompanied with pH, salts, metals, or solvent resistance [108,109]. Key enzymatic reaction may benefit from these cross-stabilities. Transformation of cellulose into biofuels is a promising eco-friendly process. However, it requires the enzymes involved in the process to be thermostable, halostable and organic solvent-stable. A cellulase presenting all these characteristics was identified through metagenomic from a deep sea foil reservoir which could be a valuable candidate [110]. Hydrogen is considered as an energy vector for a low carbon economy. Its production and conversion by enzymes should be promoted through operation on a wide range of temperatures. The hyperthermophilic hydrogenase (HASE) from *Aquifex aeolicus* was demonstrated not only to be able to operate at high temperatures for H₂ oxidation but was also much more stable at room temperature than the HASE from *Ralstonia eutropha*, a mesophilic homologue [111] (Figure 7). The structure of this hyperthermostable enzyme reveals more salt-bridges compared to mesophilic HASE, that contribute to its thermostability [112].

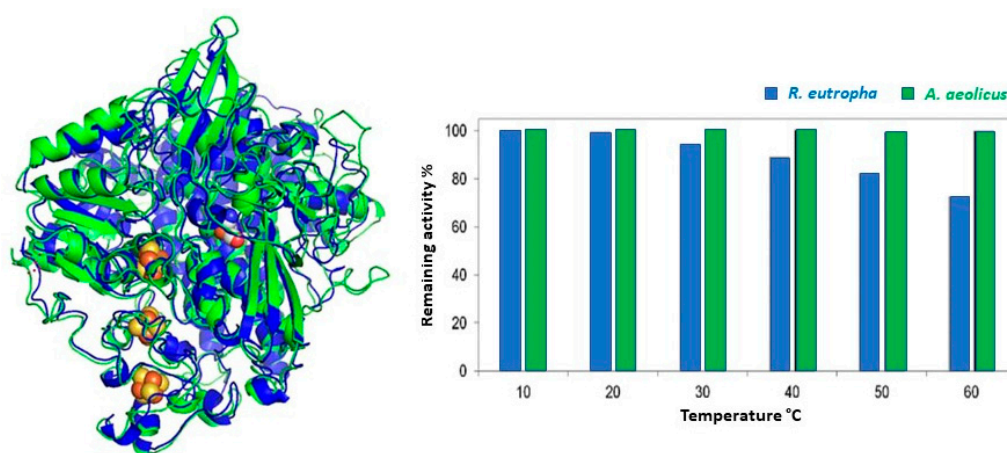


Figure 7. *A. aeolicus* and *R. eutropha* are two homologous NiFe HASEs with different thermostability. (Left) Structural alignment of mesophilic *R. eutropha* (blue) and hyperthermophilic *A. aeolicus* (green) HASEs, (right) remaining activity of the two HASEs after 360 s incubation at increasing temperatures. Adapted with permission from [111].

4. Strategies for Enzyme Stabilization in the Immobilized State

The discussion above has emphasized that the less flexible enzymes are, the most stable they are. In line with this assessment, it is quite straightforward that the immobilization of an enzyme on a support will decrease the movement of the protein, tightening the structure by single or multipoint binding and hence will increase its stability. The extent of the stabilization will depend on the enzyme, the nature of the support and the mode of enzyme attachment to the support (simple adsorption, covalent attachment, entrapment in pores, etc.) This means that the support must be amenable to surface modification for further enzyme attachment. The material acting as a support must also be biocompatible, stable, and able to host high enzyme loadings. A delicate balance between stability and activity of the enzyme will be engaged, with an additional advantage of immobilization being that the support itself can help in the stabilization by consumption of inhibitors or by providing buffer properties as examples [47]. In the following, we will especially discuss immobilization strategies that can enhance enzyme stability. We will not report an exhaustive list of the coatings that can simply prevent enzyme leaching, but we will emphasize the role of the support structuration on the enzyme conformation, hence its stability, although both concepts are closely linked. We will extend the discussion to modes of immobilization that do not require any carrier, like cross-linking of enzyme aggregates (Figure 8).

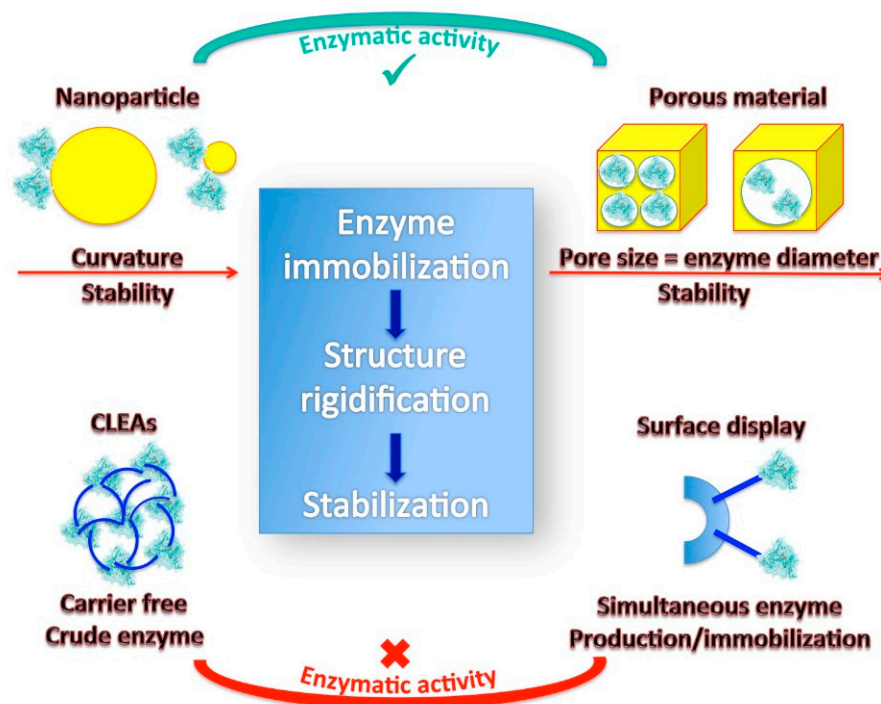


Figure 8. Strategies for enzyme stabilization in the immobilized state.

4.1. Some Fundamentals on Enzyme Immobilization on a Solid Support

4.1.1. Various Types of Interactions

The key point to develop immobilization strategies able to enhance protein stability is to understand how the interactions between the support and the immobilized enzyme may modulate the enzyme internal motion and conformation. The specific structural features of enzymes make their immobilization process very different from rigid particles that simply attach to or detach from a support with certain adsorption and desorption probabilities. The interactions that drive protein adsorption range from high energy covalent bonds (disulfide bridges 320 kJ/mol) to electrostatic interactions (35–90 kJ/mol), hydrogen bonds (8–40 kJ/mol), van der Waals interactions and hydrophobic interactions (4–12 kJ/mol) [113]. Using the concept of “hard” and “soft” proteins based on structural rigidity scale, it can be categorized that adsorption of “hard” proteins will be driven by electrostatic interactions, while “soft” proteins will be able to adsorb either on hydrophobic or hydrophilic surfaces [114].

4.1.2. Enzyme Orientation on the Surface

Upon immobilization of an enzyme onto a support, several processes are going to take place: change in the state of hydration of the enzyme surface, enzyme structural rearrangements, redistribution of charge groups, or surface aggregation [115]. These are slow processes since they involve a whole cascade of rotations. While proteins can rotate freely in solution, they will adopt on a surface one preferential orientation that exposes one part of the enzyme to the surface and the other part to the bulk solution. However, the final orientation can be very different from requirements for optimal activity. Favored orientation is linked to the minimum free energy resulting from attractive coulomb and van der Waals interactions, hydrogen bonds, and the entropy gain of solvent molecules or counter ion release [115]. In addition, rotation of the enzyme can occur even in the adsorption state when local conditions change [116]. In the case of immobilized enzyme, it was expected that only the amino acids on the surface of the enzyme will sense the support. However, by looking at the rigidity profile obtained by Brownian dynamics simulations, it was very recently shown that even amino acids in the core of the enzyme can be affected depending on the surface charge of the support [117].

4.1.3. Conformation Changes upon Immobilization

While electrostatic interactions between the enzyme and the support may drive the adsorption process and prevent enzyme leaching, strong interactions between two charged entities can affect the structure of the enzymes. Flattening of the structure was for example observed when proteins were immobilized on gold metal [118], while no change in the secondary structure was detected when immobilization occurred on a gold surface modified by a self-assembled-monolayer (SAM) of thiol [116]. In the course of adsorption, protein density increases on the surface, and enzyme/enzyme interactions may surpass enzyme/support interactions. Low surface coverage can induce modification of the conformation because the enzyme molecules maximize their contact surface. At higher enzyme loading, it can be expected that protein-protein interactions decrease the interaction with the surface and preserve enzyme conformation. Protein-protein interactions may otherwise induce repulsion between the neighbors which increases with the decrease of the distances between the adsorbed proteins. A variety of methods exists to gain information on the conformation of the enzyme in the immobilized state including CD, surface plasmon resonance (SPR), ellipsometry, fluorescence, and Raman and FTIR spectroscopies. However, characterization methods that can separate effects due to complex coupled mechanisms upon enzyme immobilization are lacking, and data often result in spatial and temporal averages.

4.1.4. Adsorption Versus Multipoint Attachment

Adsorption of proteins on surfaces is a straightforward protocol that is susceptible to maintain high enzyme activity, but it may induce enzyme leaching. Covalent attachment fixes the enzyme on the surface, thus preventing enzyme leaching, but must be carefully considered because the mode of attachment can greatly affect the protein structure, hence both stability and activity. Different protocols can be used to attach an enzyme covalently to a support [20]. The most widely used methods are maleimide and carbodiimide coupling, amine aldehyde condensation and various click chemistry reactions. They allow covalent coupling between one available functional group naturally available or engineered on the surface of the enzyme and a complementary function created on the support where the enzyme is immobilized [20]. A spacer can be added to induce some flexibility required for the activity [119]. Multipoint attachment has been widely suggested to be more suitable than one-point attachment for increased stability because of reduced dynamics of the protein [120–122]. On the other hand, a multipoint attachment is challenging, and both the reactive groups on the support and on the enzyme must be carefully chosen to prevent steric hindrance. Furthermore, the decrease in the essential motion of the folded enzyme state required for catalysis often affects the activity. Stabilization factors more than 1000 were for example reported for formate dehydrogenase or alcohol dehydrogenase after immobilization on activated glyoxyl-agarose, while activity decreased by 50 and 10%, respectively [123].

4.2. Nanomaterials for Stabilizing Enzyme in the Immobilized State

Interest in nanomaterials is increasingly growing thanks to their intrinsic physicochemical properties that allow to envision many applications when combined with enzymes for energy conversion, biosensing, drug delivery, etc. The most attractive feature of nanomaterials is their large surface-to-volume ratio that enables enhanced catalysis thanks to an increased loading of enzymes. Nanomaterials are easily functionalized for further enzyme attachment via classical covalent coupling or click chemistry. However, they also present heterogeneity in terms of size of particles [124], number of sites on the surface available for enzyme attachment, or local curvature that will greatly influence enzyme immobilization. Particle agglomeration, caused by low colloidal stability of the particles in buffer, can also hamper the storage stability of the immobilized biosystems [125].

Nanoparticles (NP) are widely used in medicine, cosmetics, or food industries. Hence, the effect of enzyme immobilization on NPs on both activity and stability has been largely studied over the last ten years. Enhanced thermal or storage stability are reported, the

reasons being often related to the mode of attachment of the enzyme [126,127]. As examples, enhanced thermal and long term stabilities, resistance to urea or to acidic conditions were shown for GOx on ferritin [128] or on Fe₃O₄-based NPs [129], for lipase on Fe₃O₄-based NPs [130], for galactosidase on ZnO-NPs [131], or for cellulase on magnetic NPs [132]. The linkage to the NP was assumed to prevent unfolding of the enzyme no matter of the NP intrinsic property.

Other aspects that account for enzyme stability enhancement on NPs need to be discussed. One of the challenges is the control of the number of grafted enzymes, which may have a direct impact on enzyme flexibility, hence stability. Beyond conjugation of the enzyme to the NP that can affect aggregation, role of the charge, size, and morphology of the NP, local pH and ionic strength may be key parameters involved in the stabilization process [127]. For instance, NP size was shown to have a direct effect on the stability of the enzyme [133]. Varying the size of NPs induces the variation of the NP surface curvature, that will offer distinguished surface of contact for the enzyme. High NP surface curvature (diameters of NP less than 20 nm) was shown to preserve enzyme native conformation [134]. Smaller area for protein contact as well as suppression of unfavorable protein–protein lateral interactions are most probably the reasons that can account for stabilization effect of nanomaterials [135,136]. Curvature-based stabilization of enzymes can be extended to other nanomaterials such as carbon nanotubes (CNT) [4,135]. Morphology of the NP was also reported to tune the enzyme stability. For example, switching from nanospheres to nanorods decreases enzyme stability, most probably because of the impact of the flat cylindrical axial surface of nanorods [137].

4.3. Encapsulation in Porous Materials

4.3.1. Key Role of Pore Size

Porous materials are attractive and versatile supports for enzyme stabilization. Once encapsulated, the enzyme should be protected from the environment, while being able to be attached via suitable chemical modification of the walls of the pores. The chemical conditions used for the porous material synthesis, as well as pore size and interconnectivity in the matrix for diffusion of substrate and product in and out, while ensuring that the protein cannot diffuse out are main issues to be considered. Depending on the materials and the synthetic procedure, the diameter of pores can be tuned and adapted to a specific enzyme. We should distinguish here micro, meso and macroporosity that are described by the diameter of pores being, respectively, less than 2 nm, between 2 and 50 nm and more than 50 nm. While mesopores are required for enzyme encapsulation, macroporosity will enable substrate diffusion. Hence, getting a material with hierarchical porosity is highly desirable in most cases. In general, pore size close to enzyme size favors stabilization. Multipoint interactions may be one explanation for such a result [138]. It was also suggested that modification of the water structure in nano-containers can induce higher enzyme stability [23]. Given the average size of enzymes in the range of about 3–10 nm, some microporous materials with controlled pore size and geometry are unfortunately not suitable for enzyme encapsulation. This is the case of silica films presenting vertically aligned pores [139], or of the well-known silica SBA15 porous matrix [140]. However, porous materials, with pore size compatible with enzyme diameter, can be obtained by different strategies [141]. Carbonization of MgO-templated precursors yields a pore size-tunable material (from around 30 to 150 nm) with interconnected mesopores [142]. Increased half-life stability was shown when the pore size was the closest to the hydrodynamic enzyme diameter [143].

4.3.2. Metal-Based Porous Matrix

Nanoporous gold (NPG) can be obtained by acidic treatment of alloys containing 20–50% gold, or by electrochemical treatment (dealloying process). NPG structure presents interconnected ligaments and pores of width between 10 and several hundred nm. NPG displays various surface curvatures that offer a different environment for enzyme immobilization. Different enzymes have been immobilized in NPG for various purposes

showing a pore size-dependent enhanced stability as compared to enzyme in solution [144]. Alternatively, enzymes can be encapsulated in gold nanocages within a 3D gold network obtained by in situ reduction of gold salts in the presence of the enzyme [145]. Complexes formed between cations such as Cu(II) and protein molecules can serve as nucleation sites for micrometer-size particles with unique flower petal-like morphology. Enzymes confined in such structures exhibit enhanced stability [146]. Other hierarchical materials presenting mesoporous structures can be obtained by using networks of CNT or nanofibers [19].

Polymeric metal-organic-frameworks (MOFs) are matrices currently under great consideration. They consist of metal ions or clusters coordinated to organic ligands to form two- or three-dimensional structures. Cavities of mesoporous MOFs are greatly suitable for enzyme immobilization. In addition to enhanced enzyme loading and reduced leaching, the strictly controlled pore size can provide selectivity for substrates. Enzymes can be immobilized by infiltration process, requiring MOF pore size larger than protein size. Enzymes can alternatively be encapsulated in the lattices of the MOF structure by mixing the enzyme with the metal and the ligand. In this case, encapsulation proceeds through a nucleation mechanism where the enzyme acts as a nucleus for MOF growth, leading to enzymes protected in pores with size close to the radius of gyration of the protein [147]. However, in the latter case, synthesis conditions must be mild enough to avoid protein denaturation. It is admitted that the framework around the enzyme maintains the conformation of the active enzyme species [148]. Many studies report increased stability of various enzymes when embedded in the pores of MOFs. Enhanced thermal and pH stability was observed for different enzymes, as well as protection against inhibitors, or maintaining of activity in non-aqueous solvents [149–154]. MOF can also be used to encapsulate cascade of enzymes with enhanced stability and spatial control of the proteins inside the lattices [155]. However, care should be taken with solubility of MOFs in the presence of various compounds such as amino acids, some organic acids or buffers that present high affinity for the MOF-metal, inducing leaching of the enzyme via MOF dissolution [156,157]. Covalent organic frameworks, only composed of light elements (H, C, B, N, and O) and covalent bonds, with higher stability than MOFs, can be alternatives as efficient matrices for enzymes [158].

In MOFs, enzymes are statistically entrapped. It should be even more elegant to engage each individual enzyme with well-defined protecting shell surrounding it [159]. This strategy, known as single enzyme nanoparticles (SEN), is based on the controlled formation of a shell of polymer around one enzyme by in situ polymerization from the enzyme surface. The shell is thin and permeable so that substrates can freely diffuse to the enzyme core. SEN strategy is reported to enhance thermal stability, organic solvent, and acid/base tolerance even in aggressive environments [160,161]. Both protection by biocompatible polymer shell and multipoint covalent attachments within the nanocapsule were suggested to explain the enhanced enzyme stability. This last strategy recalls less recent examples reported in Section 2 of this review and based on polymer protection around the enzyme.

4.3.3. Other Polymeric Matrices

Hydrogels are polymeric networks that are of great interest for protein immobilization because they present the double advantage of high water content and a tunable porous structure [162]. Natural polysaccharides such as alginate can produce beads when cross-linked with certain metals. Alginate concentration can be tuned to control the porosity of alginate beads (in the range 5 to 200 nm diameter) and to find the best compromise between substrate diffusion and enzyme conformation preservation and leaching [163]. Enzymes embedded in DNA hydrogels often show enhanced thermal stability and improved stability during freeze-thaw cycles or in the presence of denaturants such as organic solvents. Conformation of the enzyme is proposed to be maintained thanks to extensive inter- and intra-strand weaving of long DNA building blocks. The hydrophilicity of the hydrogel further protects the enzyme against organic solvent [164]. Gel nanofiber made of Zn²⁺ and adenosine monophosphate was also used to encapsulate an enzyme cascade for glucose

detection. The biomaterial exhibited enhanced stability against temperature variation, protease attack, extreme pH, and organic solvents. Porosity and water content of the gel allowed to maintain 70% of the activity after 15 days storage while free enzymes lost activity [165].

4.4. Cross-Linked Enzyme Aggregates (CLEAs)

The addition of salts, water miscible organic solvents, or non-ionic polymers to protein solution induces their precipitation as physical protein aggregates, held together by non-covalent bonding. Enzyme tertiary structure can be maintained in the aggregates. Note this is also the traditional procedure for protein purification (in particular see in Section 3 the discussion about salting-out processes) [166]. Subsequent cross-linking of these physical aggregates renders them permanently insoluble while maintaining their pre-organized structure (Figure 9). Covalent binding or cross-linking of enzyme to enzyme to form aggregates is commonly referred to as CLEAs. CLEAs constitute a simple way of enzyme immobilization which is carrier-free and can be used in any reaction medium [22,167,168]. One more advantage of CLEAs is that they can be formed starting from crude enzyme preparations and do not require highly purified enzymes. Typical cross-linking agents are GA, ethylene glycol diglycidyl ether (EGDGE), and dextran, but also polyethyleneimine (PEI) that can generate covalent bonds between two or more biomolecules in the system through the enzyme amino and/or carboxyl surface groups [169]. FTIR analysis of CLEAs highlighted changes in the secondary structure of enzymes, with an increase in β -sheet and α -helix components and a decrease in β -turns compared to free enzymes, showing the ability of CLEAs to stabilize enzymes [169–171].

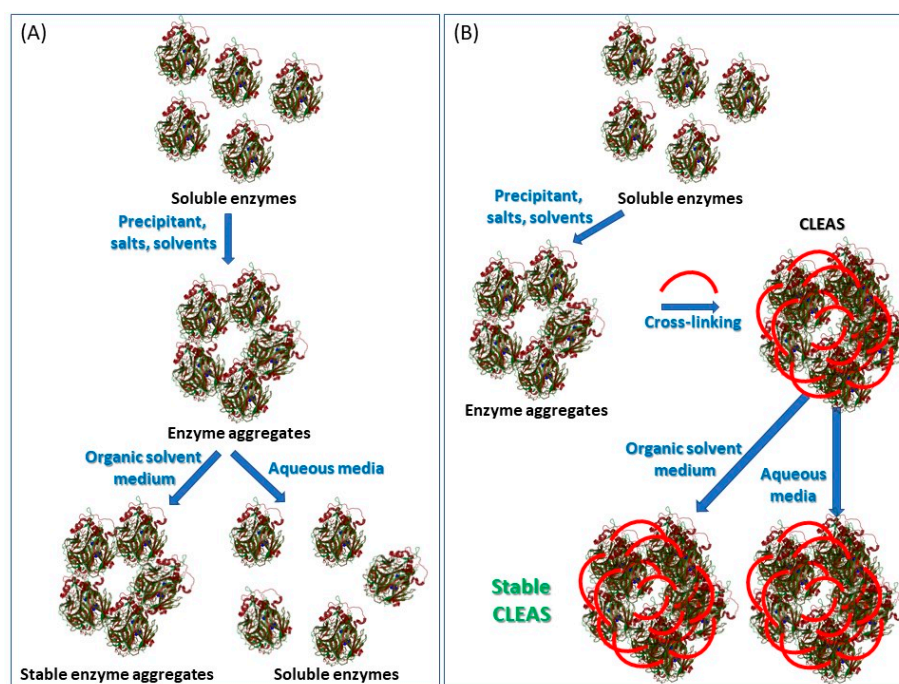


Figure 9. (A) formation and redissolution of enzyme aggregates, (B) stable CLEA preparation.

A wide variety of enzymes, including hydrolases, oxidoreductases, lyases, and transferases have been used as CLEAs especially for organic synthesis [172,173], displaying enhanced stability under various conditions: protection against organic solvents [174], enhanced thermostability [175], reduced substrate inhibition [176,177], enhanced stability in acidic or alkaline conditions [178,179] or under storage [180]. Magnetic CLEAs combined the advantages of CLEAs and covalent immobilization onto Fe_3O_4 magnetic particles and may show increased stability to changes of pH and temperature [181,182]. Enzyme cascade can also be combined as CLEAs showing enhanced thermal and pH stability [183,184].

Despite a high enzyme concentration per unit volume, decrease in activity is often observed using CLEAs. Diffusional limitation of mass transfer is one of the main issues. Alteration of the enzyme tertiary structure by one of the components required for CLEA preparation or steric hindrance within the aggregate of high particle size hampering inner enzyme activity can also explain the decrease in activity. Hence, the choice of precipitant, cross-linker, and ratio of cross-linker protein is a critical step for maintaining required flexibility of the structure for high activity [185]. These parameters strongly depend on the enzyme, making the CLEA technology delicate [174].

4.5. Bio-Surface Display of Enzymes

Bacteriophages, spores, yeast, and bacterial cells can be used as enzyme carriers in so-called surface protein display systems [186,187]. *E. coli* bacterium is one of the most studied cells for enzyme surface display. Surface display of the targeted enzyme (the passenger) is realized by genetically fusing it to a carrier protein, which facilitates export across the cell envelope (inner membrane and outer membrane separated by the periplasm). The protein of interest is ultimately secreted and immobilized on the cell wall. Interestingly, enzymes are thus simultaneously produced and immobilized on the bio-component. The anchoring motif can be fused to the N- or C- end of the protein, or the protein can be inserted within the sequence of the anchor protein. The anchor protein must be able to ensure transport of the heterologous protein through the secretory pathway, proper folding of the fusion protein, and strong binding at the cell wall surface. Contrary to purified immobilized proteins, expressing enzymes on cell surfaces is considered advantageous as enzymes can be used repeated for extended periods with no loss of enzyme activity. Stability of immobilized proteins by such a natural procedure against organic solvents, extreme pH, or high temperature has been reported [188,189]. Yeast and spores are also currently explored as enzyme display surfaces allowing enzyme enhanced thermal stability [190,191]. However, the efficiency of the display systems in terms of immobilized enzyme amount and specific activity needs to be improved for envisioning any biotechnological application [192].

5. Specificity of the Stabilization of Redox Enzymes on Electrodes for Bioelectrocatalysis

5.1. Bioelectrocatalysis: When Enzymes Meet a Foreign Conductive Surface

5.1.1. Electron Transfer in Metabolic Energy Chains

Most cellular functions, such as cell motility, key molecule biosynthesis or transport across membranes, require energy. Life energy is generated by redox transformations of nutrients present in the environment or by sunlight to create the proton gradient across the membrane. This gradient is later used to produce ATP, the universal molecular “coin” driving metabolic reactions. In these processes, complex but highly specific molecular chains are involved that couple electron transfer (ET) to the diffusion of protons across cell membranes. Focusing on bacteria, a wide range of energy substrates can be metabolized: lactate, glucose, H₂, H₂S, O₂, sulfate, fumarate, etc. thanks to the presence of a large variety of redox enzymes interacting with membrane lipids or with redox proteins acting as electron shuttles. To enable metabolism achievement, ET must proceed fast through highly specific protein–protein interactions. According to Marcus theory, the distance between the donor and the acceptor will drive the rate of ET [193]. It is admitted that electrostatic interactions serve for pre-orientation of interacting partners; then, hydrophobic interactions drive a rearrangement of the transitory complex allowing ET [194]. Pre-orientation is guided by the heterogeneity of charge distribution on the protein surface which induces dipole moments that can be as high as thousands of debyes [112]. As such, one or more amino acids defining a charged patch on the surface of one protein partner are often involved for the specific interaction with the other partner.

5.1.2. Electron Transfer Mechanisms Involving Redox Enzymes at Electrochemical Interfaces

Redox enzymes can operate very efficiently in bioelectrocatalytic processes for the redox transformation of a variety of substrates. As stated in the introduction of this review,

various applicative domains are concerned from bioelectrosensing, bioenergy to bioelectrosynthesis. One prerequisite is the use of a conductive support, the electrode, to provide or accept the electrons for the redox transformation to take place. The question directly arises whether the electrode would gently replace the physiological redox partner? Actually, many materials used as electrodes (carbon, gold, nano- or porous structures, etc.) can be chemically functionalized to provide an enzyme environment mimicking the physiological one. It was clearly demonstrated that the oriented approach of the enzyme to the electrode surface was guided by electrostatic interactions driven by the enzyme dipole moment. The example of multicopper oxidases (MCO), the key enzymes for O_2 reduction into water, is highly relevant in that sense. Four copper sites are involved in the catalytic process, CuT1 being the first electron acceptor, and electrons generated travelling intramolecularly to the trinuclear Cu site where O_2 binds and is reduced. Bilirubin oxidase (BOD) from the fungus *Myrothecium verrucaria* has a dipole moment of 910 D at pH 5 pointing positive towards the CuT1. At the same pH, BOD from the bacterium *B. pumilus* and laccase (Lac) from *Thermus thermophilus* have dipole moments of 1830 and 860 D, respectively, but pointing positive opposite to the CuT1. In accordance with this structural feature, ET was obtained on negatively or positively charged electrodes in the case of *M. verrucaria* BOD or *B. pumilus* BOD and *T. thermophilus* LAC, respectively [116,195,196]. One specificity of bioelectrocatalysis stems from the substrate and product coming in and out to/from the active site that may be hampered by the required enzyme orientation for ET. Not only activity but also stability in case of substrate or product accumulation may be affected [197]. This point is however understudied in bioelectrochemistry. When direct ET (DET) is not possible, mainly because there is no surface electron relay identified, either because the enzyme 3D structure is not known or because the active site is electrically isolated in the protein moiety, mediated ET (MET) can be used instead. Typically, MCOs, enzymes with hemic cofactor such as cellulose dehydrogenase, and enzymes with surface FeS clusters such as HASEs are reported to undergo DET, while GOx is only electrochemically addressed through MET. In this latter case, a small molecule acting as a fast and reversible electrochemical system will make the electron shuttle between the electrode and the FAD cofactor in the enzyme. Redox potential of the redox mediator as well as its affinity for the enzyme will drive the electrocatalysis. One important question is whether the enzyme will be more stable under DET or MET processes (Figure 10).

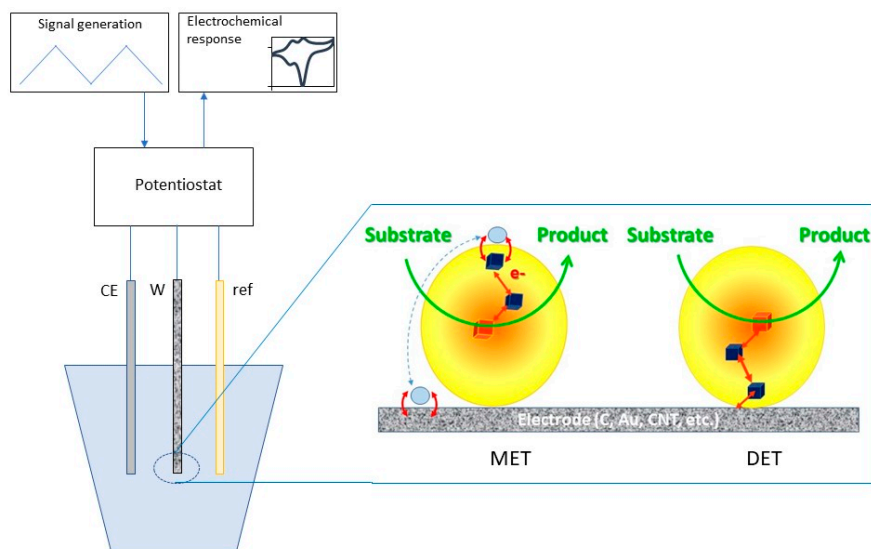


Figure 10. Scheme of a typical bioelectrochemical experiment showing the set up and the adsorption of a protein on the electrode surface either in a MET or a DET mode. The active site of the enzyme, the electronic relays and the redox mediator are represented as red squares, dark blue squares, and light blue spheres, respectively. CE, W, and ref represent counter, working, and reference electrodes, respectively.

5.2. Stabilization Strategies for Bioelectrocatalysis

5.2.1. How Far Can General Enzyme Stabilization Strategies Be Extended to Bioelectrocatalysis?

Table 1 reports bioelectrode stability for two main enzymatic reactions, i.e., O₂ reduction and H₂ oxidation. These two enzymatic reactions have been chosen as relevant for the development of biofuel cells, devices currently developed as alternatives to platinum-based fuel cells. As can be seen, many of the strategies detailed in the previous chapters of this review are involved in bioelectrode stabilization. It should be noted that in most cases stabilization refers to operational duration. Thus, the stability parameter is mainly evaluated through the percentage of preserved catalytic current. Although crucial for improving bioelectrocatalysis, only rare studies report enzyme conformational changes upon redox immobilization of enzymes on electrode.

From the survey of the literature reported in Table 1, general features of enzyme stabilization inducing bioelectrode stability can be recognized. This is the case for redox enzymes extracted from extremophiles yielding efficient bioelectrocatalysis while expected to be more stable than their mesophilic homologues even at room temperature. We already provided in Section 3 one relevant example showing that the NiFe HASE from the hyperthermophilic bacterium *A. aeolicus* was much more stable than its mesophilic homologue from *R. eutropha* [111]. This enhanced stability of the hyperthermophilic enzyme is fruitfully exploited to design an H₂/O₂ fuel cell displaying at the same time high catalytic currents reported to the mass of enzymes (in the order 1 A/mg enzyme), delivering mWs of power in a range of temperature 20–60 °C, and a half-life for the bioanode of one month, a quite encouraging stability compared to other reported devices [198]. It should be also mentioned that at the cathodic side, the thermostable BOD from *B. pumilus* is used which also shows enhanced stability compared to the widely used *M. verrucaria* BOD. Other recent works proved the efficiency of extremophilic enzymes in bioelectrochemical systems, as illustrated in the two following examples. *Bacillus* sp. FNT thermophilic LAC showed 60–80% of remaining activity after two weeks of storage at room temperature when the activity of mesophilic *T. versicolor* LAC was zero in the same conditions [199]. The activity of cellobiose dehydrogenase from *Corynascus thermophilus* retained more than 50% activity after 5 days of multicycle voltammetry mode and about 30% after 9 days [200].

As for non-redox enzymatic catalysis, stability of enzymatic electrodes requires to avoid enzyme leaching from the electrode. Entrapment in porous matrices and covalent immobilization through suitable functionalization of the electrode are ways to improve redox enzyme-based bioelectrode stabilization. However, it must be considered that the redox enzyme will sense an electric field during a bioelectrocatalytic process and that some species can be generated through the electrochemical potential application, thus requiring stabilization strategies more specific to bioelectrochemistry. In addition, the electron exchange between the electrode and the enzyme which is the basis of bioelectrocatalysis imposes specific constraints that may prevent the use of the strategies developed above. Among these constraints, the host matrix must be conductive, cross-linking that yields heterogeneities in enzyme orientation can make a population of enzymes incapable of electron transferring; addition of polyols may electrically isolate the enzyme preventing any electron transfer, or use of high concentrations of salts in the electrolyte solution can favor the leaching of the enzymes from the electrode surface. Hence, any stabilization protocols described above must be evaluated in light of their adaptability to bioelectrochemistry with redox enzymes.

Table 1. Bioelectrode stability: cases of multicopper oxidases (MCOs) and hyperthermophilic hydrogenase (HASEs).

Enzyme	Bioelectrode Design	Electrochemical Conditions	Reaction Followed/Purpose	Stability	
<i>Cerrena unicolor</i> C-139 LAC	Enzyme polymerized at a glassy carbon electrode through cold plasma	Acetate buffer pH 5, 25 °C	Rutin biosensing	42% of current is recovered after 8 days at pH 5.	[201]
<i>Streptomyces coelicor</i> LAC	Enzyme adsorbed on zinc oxide NPs capped with <i>p</i> -amino thiophenol and attached to graphene oxide	0.1 M phosphate buffer pH 5	Sucralose sensing	83% and 73% of the initial activity after 5 and 10 days, respectively.	[202]
<i>Trametes hirsuta</i> LAC GreeDo mutant obtained by combining computational design	Enzyme covalently attached to AuNPs grafted on graphite electrode	0.1 M acetate buffer pH 4	O ₂ reduction	80% of initial activity after 96 h incubation at pH 4 60% of initial activity after 2 h of continuous operation	[203]
LAC	Enzyme adsorbed on AuNPs electrodeposited on a screen-printed carbon electrode (SPCE) modified with polypyrrole	0.1 M acetate buffer pH 3.5 25 °C	Polyphenol sensing	85% of the initial activity after 1 month (storage at 4 °C)	[204]
<i>Trametes versicolor</i> LAC	Enzyme and Cu ²⁺ co-adsorbed on pyrene-terminated block polymer on pyrolytic graphite surface and graphene papers	0.1 M acetic acid buffer pH 5	Pyrocatechol sensing	70% of original activity upon 90 days of the freeze-dried powder. 80% of activity after 3 freeze-thaw cycles. 31% activity at 70 °C. 96% of the initial activity after 30 days storage at 4 °C.	[205]
<i>Trametes versicolor</i> LAC	Enzyme entrapped within graphene-cellulose microfiber composite modified SPCE.	0.1 M sodium phosphate buffer pH 5	Catechol sensing	97% of the initial activity after 130 h storage.	[206]
<i>Trametes versicolor</i> LAC	Enzyme with Cu-nanoflowers mixed with CNTs	0.01 M phosphate buffer pH 7.4	O ₂ reduction in a H ₂ /O ₂ hybrid biofuel cell	85% of biofuel cell initial power density for 15 days at room temperature.	[207]
LAC	Enzyme absorbed on AuNPs-MoS ₂ composite glued on a glassy carbon electrode (GCE) by Nafion	0.2 M acetate buffer pH 4	Catechol sensing	95% initial activity after 15 days of storage stability.	[208]
<i>Trametes versicolor</i> LAC	Enzyme entrapped in chitosan-CNT matrix	0.1 M phosphate buffer pH 7.4, 20 °C	O ₂ reduction	82% of the initial activity within 10 days.	[209]

Table 1. Cont.

Enzyme	Bioelectrode Design	Electrochemical Conditions	Reaction Followed/Purpose	Stability	
<i>Trametes versicolor</i> LAC	Enzyme entrapped with Fe ₃ O ₄ magnetic nanoparticles in chitosan matrix	0.2 M phosphate buffer	O ₂ reduction	50% of the initial activity after 20 days.	[210]
<i>Trametes versicolor</i> LAC	Enzyme crosslinked with GA in a matrix made of room temperature IL-CNTs	50 mM acetate buffer pH 5	Polyphenol biosensing	33% of the initial activity after 20 days.	[211]
<i>Bacillus subtilis</i> LAC	Enzyme adsorbed on the electrode modified with thiol graphene-AuNP nanocomposite film	0.1 M HAc-NaAc buffer solution pH 4.6, 25 °C	Hydroquinone sensing	87% of the initial current response after 100 days	[212]
<i>Trametes versicolor</i> LAC	Enzyme and nanocopper incorporated in polyacrylonitrile/polyvinylidene electrospun fibrous membranes		Trichlorophenol removal	68% of the initial activity after 30 days.	[213]
<i>Bacillus subtilis</i> LAC	Enzyme covalently bound on functionalized CNTs		O ₂ reduction	70% of initial activity after two weeks of storage at room temperature.	[199]
LAC	Enzyme cross-linked on electropolymerized L-lysine molecules on a graphene modified GCE	0.1 M sodium phosphate buffer pH 6	17β-estradiol sensing	68% of initial activity after 30 days storage at 4 °C.	[214]
<i>Aspergillus sp.</i> LAC	Enzyme adsorbed on polypyrrole-modified nanotubes and SrCuO ₂ microseeds composite on graphite electrode	0.1 M phosphate buffer pH 7	2,4-dichlorophenol sensing	80% of initial activity after 14 days of storage at 4 °C.	[215]
<i>Trametes versicolor</i> LAC	Enzyme deposited by electrospray on carbon black modified screen-printed electrodes	0.1 M citric acid/sodium citrate buffer pH 4.5	Catechol detection	Valuable working and storage stability of the biosensor that remains 100% of its performances for up to 25 measurements and can be preserved at room temperature for at least 90 days.	[216]
LAC	Enzyme mixed with polyvinylacetate and AuNPs electrospun on platinum electrode	Phosphate buffer	Ascorbic acid sensing	Stability for 76 days.	[217]
LAC	Enzyme adsorbed on polyaniline/magnetic graphene composite	pH 5	Hydroquinone sensing	90% initial response after 30 days.	[218]
<i>Trametes versicolor</i> LAC	Enzyme embedded in polydopamine NPs with anchored AuNPs	0.1 M ABS pH 5	Norepinephrine sensing	91% initial response after 30 days.	[219]

Table 1. Cont.

Enzyme	Bioelectrode Design	Electrochemical Conditions	Reaction Followed/Purpose	Stability	
LAC	Enzyme covalently bound to a composite made of acrylate microspheres and AuNPs coated on a carbon paste screen-printed electrode	0.1 M phosphate buffer pH 5	Tartrazine sensing	51% initial response after 90 days.	[220]
<i>Botryosphaeria rhodina</i> LAC	Enzyme entrapment into nanostructured carbon black paste electrode	0.1 M phosphate buffer pH 6	Epinephrine sensing	93% initial response after 7 days.	[221]
<i>Myrothecium. Sp</i> BOD	Enzyme crosslinked into a biogel matrix made of Nafion deposited on carbon NPs	0.1 M phosphate buffer pH 7.2, 25 °C	O ₂ reduction	Electrode potential decrease from 0.37 to 0.31 V after 24 h of operation at 1 mA·cm ⁻²	[222]
<i>Magnaporthe orizae</i> BOD	Enzyme entrapped in osmium-based hydrogels deposited on CNTs modified by electrografting of aryldiazonium salts	0.1 M phosphate buffer pH 5	O ₂ reduction	After 1 day loss of 27% of the initial activity then stable for several days.	[223]
<i>Myrothecium verrucaria</i> BOD	Enzyme adsorbed on carbon cloth modified with aminobenzoic acid. Gas diffusion electrode.	0.1 M phosphate buffer pH 7.4	O ₂ reduction	80% of initial activity after 1.3 h of operation of the H ₂ /O ₂ biofuel cell.	[224]
<i>Myrothecium verrucaria</i> BOD	Enzyme covalently linked to carbon cloth modified by aminobenzoic acid and coated with a microporous hydrophobic Nafion layer. Gas diffusion electrode.	0.1 M phosphate buffer pH 7, 25 °C	O ₂ reduction	80% of initial current after 6 h of continuous operation at 0 V vs. Ag/AgCl.	[225]
<i>Myrothecium verrucaria</i> BOD	Enzyme adsorbed on CNTs and protected by a carbon-coated magnetic nanoparticle layer	0.1 M HEPES buffer pH 7,	O ₂ reduction	80% of initial activity after 48 h of continuous operation at 0 V vs. Ag/AgCl in the presence of 1 nM proteinase. 70% initial activity after 30 days of storage at room temperature.	[226]
<i>Magnaporthe orizae</i> BOD	Wild type enzyme adsorbed and mutants covalently bound to a maleimide CNT modified electrode	200 mM phosphate buffer 100 mM citrate buffer pH 7	O ₂ reduction	40% and 10% initial activity after 3 days and 6 days, respectively, in the adsorbed mode. 95% and 52% initial activity after 3 days and 6 days, respectively, in the covalent attachment mode	[227]

Table 1. Cont.

Enzyme	Bioelectrode Design	Electrochemical Conditions	Reaction Followed/Purpose	Stability
<i>Myrothecium verrucaria</i> BOD	Enzyme adsorbed or electrochemically deposited on Au polycrystalline electrode	0.1 M acetate buffer pH 5, 25 °C	O ₂ reduction	Adsorption mode: 5% initial activity after 100 potential cycles between 0 and 0.8 V vs. Ag/AgCl at 50 mV/s. Electrochemical deposition mode: 80% initial activity after 200 cycles [228]
<i>Myrothecium verrucaria</i> BOD	Enzyme adsorbed on MgOC modified with 6 amino 2-naphtoïque acid	0.1 M acetate buffer pH 5, 24 °C	O ₂ reduction	50% of the initial activity after 5 days. [229]
<i>Myrothecium verrucaria</i> BOD	Enzyme covalently bound to reduced graphene oxide modified by 4-aminobenzoic acid to reduce its aggregation	0.1 M phosphate buffer pH 7	O ₂ reduction	55 h half-life. [230]
<i>Myrothecium verrucaria</i> BOD	Enzyme adsorbed on buckypaper CNTs	Phosphate buffer pH 6.5, 25 °C	O ₂ reduction	10 h half-life [231]
<i>Magnaporthe oryzae</i> BOD	Molecular engineering for covalent immobilization in macroporous gold electrode	0.1 M phosphate buffer pH 7.2, 25 °C	O ₂ reduction	75% of the initial activity after incubation for 5 days. [232]
<i>Myrothecium verrucaria</i> BOD	<i>Mv</i> BOD entrapped with ABTS in polydopamine layer on CNTs	0.1 M phosphate buffer pH 7, 25 °C	O ₂ reduction	<i>Mv</i> BOD stable for 22 h of operation at 0.1 V vs. Ag/AgCl. [233]
<i>Bacillus pumilus</i> BOD	<i>Bp</i> BOD: entrapped in pyrenebetaine on CNTs	50 °C	O ₂ reduction	Rapid drop in activity, almost 0 after 3 h of operation at 0.1 V vs. Ag/AgCl [233]
<i>Bacillus pumilus</i> BOD	Enzyme entrapment in a carbon felt modified by pyrene-NH ₂ modified CNTs	0.2 M phosphate buffer pH 6,	O ₂ reduction	7 days half-life at 25 °C upon continuous operation of a H ₂ /O ₂ biofuel cell. [198]
<i>Pyrococcus furiosus</i> HASE	Enzyme adsorbed onto a CNT modified carbon felt electrode	50 mM phosphate buffer pH 7, 50 °C	H ₂ oxidation	Voltage retains 90% of the initial value 33 h operation in a hybrid fuel cell. [234]
<i>Desulfovibrio vulgaris</i> HASE	Enzyme embedded in viologen-based redox hydrogel modified porous carbon cloth.	0.1 M phosphate buffer pH 7.4	H ₂ oxidation	60% of initial activity after 20 h at 0.16 V vs. SHE. [224]
<i>Desulfomicrobium baculatum</i> HASE	Oriented covalent immobilization of the enzyme on modified CNTs	50 mM phosphate buffer pH 7.6, 25 °C	H ₂ oxidation	80% of initial activity after 1 h in the biofuel cell. [235]

Table 1. Cont.

Enzyme	Bioelectrode Design	Electrochemical Conditions	Reaction Followed/Purpose	Stability	
<i>Desulfovibrio desulfuricans</i> HASE	Enzyme embedded in viologen-based redox hydrogel on carbon cloth-based electrode	0.1 M phosphate buffer pH 7.4	H ₂ oxidation	50% of initial activity after 11 h at 0.16 V vs. SHE.	[236]
<i>Desulfovibrio vulgaris</i> HASE	Enzyme embedded in viologen-based redox hydrogel and protected by catalase-GOx layer.	0.1 M phosphate buffer pH 7.4	H ₂ oxidation	60% initial activity after 8 h in the presence of 5% O ₂ at 0.016 V vs. SHE.	[143]
<i>Aquifex aeolicus</i> HASE	Enzyme adsorption on CNT modified by π - π stacking with PyrNH ₂	0.2 M phosphate buffer pH 7, 25 °C	H ₂ oxidation	1 month half-life at 25 °C upon continuous operation of a H ₂ /O ₂ biofuel cell.	[198]
[NiFeSe] <i>Desulfovibrio vulgaris</i> Hildenborough HASE	Enzyme entrapped in methylviologen-based redox polymer films deposited on carbon cloths	0.1 M phosphate buffer pH 7.4, room temperature	H ₂ oxidation	25% and 50% of initial activity depending on the variant after 7 h in chronoamperometry experiments.	[237]

5.2.2. Engineering of Enzymes Seeking for Both Enhanced ET Efficiency and Stability

The general engineering procedures developed to enhance enzyme stability can be adapted for redox enzymes, including introduction of stronger bonds, removal of potential degradation sites, or oligomeric structure formation [238–240]. However, the most interesting strategies here are to obtain enhanced stability and ET efficiency at the same time. Then, the main targets for protein engineering will lie (i) in the vicinity of the active site or (ii) at specific points of the enzyme surface able to anchor it with the best orientation for the highest ET rate (Figure 11). For strategy (i), the vicinity of the heme cavity of peroxidase [241] or of the CuT1 site of LAC has been targeted [242,243]. Two recent reports illustrate this concept. Two alanine residues were mutated to one leucine and one valine. Not only did the introduction of hydrophobic residues increase the redox potential of the CuT1 site by 50 mV, but it also protected the CuT1 site from the solvent as well as enhanced temperature and pH stability of the variant. The mutant was stabilized at the electrode. It retained roughly 80% of its initial activity after 96 h incubation at pH 4.0 and presented a half-life of 60 min at 70 °C against 23 min for the wild type protein [203]. With the aim of electricity production directly from seawater recycling, recombinant forms of CotA LAC from *B. licheniformis* were produced [244]. A double mutation, one in a region close to the CuT1 and the other on the surface of the protein, was shown to induce a synergic effect in bioelectrocatalysis. Conformational changes in the double mutant were proved by CD and fluorescence that allow the variant to catalyze O₂ reduction in seawater, a very unusual property for classical LACs. Protein leaching under such high ionic strength conditions must however be solved.

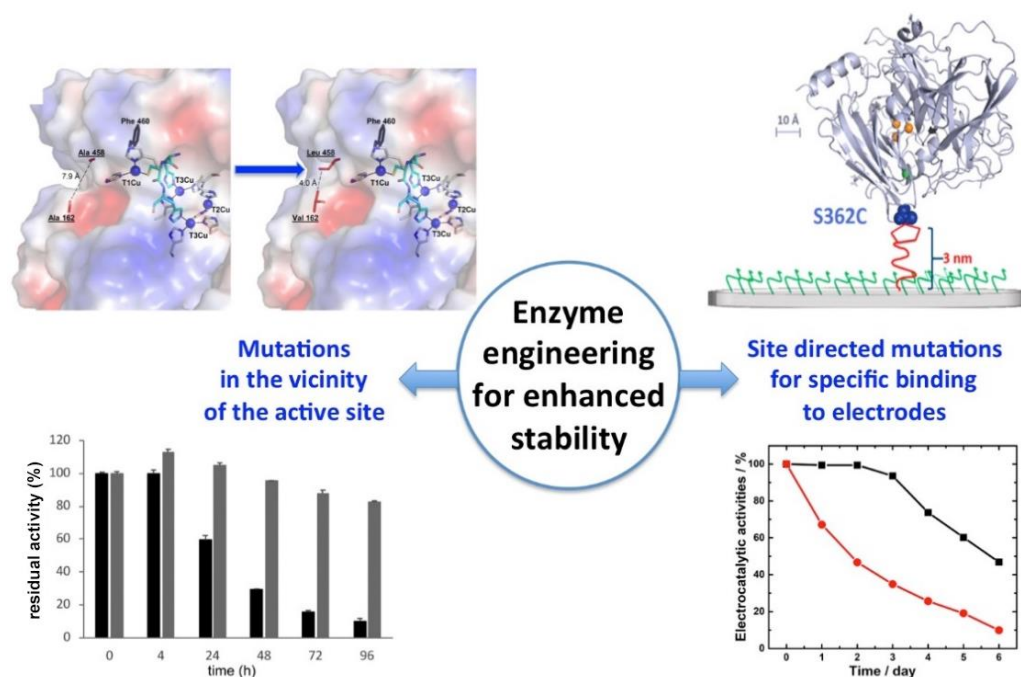


Figure 11. Enzyme engineering strategies for enhanced stability. (Left) Mutations in the vicinity of the active site; computer-guided mutagenesis and directed evolution of a fungal LAC in CuT1 vicinity induce enhanced stability at pH 4 compared to the WT. Reproduced with permission from [243]. (Right) Covalent immobilization of BOD through site-directed mutagenesis and reaction with maleimide groups on the electrode surface induce enhanced stability of the mutant (black curve) compared to the WT (red curve). Adapted with permission from [227].

For strategy (ii), covalent immobilization of enzymes at electrodes was realized by producing site-directed variants with cysteine residues located at different sites of the enzymes able to react with maleimide groups immobilized on the electrode. This elegant method combines controlled orientation of the protein at the electrode for ET, sufficient flexibility

for activity, and expected enhanced stability. In the case of cellulose dehydrogenase, 40% of initial electroactivity was recovered after 2 months of storage while the wild type enzyme loses progressively its activity within 20 days [245,246]. In addition, controlled orientation allowed investigating mechanistic aspects of the ET. The immobilization method was extended to BOD from *Magnaporthe oryzae* showing an enhanced stability with almost no loss of electroactivity for 3 days [227] (Figure 11).

5.2.3. Conductive Porous Material as Redox Enzyme Host Matrices Favoring Fast ET

We discussed in the previous sections how porous materials can be beneficial for the stabilization of embedded enzymes. The further requirements for their use as host matrices of redox enzymes are that either the porous material is conductive to ensure DET, or redox mediators can be added either diffusing or co-immobilized within the matrix. We emphasized that MOFs are nowadays considered as very attractive materials. To ensure electron conduction within MOFs, multicomponent systems can be synthesized composed of MOFs, enzymes and conductive nanomaterials such as graphene nanosheets or CNTs [147]. A nice example is provided by Li et al. who encapsulated a LAC in ZIF-8 in the presence of CNTs (LAC@ZIF-8) [247]. Fluorescence measurements highlighted a negligible enzyme leaching. When compared to free enzyme or to enzyme embedded in MOF with no CNT, the LAC@ZIF-8 hybrid displayed improved thermal stability, enhanced resistance to solvents as well improved long-term storage stability. However, although DET was demonstrated, the catalytic efficiency was greatly enhanced by redox mediator addition, suggesting that a large enzyme population was not directly wired in the hybrid material. Mesoporous silica nanotubes are another example of a suitable matrix when coated with a graphene sheet layer to enhance its electrical conductivity. BOD entrapped in the material was able to reduce O₂ in the absence of redox mediators, and the bioelectrode stored in water at 4 °C for 15 days retained around 80% of initial current [248]. The stability of the bioelectrode was suggested to be linked to the size of the nano-channels (12 nm) being close to the size of the enzyme, limiting its mobility. Fructose dehydrogenase and HASE were immobilized in MgOC with pore size in the range 10–150 nm [249,250]. DET occurred between enzymes and the material regardless of the pore size, but a pore diameter close to the enzyme size enhanced the thermal and long-term stabilities.

The relationship between pore size and stability is shared by non-redox and redox enzymes. However, for redox ones, the orientation of the enzyme toward the material wall must also be considered for a direct wiring. In pores presenting a diameter close to the enzyme size, the distance between electrical relays on the surface of enzymes and the material will be statistically minimized. Multi-point contacts are expected to occur at the same time. This means that both stability and ET rates should be enhanced simultaneously [238,251]. Porous gold obtained either by dealloying processes or anodization is increasingly used for immobilization of redox enzymes. Their pore sizes are compatible with efficient enzyme entrapment [144]. Using electrochemistry, a narrow distribution of orientation of BOD favorable for enhanced DET was measured [252]. A model based on close packing spheres explained why the curvature of pores was beneficial for DET. Unfortunately, no examination of the enzyme conformation in the porous gold material was provided. Effect of nanomaterial curvature was evoked in another work to explain LAC properties once immobilized in a CNT network in the presence of ethanol [253]. An improved direct catalytic current for O₂ reduction as well as reduced chloride inhibition was measured. CD and ATR-IR demonstrated a net difference in the secondary structure when the enzyme/CNT/ethanol system was immobilized at the electrode as compared with enzyme in solution. The structure stabilization suggested that ethanol favors contact between CNT and LAC in its native form with an orientation favorable for DET. Although not deeply investigated, CNT curvature was suggested to help in the stabilization of the immobilized dehydrated enzyme.

5.2.4. Redox Enzyme Encapsulation in Hydrogels for Bioelectrocatalysis

Entrapping redox enzymes into hydrogels is expected to provide a suitable hydrated environment able to maintain the enzyme in a functional active state. Some examples of use of a sole polymer for direct electrocatalysis involving redox enzymes were recently reported [254]. Conductive polyaniline (PANi) forms a nanostructured hydrogel once deposited on an electrode [255]. The PANi hydrogel exhibits a continuously connected hierarchical 3D network with pore diameter of 60 nm, allowing a short electron diffusion length. The PANi-formate dehydrogenase electrode was efficient for catalytic reduction of CO₂ into formate. Although no exhaustive study of stability was made, conversion of CO₂ was efficient for 12 h. However, hydrogel matrices are very often poorly conductive, and conductive nanostructures or redox mediators must be co-immobilized in the gel to ensure electron conduction. Chitosan is a natural polyamino-saccharide that forms thin hydrogel films at electrodes through controlled electrodeposition process. The amine groups are available for attachment to a functionalized electrode or for anchorage of the enzyme. CNTs mixed with chitosan render the material conductive. Hosting a LAC, the so-built bioelectrode retained 70% initial current after 60 days of continuous measurement [209,256]. The same authors reported an improved bioelectrode using genipin as a cross linker. The LAC-based electrode was implanted in rats and remained operational for 167 days *in vivo* [257].

Alternatively, redox mediators can act as electron relays between the electrode and the enzyme inside the hydrogel. In the search for enzyme stabilization, Matsumoto et al. prevented leaching of a biotinylated GDH by immobilizing it into a streptavidine-hydrogel prepared by click chemistry between sortase A and PEG [258]. In the presence of a ferrocene derivative as a redox mediator, the so-designed electrode showed improved stability when compared to the electrode with no hydrogel. One issue was the weak stability of the hydrogel itself on the electrode. This last result points out one more requirement for redox enzyme-based electrode stabilization: Not only the enzyme must be stable but the interaction between the electrode and the hybrid enzyme-host matrix must also be strong enough to avoid leaching of the whole biomaterial. To ensure stability of the bioelectrode, hydrogel can be combined within porous conductive material. As an illustration, a hydrogel formed by cross-linking bovine serum albumin, GOx and arginine was interlocked within the pores of a carbon cloth [259]. Leaching of enzyme was less than 0.5% of the total amount of embedded protein within 48 h. UV-Visible spectrometry and CD demonstrated that 90% of the enzyme secondary structure was preserved in the network. In the presence of ferricyanide as a redox mediator, the current density for glucose oxidation was maintained for 25 days.

Diffusing redox mediators are however undesirable in many cases, either because they limit the rate of reaction or because they can be toxic when leaching to the environment in which the enzyme operates. Redox hydrogels, introduced 30 years ago by Adam Heller, are now widely exploited for immobilization of a variety of enzymes [260]. These hydrogels combine the advantages of a hydrated matrix ensuring protection of the enzyme and rapid diffusion of the substrate with the presence of tethered redox moieties (they can be based on osmium, ruthenium, ferrocene, cobaltocene, quinone, or viologen derivatives) that can electrically wire the enzyme by electron hopping inside the gel [261–263]. The redox potential of the hydrogel matrix can be adapted to the desired reaction to be catalyzed by tuning the ligands of the redox moieties. Ferrocene entity was tethered to linear PEI and used to cross-link GOx [264]. Of initial current, 70% and 36% was retained after 21 days of storage and 6 h of continuous operation, respectively. This marked difference underlines the effect of applied potential on the stability of the bioelectrode, an issue that we will further discuss in Section 5.3.2. Os-tethered hydrogel embedding GDH was loaded in porous MgOC deposited by ink-drop-casting on an electrode [265]. The high catalytic currents for glucose oxidation were linked to the controlled pore diameter of the MgOC matrix that allows high loading of redox polymer and rapid substrate diffusion. Moreover, the combined advantage of hydrated redox polymer and porous structure

allowed improved stability. Of initial catalytic current, 44% was recovered after 10 days of operation against 3% for the hydrogel-enzyme hybrid deposited on a glassy carbon electrode. Direct oxidation of glucose by *Corynascus thermophilus* cellobiose dehydrogenase was compared to the mediated one obtained when the CNT-based electrode was further modified by an Os-based redox hydrogel [200]. MET process generated higher catalytic currents than DET one proceeding at a lower potential through the FAD cofactor instead of the heme domain in the case of the DET process. Of the mediated electrocatalytic current, 30% remained after 9 days of CV cycling. In such configuration, it will be interesting in the future to get the comparative stability through the DET process. Last but not least, redox hydrogels have been shown in recent years to act as shields against O₂ for sensitive enzymes. This topic will be further developed below in Section 5.3.3.

5.2.5. When Aggregates or Partially Unfolded Enzymes Operate in Bioelectrocatalysis

We clearly stated in the introduction of this review that the secondary and tertiary structure of enzymes control their activity. Any change in the conformation was thus expected to modify the activity, yielding inactive states upon denaturation. We otherwise underlined that aggregated enzymes, for example in the form of CLEAs, could maintain the native conformation showing a stable, although often lower, enzymatic activity. Efforts to maintain stable enzyme electroactivity are mainly directed toward enzymes with unchanged conformations. However, and contrary to these strategies, examples of aggregates or partially unfolded forms of proteins have been reported to promote bioelectrocatalytic properties. Aggregated proteins immobilized on nanostructured carbon-based electrodes may enabled direct electrocatalysis showing enhanced stability compared to non-precipitated proteins [266,267]. Pyranose oxidase was immobilized on a CNT-based electrode via three different procedures: (i) covalent attachment (CA), (ii) enzyme coating (EC), (iii) enzyme precipitate coating (CLEA). After 34 days at room temperature, CLEA retained 65% of initial electroactivity toward glucose oxidation, while CA and EC maintained 9.2% and 26% of their initial activities, respectively. LAC aggregates were formed by computational design through production of a new dimeric interface that induces self-assembly of the protein into crystalline-like assemblies [268]. Combined with CNT incorporated in the aggregates, the bioelectrode showed high direct electroenzymatic rate for O₂ reduction with enhanced thermostability. LAC from *T. versicolor* was precipitated in the presence of Cu²⁺ yielding flower-like particles [207]. The Cu/LAC nanoflowers were integrated in carbonaceous nanomaterials and tested as catalysts for O₂ bioelectroreduction. A well-shaped direct electroenzymatic signal was observed, demonstrating the functionality of the electron pathway through CuT1 in the flower particles (Figure 12). The bioelectrode delivered 72% initial current after 6 days of daily 2 h discharge, and the H₂/O₂ fuel cell constructed based on the Cu/LAC flower-based biocathode maintained 85% initial power after 15 days of operation.

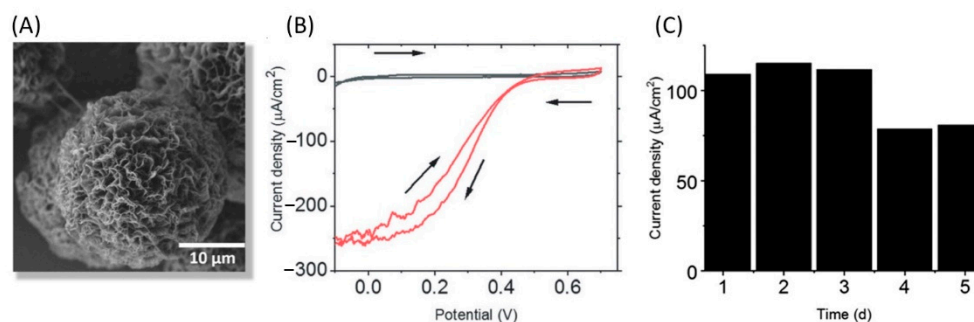


Figure 12. LAC assembled through Cu-flower like particles displays direct and stable electrocatalysis of O₂ reduction. (A) SEM image of a Cu/LAC nanoflower, (B) Catalytic reduction of O₂ (red curve) by LAC in Cu nanoflowers on CNTs, (C) Operational stability. Adapted with permission from [207].

It was also recently shown that the large sub-unit of a NiFe HASE was able to sustain H₂ oxidation by itself, showing that an incomplete structure still allows catalysis [269]. As another illustration, LAC from *Aspergillus* sp. was immobilized on Fe₂O₃ NPs [270]. Careful spectroscopic analysis, including FT-IR, fluorescence and EPR, demonstrated a partial unfolding of the protein which tends to a higher exposure of the CuT1. A large direct catalytic current in the range of 3 mA/cm² was observed, with an electrochemical CV shape denoting fast ET. However, it should be stressed that heterogeneity of enzyme population certainly exists at the electrochemical interface, and methods are now required to distinguish whether the electrochemical activity is actually linked to the unfolded proteins or to the small fraction of proteins remaining correctly folded.

5.3. Parameters Specific to Bioelectrocatalysis Stabilization

Bioelectrocatalysis implies not only the immobilization of the enzyme on a conductive support but also the application of a potential that the enzyme will sense. Hence, the stability of a bioelectrode will include the stability of the enzyme in the immobilized state and the stability of the electrocatalytic response under an electric field which is reflected in most cases by a measure of a current, a voltage or the impedance of the system. However, the variation of the electrochemical signal may have different origins. Progressive leaching of the enzymes from the electrochemical interface can explain a decrease in the catalytic current, while changes in the conformation or in the reorientation of the enzyme can explain modification in the catalytic response due to lower electron transfer rates. Methods probing the relationship between electroactivity and amount of proteins on the electrochemical interface, as well as the relationship between electroactivity and changes in enzyme conformation, are not readily available. Actually, many bioelectrocatalysis-related studies report a decrease of the catalytic current with time. This decrease has long been named as “film loss”, suggesting that enzyme leaching from the electrode would be responsible for the current evolution. However, coupling SPR and quartz crystal microbalance with dissipation (QCM-D) to electrochemistry, it was shown that other phenomena than simple enzyme desorption must account for bioelectrode instability [271,272]. In the following, we would like to emphasize some critical parameters that will affect the overall electrocatalytic response stability and the methods developed to get more insights in the overall process.

5.3.1. Reorientation of the Immobilized Enzyme

We stated just before that one key issue in order to enhance the interfacial ET between a redox enzyme and an electrode is the orientation of the enzyme on the solid surface so that the electronic relay on the surface of the protein can be positioned at a distance compatible with fast ET. In many studies reporting enzyme orientation, hydrophobic or electrostatic interactions are used to control the enzyme positioning. These interactions are relevant because they mimic *in vivo* recognition with the substrate or between redox partners. LAC, as an example, is involved in transformation of many substrates such as phenolic compounds. In accordance, the Cu T1 is engaged in a hydrophobic pocket that can be recognized by the electrode modified by phenyl or anthracenyl groups, leading to an orientation favoring efficient electron transfer [273]. The recognition between HASE and its redox partner cytochrome *c*₃ is another example illustrating electrostatic parameters to be considered in ET. By NMR docking and by resolving the Poisson–Boltzmann equation, it was established that a functional complex is formed thanks to a small negatively charged region on the HASE surface that can interact with the positively charged cytochrome. Such local electrostatic interaction was able to overcome electrostatic repulsion of the overall positive charges of the interacting proteins [274,275]. The same situation arises in bioelectrocatalysis, considering the electrode as the redox partner. Local charges are reflected by charge heterogeneity on the surface of the enzyme and rationalization can be obtained through the calculation of the dipole moment direction. This latter will depend on the pH of the enzyme environment. Hence, it can be expected that an enzyme takes an orientation favorable to ET at one pH but rotates on the electrode when the

pH of surrounding solution is modified. It is the most crucial when electrocatalysis involves proton consumption or production, as it is the case for many electroenzymatic reactions, thus inducing local changes in pH in the weakly buffered solution and potential modification of the catalytic signal.

Evidence of the rotation of BOD was demonstrated on gold electrodes modified by thiol-based SAMs [116]. Both the pH at which the enzyme was adsorbed and the pH of the electrolytic solution were varied. By doing so, not only the charge of the electrode but also the charge of the enzyme varied. Coupling electrochemistry to ellipsometry, SPR, and Phase Modulation Infrared Reflection Absorption Spectroscopy (PMIRRAS), it was shown that the global charge of the protein controls the amount of adsorbed molecules as a function of electrostatic interactions tuned by the pH of adsorption. It was also demonstrated that the local charge in the vicinity of the CuT1 controls the orientation of the enzyme, hence the catalytic current for O₂ reduction. Hence, when the amount of enzyme and its orientation were a priori fixed by adsorption at a fixed pH, the catalytic current recorded in buffers of various pHs nevertheless varied following rotation of the enzyme to adopt the most favorable orientation. It was clearly shown that orientation could be reversibly tuned by changing the pH of the electrolyte, shifting the catalysis from a slow ET rate to a fast one (Figure 13).

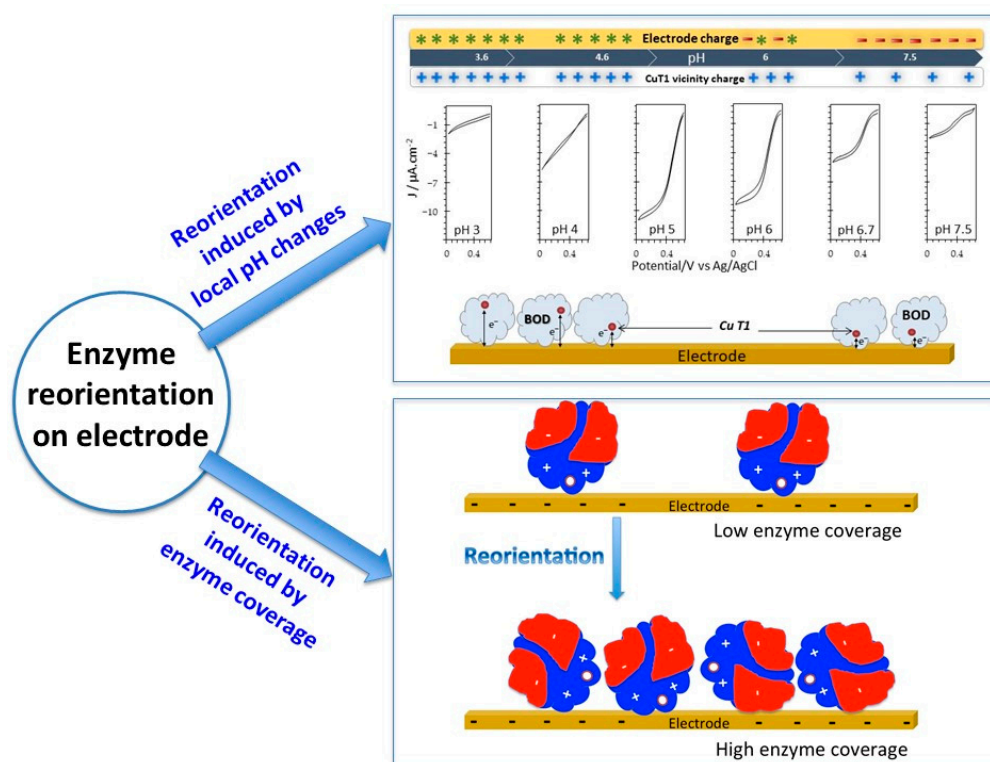


Figure 13. Reorientation of enzymes on electrode may alter enzyme stability. **(Top)** Tuning the pH of the electrolyte induces rotation of the adsorbed bilirubin oxidase on the electrode surface, hence induces modification in bioelectrocatalysis for O₂ reduction. Adapted with permission from [116]. **(Down)** Scheme of the reorientation of enzymes on an electrode induced by surface coverage. The white sphere represents the active site. Adapted with permission from [115].

Enzyme reorientation, leading to potential bioelectrocatalysis instability, may have another origin. In the course of protein adsorption, protein-protein interactions are increasingly dominating. Hence, while the adsorption of the first proteins in a favorable orientation for ET can be controlled by electrostatic interactions, the interactions between neighboring adsorbed proteins may induce reorientation to decrease the repulsive forces [115] (Figure 13). Coupling electrochemistry to QCM and interferometry for studying O₂ reduc-

tion by BOD on a gold electrode, Blanford et al. clearly demonstrated that an optimum surface coverage exists yielding the highest stable electrocatalytic current [276]. Although proof of enzyme reorientation was not provided, QCM-D allowed to conclude that this optimum was linked to a balance between rate of enzyme adsorption and deformation.

5.3.2. Effect of the Electric Field

Compared to other catalytic processes, the special feature of bioelectrocatalysis lies in the electric field imposed at the electrode interface. Although partially shielded by the ions present in the solution, the extent of the electric field can still reach the size of immobilized enzymes, especially in weakly supported electrolytes. It should be expected to have a major impact, but only few studies report the effect of the electric field on enzyme or bioelectrode stability. This lack of information most probably comes from the difficulty to determine which effect among protein leaching, denaturation or reformation can be responsible for any variation in the electrocatalytic response. The recent use of coupled methods with electrochemistry will certainly lead to major advancements in that field. Adsorption of MCOs on planar gold electrodes was taken as a model for such studies. It was shown using electrochemistry coupled to QCM-D that cycling the potential for O₂ reduction by *M. verrucaria* BOD accelerated mass decrease compared to applying a fixed potential [272]. It was hypothesized that varying the electric field near the surface may distort the adsorbed protein, expelling water and contributing to enzyme denaturation. It was further shown with the same enzyme that continuous cycling induced more stability of the bioelectrode than cycling during a same period but at regular intervals, the electrode being at the open circuit potential (OCP) when not cycling [116]. This result suggests a much lower stability of the bioelectrode when the applied potential was close to the OCP. Considering the potential of zero charge (E_{pzc}) of the electrode, it could be concluded that the strong electric field generated when holding the potential far away from E_{pzc} induced bioelectrode destabilization. Kano's group rationalized these experimental data by modeling the electrostatic interactions between enzymes and electrodes in the electric double layer [275]. Taking the copper efflux oxidase (CueO) enzyme as a model enzyme adsorbed either at bare or butanethiol-modified gold electrodes, the authors demonstrated how the electrical double layer plays a key role in enzyme stability for bioelectrocatalysis. It can be argued that the diameter of the enzyme is much higher than the length of the electrical double layer (5 nm vs. 1 nm at a typical ionic strength for electrocatalysis). However, the domain of CueO facing the electrode is indeed located in the double layer and will face an electric field whose force depends on the applied potential and on the E_{pzc} of the electrode. Hence, at the bare gold electrode, the strong electric field induced by an applied potential much more positive than E_{pzc} of the electrode, in addition to the complementary charges chosen to favor DET orientation, leads to denaturation of the protein.

Heterogeneity of the electric field inside the pores of a porous matrix otherwise affects enzyme stabilization. A model developed in the group of Kano demonstrated the existence of an inner pore region where the electric field remains low, and where weak electrostatic forces help in protein stabilization [238,277,278]. The higher electric field at the entry of the pore should enhance the ET, while inducing less stability [279,280]. This effect known as the "edge effect" was recognized early in the history of bioelectrochemical studies using cytochrome *c* and graphite and may explain efficient bioelectrocatalysis at carbon nanofibers (CNFs) [281–284].

Finally, it should be mentioned the role of the electric field sensed by the enzyme within the course of mediated electrocatalysis against direct electrocatalysis. A relevant example is bioelectrocatalytic oxidation of hydrogen by HASEs. It is known that HASEs are reversibly inactivated at high potentials [285]. In a typical cyclic voltammetry experiment where the enzyme is adsorbed on an electrode, this inactivation results in a decrease in the catalytic current in the forward scan at a potential higher than ca. -0.4 V vs. Ag/AgCl at pH 7. Current recovers when the potential is reversed. It was shown that pushing the potential

to even more positive values induces an irreversible inactivation of the enzyme [286]. Such inactivation process may have consequences on the operation of fuel cells using HASE as anode catalyst, requiring regular steps of reducing voltages to reactivate the enzyme. Alternatively, it was shown that embedding the hydrogenase in a viologen-based hydrogel protected the enzyme from high potential deactivation. In this MET process, the enzyme no longer senses the high potential of the electrode but the potential of the viologen redox couple which is sufficiently negative to prevent HASE inactivation [287–289]. Nevertheless, the use of redox mediators induces other detrimental effects towards enzyme stability, such as production of reactive oxygen species (ROS) that will be discussed in the next section.

5.3.3. Protection against Reactive Oxygen Species (ROS) Production

Two electron reduction of O_2 yields the formation of unstable superoxide $O_2^{\bullet-}$ which is the precursor for other reactive species including H_2O_2 and $\bullet OH$. Incomplete oxygen reduction can be encountered in the course of certain enzymatic reactions, or when O_2 is directly reduced at an electrochemical interface. A relevant example of ROS produced by enzymatic reactions is the oxidation of sugars by the flavin-based GOx. Here, O_2 is a co-substrate of the enzyme and is reduced to H_2O_2 after the release of D-glucono- δ -lactone within glucose oxidation [290]. Identically, oxidation of lactate-by-lactate oxidase produces H_2O_2 . To avoid any detrimental effect of H_2O_2 , one solution is to electroenzymatically reduce this latter by peroxidases [291]. Alternatively, catalase has been used to decompose H_2O_2 [292]. Engineering of flavoproteins is also largely reported to decrease O_2 activity [293,294]. Such strategy is particularly useful when the flavoprotein is embedded in redox hydrogels, where the competition between reaction of the enzyme with the redox mediator or O_2 occurs within the polymer, decreasing the efficiency of the bioelectrocatalysis. An additional issue comes from the reduction of O_2 directly by the redox entities of the polymer.

Reactions other than the oxidation of sugar by GOx embedded in Os-based polymers can expose enzymes to ROS. Actually, low potential viologen-based redox polymers developed to protect HASEs against high potential inactivation also serve as shields against O_2 [224,237,288]. However, the viologen-based matrix itself may generate ROS in the course of the HASE protection mechanism, inducing its progressive decomposition [295]. To tackle this issue, a top polymer layer containing both GOx and catalase was used to ensure a complete HASE protection [143]. Alternatively, iodide was added in the whole system to induce dismutation of H_2O_2 . An improvement of the half-life of the HASE in the presence of O_2 was demonstrated [295]. In the case of O_2 -tolerant HASEs, their specific sensitivity/tolerance to O_2 has been shown to lead to an even greater sensitivity to ROS. Hence, it was reported that ROS formed by applying low potentials to a HASE-based carbon felt electrode in the presence of O_2 irreversibly deactivated the enzyme contrary to reversible O_2 inactivation [111,198] (Figure 14). In this case, a protective upper layer composed of a 3D porous carbon matrix increased the stability by 4–6 times against ROS compared to a 2D electrode. It was proposed that the 3D matrix could scavenge ROS before reaching the enzymes inside the pores.

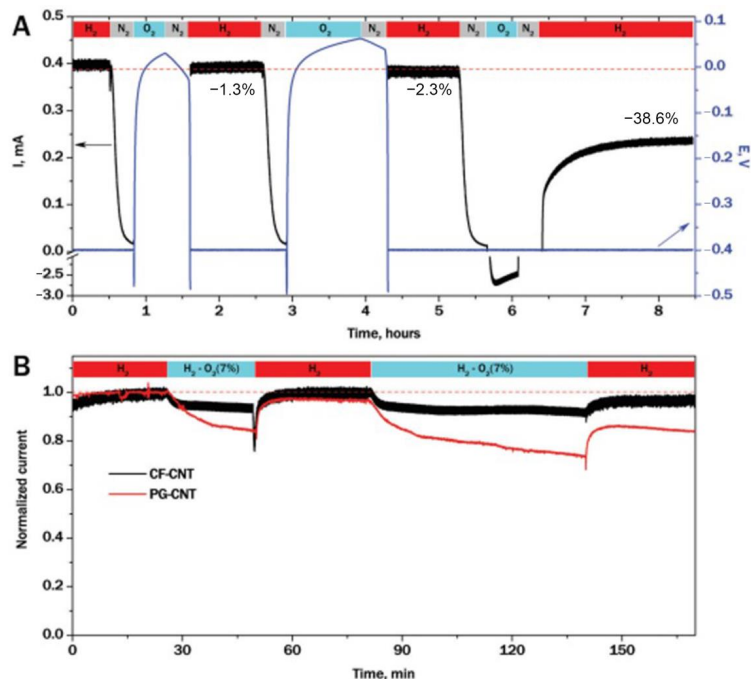


Figure 14. Chronoamperometric response for H_2 oxidation by *A. aeolicus* HASE embedded in a CNT-modified carbon felt electrode showing the inactivation of the enzyme by ROS electrochemically produced (A) and protection by a porous matrix (B). Reproduced with permission from [198].

6. Conclusions and Future Directions

Electrocatalysis involving redox enzymes takes advantage of the high selectivity and affinity of the biomolecules, as well as the large diversity of identified enzymes, hence a large variety of substrates. Possible applications range from implantable medical devices (insulin pump, neurological stimulator, artificial organs, etc.), wearable sensors, and environmental diagnostic to energy converting devices or CO_2 capture [16,17,296–299]. Many strategies are available to enhance enzyme stability in general. However, the specificity of redox enzymes that sense an electric field and require a controlled orientation to operate on electrochemical interfaces makes the stability of redox enzymes one of the most important issues to resolve before a large-scale commercial development of bioelectrocatalysis. The search for a good balance between stability and activity of enzymes is a prerequisite, even complexified by the search for efficient ET in the case of redox enzymes. Recent examples in the literature concerning MCOs revealed the difficulty of getting improved interfacial ET parameters or improved redox properties while maintaining both the stability and the activity of the enzyme [300,301]. No doubt that protein engineering, which is increasingly carried out with the aid of innovative solutions based on emerging genetic tools, will offer new opportunities of producing stable enzymes. There is also no doubt that the screening of the biodiversity will allow the discovery of redox enzymes with outstanding properties, which can be applied either directly in bioelectrochemical devices, or as model enzymes for protein engineering for high stability.

Alternative strategies can be envisioned in case enzyme stability is limiting the targeted device. The first one would be to refresh the bioelectrodes regularly, so as to renew inactivated enzymes by new active ones. Increasing salt concentration in the medium was reported to allow LAC desorption, rendering the electrode available for fresh enzyme adsorption [209]. Refreshment of the bioelectrode can also be done by adsorbing the enzyme on magnetic nanoparticles [302]. Applying a suitable magnetic field may allow assembling or release of the biocatalyst on the electrode. Cosnier et al. proposed to use enzymes and redox mediators encapsulated in glyconanoparticles, both diffusing in solution [303]. This strategy was supposed to allow protein and mediators to freely rotate for an efficient ET and to offer in addition the possibility of easy refreshing of the biocatalyst

by a simple exchange of the solutions. Although suitable to overcome enzyme instability, these procedures based on enzyme renewal, however, do not appear to be sustainable or cost effective. Nanozymes, or bioinspired catalysts, could be desirable alternatives to enzymes in the future [304–307]. Taking benefit of the fundamental understanding of bioelectrocatalysis, these synthetic catalysts may provide higher stability while operating the closest to the enzymatic catalysis.

Should redox enzymes or biosynthetic catalysts be used, novel methodologies must be developed in order to get new insights in the parameters that limit the stability of bioelectrocatalysis. *In situ* and *in operando* methods are certainly the most appealing within the objective of understanding and enhancing bioelectrode stability [308,309]. Recent reviews by Reisner et al. and by Crespilho et al. discussed various methods, and especially coupled methods, currently available to study bioelectrode interfaces [309,310]. Methods allowing mass or layer thickness quantification, i.e., SPR, QCM-D and ellipsometry, coupled to electrochemistry will give access to the relationship between enzyme loading or release and catalytic response [21,116,271,272,311]. Electrochemistry coupled to spectroscopies (IR (including SEIRA, PMIRRAS), XAS, fluorescence, Raman (including SERRS), EPR, CD, mass spectrometry) will help in the determination of conformational change once enzyme is immobilized or as a function of applied potential or current [312–317]. Microscopy coupled to electrochemistry will allow the mapping of the electrocatalysis [318–320]. Finally, getting more and more accurate experimental data on enzyme behavior on electrodes may be implemented in theoretical models that in return will help in bioelectrode rationalization [21,117,321–323].

Author Contributions: Writing, C.B.; review and editing, H.-M.M., A.d.P. and I.M.; writing, editing, and supervision, E.L. All authors have read and agreed to the published version of the manuscript.

Funding: This work was supported by ANR (ENZYMOR-ANR-16-CE05-0024). H-M Man grant was funded by Région PACA, France, Centre National de la Recherche Scientifique, CNRS, France and Hyseas company, Cannes, France. C. Beaufils grant was funded by Aix-Marseille University and by “Agence Innovation Defense” of the French army ministry.

Conflicts of Interest: The authors declare no conflict of interest.

References

1. Woodley, J.M. New frontiers in biocatalysis for sustainable synthesis. *Curr. Opin. Green Sustain. Chem.* **2020**, *21*, 22–26. [[CrossRef](#)]
2. Reetz, M.T. What are the Limitations of Enzymes in Synthetic Organic Chemistry? *Chem. Rec.* **2016**, *16*, 2449–2459. [[CrossRef](#)] [[PubMed](#)]
3. Hauer, B. Embracing Nature’s Catalysts: A Viewpoint on the Future of Biocatalysis. *ACS Catal.* **2020**, *10*, 8418–8427. [[CrossRef](#)]
4. Bommarius, A.S.; Paye, M.F. Stabilizing biocatalysts. *Chem. Soc. Rev.* **2013**, *42*, 6534–6565. [[CrossRef](#)] [[PubMed](#)]
5. Mandpe, P.; Prabhakar, B.; Gupta, H.; Shende, P. Glucose oxidase-based biosensor for glucose detection from biological fluids. *Sens. Rev.* **2020**, *40*, 497–511. [[CrossRef](#)]
6. Mano, N.; de Poulpique, A. O₂ Reduction in Enzymatic Biofuel Cells. *Chem. Rev.* **2018**, *118*, 2392–2468. [[CrossRef](#)] [[PubMed](#)]
7. Lojou, E. Hydrogenases as catalysts for fuel cells: Strategies for efficient immobilization at electrode interfaces. *Electrochim. Acta* **2011**, *56*, 10385–10397. [[CrossRef](#)]
8. Lubitz, W.; Ogata, H.; Rudiger, O.; Reijerse, E. Hydrogenases. *Chem. Rev.* **2014**, *114*, 4081–4148. [[CrossRef](#)]
9. Alfano, M.; Cavazza, C. Structure, function, and biosynthesis of nickel-dependent enzymes. *Protein Sci.* **2020**, *29*, 1071–1089. [[CrossRef](#)]
10. Najafpour, M.M.; Zaharieva, I.; Zand, Z.; Hosseini, S.M.; Kouzmanova, M.; Holynska, M.; Tranca, I.; Larkum, A.W.; Shen, J.R.; Allakhverdiev, S.I. Water-oxidizing complex in Photosystem II: Its structure and relation to Manganese-oxide based catalysts. *Coord. Chem. Rev.* **2020**, *409*. [[CrossRef](#)]
11. Morello, G.; Megarity, C.F.; Armstrong, F.A. The power of electrified nanoconfinement for energising, controlling and observing long enzyme cascades. *Nat. Commun.* **2021**, *12*, 340. [[CrossRef](#)] [[PubMed](#)]
12. Stolarczyk, K.; Rogalski, J.; Bilewicz, R. NAD(P)-dependent glucose dehydrogenase: Applications for biosensors, bioelectrodes, and biofuel cells. *Bioelectrochemistry* **2020**, *135*, 107574. [[CrossRef](#)] [[PubMed](#)]
13. Alvarez-Malmagro, J.; Garcia-Molina, G.; De Lacey, A.L. Electrochemical Biosensors Based on Membrane-Bound Enzymes in Biomimetic Configurations. *Sensors* **2020**, *20*, 3393. [[CrossRef](#)] [[PubMed](#)]

14. Bollella, P.; Katz, E. Bioelectrocatalysis at carbon nanotubes. In *Methods in Enzymology: Nanoarmoring of Enzymes with Carbon Nanotubes and Magnetic Nanoparticles*; Kumar, C.V., Pyle, A.M., Christianson, D.W., Eds.; Elsevier: Amsterdam, The Netherlands, 2020; Volume 630, pp. 215–247.
15. Wu, R.R.; Ma, C.L.; Zhu, Z.G. Enzymatic electrosynthesis as an emerging electrochemical synthesis platform. *Curr. Opin. Electrochem.* **2020**, *19*, 1–7. [[CrossRef](#)]
16. Yuan, M.W.; Kummer, M.J.; Minteer, S.D. Strategies for Bioelectrochemical CO₂ Reduction. *Chem. A Eur. J.* **2019**, *25*, 14258–14266. [[CrossRef](#)]
17. Mazurenko, I.; Wang, X.; de Poulpiquet, A.; Lojou, E. H-2/O-2 enzymatic fuel cells: From proof-of-concept to powerful devices. *Sustain. Energy Fuels* **2017**, *1*, 1475–1501. [[CrossRef](#)]
18. Xiao, X.X.; Xia, H.Q.; Wu, R.R.; Bai, L.; Yan, L.; Magner, E.; Cosnier, S.; Lojou, E.; Zhu, Z.G.; Liu, A.H. Tackling the Challenges of Enzymatic (Bio)Fuel Cells. *Chem. Rev.* **2019**, *119*, 9509–9558. [[CrossRef](#)] [[PubMed](#)]
19. Mazurenko, I.; de Poulpiquet, A.; Lojou, E. Recent developments in high surface area bioelectrodes for enzymatic fuel cells. *Curr. Opin. Electrochem.* **2017**, *5*, 74–84. [[CrossRef](#)]
20. Mazurenko, I.; Hitaishi, V.P.; Lojou, E. Recent advances in surface chemistry of electrodes to promote direct enzymatic bioelectrocatalysis. *Curr. Opin. Electrochem.* **2020**, *19*, 113–121. [[CrossRef](#)]
21. Hitaishi, V.P.; Clement, R.; Bourassin, N.; Baaden, M.; de Poulpiquet, A.; Sacquin-Mora, S.; Ciaccafava, A.; Lojou, E. Controlling Redox Enzyme Orientation at Planar Electrodes. *Catalysts* **2018**, *8*, 192. [[CrossRef](#)]
22. Iyer, P.V.; Ananthanarayan, L. Enzyme stability and stabilization—Aqueous and non-aqueous environment. *Process Biochemistry* **2008**, *43*, 1019–1032. [[CrossRef](#)]
23. Balcao, V.M.; Vila, M. Structural and functional stabilization of protein entities: State-of-the-art. *Adv. Drug Deliv. Rev.* **2015**, *93*, 25–41. [[CrossRef](#)] [[PubMed](#)]
24. Polizzi, K.M.; Bommarius, A.S.; Broering, J.M.; Chaparro-Riggers, J.F. Stability of biocatalysts. *Curr. Opin. Chem. Biol.* **2007**, *11*, 220–225. [[CrossRef](#)] [[PubMed](#)]
25. Gianfreda, L.; Scarfi, M.R. Enzyme Stabilization—State-Of-The-Art. *Mol. Cell. Biochem.* **1991**, *100*, 97–128. [[CrossRef](#)] [[PubMed](#)]
26. Stepankova, V.; Bidmanova, S.; Koudelakova, T.; Prokop, Z.; Chaloupkova, R.; Damborsky, J. Strategies for Stabilization of Enzymes in Organic Solvents. *ACS Catal.* **2013**, *3*, 2823–2836. [[CrossRef](#)]
27. Lalande, M.; Schwob, L.; Vizcaino, V.; Chirot, F.; Dugourd, P.; Schlatholter, T.; Pouilly, J.C. Direct Radiation Effects on the Structure and Stability of Collagen and Other Proteins. *Chembiochem* **2019**. [[CrossRef](#)]
28. Doster, W.; Settles, M. Protein-water displacement distributions. *Biochim. Biophys. Acta Proteins Proteom.* **2005**, *1749*, 173–186. [[CrossRef](#)]
29. Miyawaki, O. Hydration state change of proteins upon unfolding in sugar solutions. *Biochim. Biophys. Acta Proteins Proteom.* **2007**, *1774*, 928–935. [[CrossRef](#)] [[PubMed](#)]
30. Ganjalikhany, M.R.; Ranjbar, B.; Hosseinkhani, S.; Khalifeh, K.; Hassani, L. Roles of trehalose and magnesium sulfate on structural and functional stability of firefly luciferase. *J. Mol. Catal. B Enzym.* **2010**, *62*, 127–132. [[CrossRef](#)]
31. Haque, I.; Singh, R.; Moosavi-Movahedi, A.A.; Ahmad, F. Effect of polyol osmolytes on Delta G(D), the Gibbs energy of stabilisation of proteins at different pH values. *Biophys. Chem.* **2005**, *117*, 1–12. [[CrossRef](#)] [[PubMed](#)]
32. Tiwari, A.; Bhat, R. Stabilization of yeast hexokinase A by polyol osmolytes: Correlation with the physicochemical properties of aqueous solutions. *Biophys. Chem.* **2006**, *124*, 90–99. [[CrossRef](#)] [[PubMed](#)]
33. Wlodarczyk, S.R.; Costa-Silva, T.A.; Pessoa, A.; Madeira, P.; Monteiro, G. Effect of osmolytes on the activity of anti-cancer enzyme L-Asparaginase II from *Erwinia chrysanthemi*. *Process Biochem.* **2019**, *81*, 123–131. [[CrossRef](#)]
34. Chen, G.; Zhang, Q.P.; Lu, Q.Y.; Feng, B. Protection effect of polyols on *Rhizopus chinensis* lipase counteracting the deactivation from high pressure and high temperature treatment. *Int. J. Biol. Macromol.* **2019**, *127*, 555–562. [[CrossRef](#)]
35. Pazhang, M.; Mardi, N.; Mehrnejad, F.; Chaparzadeh, N. The combinatorial effects of osmolytes and alcohols on the stability of pyrazinamidase: Methanol affects the enzyme stability through hydrophobic interactions and hydrogen bonds. *Int. J. Biol. Macromol.* **2018**, *108*, 1339–1347. [[CrossRef](#)]
36. Khan, M.V.; Ishtikhar, M.; Rabbani, G.; Zaman, M.; Abdelhameed, A.S.; Khan, R.H. Polyols (Glycerol and Ethylene glycol) mediated amorphous aggregate inhibition and secondary structure restoration of metalloproteinase-conalbumin (ovotransferrin). *Int. J. Biol. Macromol.* **2017**, *94*, 290–300. [[CrossRef](#)]
37. Kaushik, J.K.; Bhat, R. Why is trehalose an exceptional protein stabilizer? An analysis of the thermal stability of proteins in the presence of the compatible osmolyte trehalose. *J. Biol. Chem.* **2003**, *278*, 26458–26465. [[CrossRef](#)]
38. Silva, C.; Martins, M.; Jing, S.; Fu, J.J.; Cavaco-Paulo, A. Practical insights on enzyme stabilization. *Crit. Rev. Biotechnol.* **2018**, *38*, 335–350. [[CrossRef](#)]
39. Scharnagl, C.; Reif, M.; Friedrich, J. Local compressibilities of proteins: Comparison of optical experiments and simulations for horse heart cytochrome-c. *Biophys. J.* **2005**, *89*, 64–75. [[CrossRef](#)]
40. Mangiagalli, M.; Carvalho, H.; Natalello, A.; Ferrario, V.; Pennati, M.L.; Barbiroli, A.; Lotti, M.; Pleiss, J.; Brocca, S. Diverse effects of aqueous polar co-solvents on *Candida antarctica* lipase B. *Int. J. Biol. Macromol.* **2020**, *150*, 930–940. [[CrossRef](#)]
41. Mukherjee, A.; Sarkar, S.; Gupta, S.; Banerjee, S.; Senapati, S.; Chakrabarty, R.; Gachhui, R. DMSO strengthens chitin deacetylase-chitin interaction: Physicochemical, kinetic, structural and catalytic insights. *Carbohydr. Polym.* **2019**, *223*. [[CrossRef](#)] [[PubMed](#)]

42. Woll, A.K.; Hubbuch, J. Investigation of the reversibility of freeze/thaw stress-induced protein instability using heat cycling as a function of different cryoprotectants. *Bioprocess Biosyst. Eng.* **2020**, *43*, 1309–1327. [[CrossRef](#)] [[PubMed](#)]
43. Dal Magro, L.; Kordecki, J.F.; Klein, M.P.; Rodrigues, R.C.; Fernandez-Lafuente, R. Stability/activity features of the main enzyme components of rohapect 10L. *Biotechnol. Prog.* **2019**, *35*. [[CrossRef](#)] [[PubMed](#)]
44. Nolan, V.; Collin, A.; Rodriguez, C.; Perillo, M.A. Effect of Polyethylene Glycol-Induced Molecular Crowding on the Enzymatic Activity and Thermal Stability of beta-Galactosidase from *Kluyveromyces lactis*. *J. Agric. Food Chem.* **2020**, *68*, 8875–8882. [[CrossRef](#)] [[PubMed](#)]
45. Jain, E.; Flanagan, M.; Sheth, S.; Patel, S.; Gan, Q.; Patel, B.; Montano, A.M.; Zustiak, S.P. Biodegradable polyethylene glycol hydrogels for sustained release and enhanced stability of rhGALNS enzyme. *Drug Deliv. Transl. Res.* **2020**, *10*, 1341–1352. [[CrossRef](#)]
46. Sasahara, K.; McPhie, P.; Minton, A.P. Effect of dextran on protein stability and conformation attributed to macromolecular crowding. *J. Mol. Biol.* **2003**, *326*, 1227–1237. [[CrossRef](#)]
47. Kuchler, A.; Yoshimoto, M.; Luginbuhl, S.; Mavelli, F.; Walde, P. Enzymatic reactions in confined environments. *Nat. Nanotechnol.* **2016**, *11*, 409–420. [[CrossRef](#)]
48. Li, J.H.; Zheng, H.Y.; Feng, C.J. Effect of Macromolecular Crowding on the FMN-Herpe Intraprotein Electron Transfer in Inducible NO Synthase. *Biochemistry* **2019**, *58*, 3087–3096. [[CrossRef](#)]
49. Shahid, S.; Hassan, M.I.; Islam, A.; Ahmad, F. Size-dependent studies of macromolecular crowding on the thermodynamic stability, structure and functional activity of proteins: In vitro and in silico approaches. *Biochim. Et Biophys. Acta-Gen. Subj.* **2017**, *1861*, 178–197. [[CrossRef](#)]
50. Christiansen, A.; Wang, Q.; Samiotakis, A.; Cheung, M.S.; Wittung-Stafshede, P. Factors Defining Effects of Macromolecular Crowding on Protein Stability: An In Vitro/in Silico Case Study Using Cytochrome c. *Biochemistry* **2010**, *49*, 6519–6530. [[CrossRef](#)]
51. Timasheff, S.N. Protein-solvent preferential interactions, protein hydration, and the modulation of biochemical reactions by solvent components. *Proc. Natl. Acad. Sci. USA* **2002**, *99*, 9721–9726. [[CrossRef](#)]
52. Hasan, S.; Isar, M.; Naeem, A. Macromolecular crowding stabilises native structure of alpha-chymotrypsinogen-A against hexafluoropropanol-induced aggregates. *Int. J. Biol. Macromol.* **2020**. [[CrossRef](#)] [[PubMed](#)]
53. Ghosh, S.; Shahid, S.; Raina, N.; Ahmad, F.; Hassan, M.I.; Islam, A. Molecular and macromolecular crowding-induced stabilization of proteins: Effect of dextran and its building block alone and their mixtures on stability and structure of lysozyme. *Int. J. Biol. Macromol.* **2020**, *150*, 1238–1248. [[CrossRef](#)] [[PubMed](#)]
54. Baykal, E.; Vardar, G.; Attar, A.; Yapaoz, M.A. Complexes of glucose oxidase with chitosan and dextran possessing enhanced stability. *Prep. Biochem. Biotechnol.* **2020**, *50*, 572–577. [[CrossRef](#)] [[PubMed](#)]
55. Das, N.; Sen, P. Size-dependent macromolecular crowding effect on the thermodynamics of protein unfolding revealed at the single molecular level. *Int. J. Biol. Macromol.* **2019**, *141*, 843–854. [[CrossRef](#)] [[PubMed](#)]
56. Mittal, S.; Chowhan, R.K.; Singh, L.R. Macromolecular crowding: Macromolecules friend or foe. *Biochim. Et Biophys. Acta-Gen. Subj.* **2015**, *1850*, 1822–1831. [[CrossRef](#)] [[PubMed](#)]
57. Lavelle, L.; Fresco, J.R. Stabilization of nucleic acid triplexes by high concentrations of sodium and ammonium salts follows the Hofmeister series. *Biophys. Chem.* **2003**, *105*, 681–699. [[CrossRef](#)]
58. Okur, H.I.; Hladilkova, J.; Rembert, K.B.; Cho, Y.; Heyda, J.; Dzubiella, J.; Cremer, P.S.; Jungwirth, P. Beyond the Hofmeister Series: Ion-Specific Effects on Proteins and Their Biological Functions. *J. Phys. Chem. B* **2017**, *121*, 1997–2014. [[CrossRef](#)] [[PubMed](#)]
59. Hofmeister, F. Zur Lehre von der Wirkung der Salze. *Arch. Exp. Pathol. Pharmacol.* **1888**, *24*, 247–260. [[CrossRef](#)]
60. Salis, A.; Ninham, B.W. Models and mechanisms of Hofmeister effects in electrolyte solutions, and colloid and protein systems revisited. *Chem. Soc. Rev.* **2014**, *43*, 7358–7377. [[CrossRef](#)]
61. Ghobadi, R.; Divsalar, A. Enzymatic behavior of bovine liver catalase in aqueous medium of sugar based deep eutectic solvents. *J. Mol. Liq.* **2020**, *310*. [[CrossRef](#)]
62. Usoltsev, D.; Sitnikova, V.; Kajava, A.; Uspenskaya, M. FTIR Spectroscopy Study of the Secondary Structure Changes in Human Serum Albumin and Trypsin under Neutral Salts. *Biomolecules* **2020**, *10*, 606. [[CrossRef](#)] [[PubMed](#)]
63. Sedlak, E.; Sedlakova, D.; Marek, J.; Hancar, J.; Garajova, K.; Zoldak, G. Ion-Specific Protein/Water Interface Determines the Hofmeister Effect on the Kinetic Stability of Glucose Oxidase. *J. Phys. Chem. B* **2019**, *123*, 7965–7973. [[CrossRef](#)] [[PubMed](#)]
64. Garajova, K.; Balogova, A.; Dusekova, E.; Sedlakova, D.; Sedlak, E.; Varhac, R. Correlation of lysozyme activity and stability in the presence of Hofmeister series anions. *Biochim. Biophys. Acta Proteins Proteom.* **2017**, *1865*, 281–288. [[CrossRef](#)] [[PubMed](#)]
65. Nemoto, M.; Sugihara, K.; Adachi, T.; Murata, K.; Shiraki, K.; Tsujimura, S. Effect of Electrolyte Ions on the Stability of Flavin Adenine Dinucleotide-Dependent Glucose Dehydrogenase. *Chemelectrochem* **2019**, *6*, 1028–1031. [[CrossRef](#)]
66. Hani, F.M.; Cole, A.E.; Altman, E. The ability of salts to stabilize proteins in vivo or intracellularly correlates with the Hofmeister series of ions. *Int. J. Biochem. Mol. Biol.* **2019**, *10*, 23–31.
67. Banerjee, S.; Arora, A.; Vijayaraghavan, R.; Patti, A.F. Extraction and crosslinking of bromelain aggregates for improved stability and reusability from pineapple processing waste. *Int. J. Biol. Macromol.* **2020**, *158*, 318–326. [[CrossRef](#)]
68. Kulkarni, N.H.; Muley, A.B.; Bedade, D.K.; Singhal, R.S. Cross-linked enzyme aggregates of arylamidase from *Cupriavidus oxalaticus* ICTDB921: Process optimization, characterization, and application for mitigation of acrylamide in industrial wastewater. *Bioprocess Biosyst. Eng.* **2020**, *43*, 457–471. [[CrossRef](#)]

69. Mayolo-Delouis, K.; Gonzalez-Gonzalez, M.; Simental-Martinez, J.; Rito-Palomares, M. Aldehyde PEGylation of laccase from *Trametes versicolor* in route to increase its stability: Effect on enzymatic activity. *J. Mol. Recognit.* **2015**, *28*, 173–179. [[CrossRef](#)]
70. El-Sayed, A.S.A.; Shindia, A.A.; Abou Zeid, A.A.; Yassin, A.M.; Sitohy, M.Z.; Sitohy, B. Aspergillus nidulans thermostable arginine deiminase-Dextran conjugates with enhanced molecular stability, proteolytic resistance, pharmacokinetic properties and anticancer activity. *Enzym. Microb. Technol.* **2019**, *131*. [[CrossRef](#)]
71. Veronese, F.M. Peptide and protein PEGylation: A review of problems and solutions. *Biomaterials* **2001**, *22*, 405–417. [[CrossRef](#)]
72. Huang, H.F.; Fang, L.; Xue, L.; Zhang, T.; Kim, K.B.; Hou, S.R.; Zheng, F.; Zhan, C.G. PEGylation but Not Fc-Fusion Improves in Vivo Residence Time of a Thermostable Mutant of Bacterial Cocaine Esterase. *Bioconjugate Chem.* **2019**, *30*, 3021–3027. [[CrossRef](#)]
73. Cummings, C.; Murata, H.; Koepsel, R.; Russell, A.J. Tailoring enzyme activity and stability using polymer-based protein engineering. *Biomaterials* **2013**, *34*, 7437–7443. [[CrossRef](#)] [[PubMed](#)]
74. Chung, S.F.; Kim, C.F.; Kwok, S.Y.; Tam, S.Y.; Chen, Y.W.; Chong, H.C.; Leung, S.L.; So, P.K.; Wong, K.Y.; Leung, Y.C.; et al. Mono-PEGylation of a Thermostable Arginine-Depleting Enzyme for the Treatment of Lung Cancer. *Int. J. Mol. Sci.* **2020**, *21*, 4234. [[CrossRef](#)] [[PubMed](#)]
75. Kovaliov, M.; Zhang, B.; Konkolewicz, D.; Szczesniak, K.; Jurga, S.; Averick, S. Polymer grafting from a metallo-centered enzyme improves activity in non-native environments. *Poly. Int.* **2020**. [[CrossRef](#)]
76. Ritter, D.W.; Newton, J.M.; McShane, M.J. Modification of PEGylated enzyme with glutaraldehyde can enhance stability while avoiding intermolecular crosslinking. *RSC Adv.* **2014**, *4*, 28036–28040. [[CrossRef](#)]
77. Sharma, A.; Gupta, G.; Ahmad, T.; Mansoor, S.; Kaur, B. Enzyme Engineering: Current Trends and Future Perspectives. *Food Rev. Int.* **2021**. [[CrossRef](#)]
78. Korendovych, I.V. Rational and Semirational Protein Design. *Methods Mol. Biol.* **2018**, *1685*, 15–23. [[CrossRef](#)]
79. de Moraes, M.A.B.; Polo, C.C.; Domingues, M.N.; Persinoti, G.F.; Pirolla, R.A.S.; de Souza, F.H.M.; Correa, J.B.D.; dos Santos, C.R.; Murakami, M.T. Exploring the Molecular Basis for Substrate Affinity and Structural Stability in Bacterial GH39 beta-Xylosidases. *Front. Bioeng. Biotechnol.* **2020**, *8*. [[CrossRef](#)]
80. Ito, Y.; Ikeuchi, A.; Imamura, C. Advanced evolutionary molecular engineering to produce thermostable cellulase by using a small but efficient library. *Protein Eng. Des. Sel.* **2013**, *26*, 73–79. [[CrossRef](#)] [[PubMed](#)]
81. Minges, H.; Schnepel, C.; Bottcher, D.; Weiss, M.S.; Spross, J.; Bornscheuer, U.T.; Sewald, N. Targeted Enzyme Engineering Unveiled Unexpected Patterns of Halogenase Stabilization. *Chemcatchem* **2020**, *12*, 818–831. [[CrossRef](#)]
82. Bulut, H.; Yuksel, B.; Gul, M.; Eren, M.; Karatas, E.; Kara, N.; Yilmazer, B.; Kocyigit, A.; Labrou, N.E.; Binay, B. Conserved Amino Acid Residues that Affect Structural Stability of *Candida boidinii* Formate Dehydrogenase. *Appl. Biochem. Biotechnol.* **2020**. [[CrossRef](#)]
83. Alvarez, C.E.; Bovdilova, A.; Hoppner, A.; Wolff, C.C.; Saigo, M.; Trajtenberg, F.; Zhang, T.; Buschiazzi, A.; Nagel-Steger, L.; Drincovich, M.F.; et al. Molecular adaptations of NADP-malic enzyme for its function in C-4 photosynthesis in grasses. *Nat. Plants* **2019**, *5*, 755–765. [[CrossRef](#)] [[PubMed](#)]
84. Zhang, Y.; Yang, J.; Yu, X.; Hu, X.; Zhang, H. Engineering *Leuconostoc mesenteroides* dextranucrase by inserting disulfide bridges for enhanced thermotolerance. *Enzym. Microb. Technol.* **2020**, *139*. [[CrossRef](#)]
85. Gomez-Fernandez, B.J.; Risso, V.A.; Sanchez-Ruiz, J.M.; Alcalde, M. Consensus Design of an Evolved High-Redox Potential Laccase. *Front. Bioeng. Biotechnol.* **2020**, *8*. [[CrossRef](#)] [[PubMed](#)]
86. Zhao, Z.X.; Lan, D.M.; Tan, X.Y.; Hollmann, F.; Bornscheuer, U.T.; Yang, B.; Wang, Y.H. How To Break the Janus Effect of H₂O₂ in Biocatalysis? Understanding Inactivation Mechanisms To Generate more Robust Enzymes. *ACS Catal.* **2019**, *9*, 2916–2921. [[CrossRef](#)]
87. Liu, Q.; Xun, G.H.; Feng, Y. The state-of-the-art strategies of protein engineering for enzyme stabilization. *Biotechnol. Adv.* **2019**, *37*, 530–537. [[CrossRef](#)]
88. Roger, M.; Castelle, C.; Guiral, M.; Infossi, P.; Lojou, E.; Giudici-Orticoni, M.T.; Ilbert, M. Mineral respiration under extreme acidic conditions: From a supramolecular organization to a molecular adaptation in *Acidithiobacillus ferrooxidans*. *Biochem. Soc. Trans.* **2012**, *40*, 1324–1329. [[CrossRef](#)]
89. Hassan, N.; Rafiq, M.; Rehman, M.; Sajjad, W.; Hasan, F.; Abdullah, S. Fungi in acidic fire: A potential source of industrially important enzymes. *Fungal Biol. Rev.* **2019**, *33*, 58–71. [[CrossRef](#)]
90. Jin, M.; Gai, Y.B.; Guo, X.; Hou, Y.P.; Zeng, R.Y. Properties and Applications of Extremozymes from Deep-Sea Extremophilic Microorganisms: A Mini Review. *Mar. Drugs* **2019**, *17*, 656. [[CrossRef](#)]
91. Guiral, M.; Prunetti, L.; Aussignargues, C.; Ciaccafava, A.; Infossi, P.; Ilbert, M.; Lojou, E.; Giudici-Orticoni, M.T. The hyperthermophilic bacterium *Aquifex aeolicus*: From respiratory pathways to extremely resistant enzymes and biotechnological applications. *Adv. Microb. Physiol.* **2012**, *61*, 125–194. [[CrossRef](#)] [[PubMed](#)]
92. Furukawa, R.; Toma, W.; Yamazaki, K.; Akanuma, S. Ancestral sequence reconstruction produces thermally stable enzymes with mesophilic enzyme-like catalytic properties. *Sci. Rep.* **2020**, *10*, 15493. [[CrossRef](#)] [[PubMed](#)]
93. Abdollahi, P.; Ghane, M.; Babaekhou, L. Isolation and Characterization of Thermophilic Bacteria from Gavmesh Goli Hot Spring in Sabalan Geothermal Field, Iran: *Thermomonas hydrothermalis* and *Bacillus altitudinis* Isolates as a Potential Source of Thermostable Protease. *Geomicrobiol. J.* **2020**. [[CrossRef](#)]
94. Hilden, K.; Hakala, T.K.; Lundell, T. Thermotolerant and thermostable laccases. *Biotechnol. Lett.* **2009**, *31*, 1117–1128. [[CrossRef](#)] [[PubMed](#)]

95. Sterner, R.; Liebl, W. Thermophilic adaptation of proteins. *Crit. Rev. Biochem. Mol. Biol.* **2001**, *36*, 39–106. [[CrossRef](#)]
96. Maiello, F.; Gallo, G.; Coelho, C.; Sucharski, F.; Hardy, L.; Wurtele, M. Crystal structure of *Thermus thermophilus* methylenetetrahydrofolate dehydrogenase and determinants of thermostability. *PLoS ONE* **2020**, *15*. [[CrossRef](#)]
97. McManus, T.J.; Wells, S.A.; Walker, A.B. Salt bridge impact on global rigidity and thermostability in thermophilic citrate synthase. *Phys. Biol.* **2020**, *17*. [[CrossRef](#)]
98. Xie, Z.H.; Zhai, L.X.; Meng, D.; Tian, Q.P.; Guan, Z.B.; Cai, Y.J.; Liao, X.R. Improving the catalytic thermostability of *Bacillus altitudinis* W3 omega-transaminase by proline substitutions. *3 Biotech* **2020**, *10*. [[CrossRef](#)]
99. Kargar, F.; Mortezavi, M.; Torkzadeh-Mahani, M.; Lotfi, S.; Shakeri, S. Evaluation of Luciferase Thermal Stability by Arginine Saturation in the Flexible Loops. *Curr. Proteom.* **2020**, *17*, 30–39. [[CrossRef](#)]
100. Enguita, F.J.; Martins, L.O.; Henriques, A.O.; Carrondo, M.A. Crystal structure of a bacterial endospore coat component—A laccase with enhanced thermostability properties. *J. Biol. Chem.* **2003**, *278*, 19416–19425. [[CrossRef](#)]
101. Brininger, C.; Spradlin, S.; Cobani, L.; Evilia, C. The more adaptive to change, the more likely you are to survive: Protein adaptation in extremophiles. *Semin. Cell Dev. Biol.* **2018**, *84*, 158–169. [[CrossRef](#)] [[PubMed](#)]
102. Cea, P.A.; Araya, G.; Vallejos, G.; Recabarren, R.; Alzate-Morales, J.; Babul, J.; Guixe, V.; Castro-Fernandez, V. Characterization of hydroxymethylpyrimidine phosphate kinase from mesophilic and thermophilic bacteria and structural insights into their differential thermal stability. *Arch. Biochem. Biophys.* **2020**, *688*. [[CrossRef](#)] [[PubMed](#)]
103. Maffucci, I.; Laage, D.; Stirnemann, G.; Sterpone, F. Differences in thermal structural changes and melting between mesophilic and thermophilic dihydrofolate reductase enzymes. *Phys. Chem. Chem. Phys.* **2020**, *22*, 18361–18373. [[CrossRef](#)] [[PubMed](#)]
104. Hou, J.; Yang, X.Y.; Xu, Q.; Cui, H.L. Characterization of a novel Cu-containing dissimilatory nitrite reductase from the haloarchaeon *Haloaroccus* sp. YCN54. *Extremophiles* **2020**, *24*, 403–411. [[CrossRef](#)] [[PubMed](#)]
105. Graziano, G.; Merlino, A. Molecular bases of protein halotolerance. *Biochim. Biophys. Acta Proteins Proteom.* **2014**, *1844*, 850–858. [[CrossRef](#)] [[PubMed](#)]
106. Qin, H.M.; Gao, D.K.; Zhu, M.L.; Li, C.; Zhu, Z.L.; Wang, H.B.; Liu, W.D.; Tanokura, M.; Lu, F.P. Biochemical characterization and structural analysis of ulvan lyase from marine *Alteromonas* sp. reveals the basis for its salt tolerance. *Int. J. Biol. Macromol.* **2020**, *147*, 1309–1317. [[CrossRef](#)] [[PubMed](#)]
107. Zheng, C.; Li, Z.; Yang, H.; Zhang, T.; Niu, H.; Liu, D.; Wang, J.; Ying, H. Computation-aided rational design of a halophilic choline kinase for cytidine diphosphate choline production in high-salt condition. *J. Biotechnol.* **2019**, *290*, 59–66. [[CrossRef](#)] [[PubMed](#)]
108. Liu, Z.; Yuan, M.; Zhang, X.; Liang, Q.; Yang, M.; Mou, H.; Zhu, C. A thermostable glucose oxidase from *Aspergillus heteromorphus* CBS 117.55 with broad pH stability and digestive enzyme resistance. *Protein Expr. Purif.* **2020**, *176*. [[CrossRef](#)]
109. Yi, Z.; Cai, Z.; Zeng, B.; Zeng, R.; Zhang, G. Identification and Characterization of a Novel Thermostable and Salt-Tolerant beta-1,3 Xylanase from *Flammeovirga pacifica* Strain WPAGA1. *Biomolecules* **2020**, *10*, 1287. [[CrossRef](#)]
110. Zhu, T.; Li, R.; Sun, J.; Cui, Y.; Wu, B. Characterization and efficient production of a thermostable, halostable and organic solvent-stable cellulase from an oil reservoir. *Int. J. Biol. Macromol.* **2020**, *159*, 622–629. [[CrossRef](#)]
111. Monsalve, K.; Mazurenko, I.; Gutierrez-Sanchez, C.; Ilbert, M.; Infossi, P.; Frielingsdorf, S.; Giudici-Ortoni, M.T.; Lenz, O.; Lojou, E. Impact of Carbon Nanotube Surface Chemistry on Hydrogen Oxidation by Membrane-Bound Oxygen-Tolerant Hydrogenases. *Chemelectrochem* **2016**, *3*, 2179–2188. [[CrossRef](#)]
112. Oteri, F.; Baaden, M.; Lojou, E.; Sacquin-Mora, S. Multiscale Simulations Give Insight into the Hydrogen In and Out Pathways of NiFe-Hydrogenases from *Aquifex aeolicus* and *Desulfovibrio fructosovorans*. *J. Phys. Chem. B* **2014**, *118*, 13800–13811. [[CrossRef](#)]
113. Coglitore, D.; Janot, J.M.; Balme, S. Protein at liquid solid interfaces: Toward a new paradigm to change the approach to design hybrid protein/solid-state materials. *Adv. Colloid Interface Sci.* **2019**, *270*, 278–292. [[CrossRef](#)]
114. Arai, T.; Norde, W. The behavior of some model proteins at solid liquid interfaces 1. adsorption from single protein solutions. *Adv. Colloid Interface Sci.* **1990**, *51*, 1–15. [[CrossRef](#)]
115. Rabe, M.; Verdes, D.; Seeger, S. Understanding protein adsorption phenomena at solid surfaces. *Adv. Colloid Interface Sci.* **2011**, *162*, 87–106. [[CrossRef](#)] [[PubMed](#)]
116. Hitashi, V.P.; Mazurenko, I.; Harb, M.; Clement, R.; Taris, M.; Castano, S.; Duché, D.; Lecomte, S.; Ilbert, M.; de Poulpiquet, A.; et al. Electrostatic-Driven Activity, Loading, Dynamics, and Stability of a Redox Enzyme on Functionalized-Gold Electrodes for Bioelectrocatalysis. *ACS Catal.* **2018**, *8*, 12004–12014. [[CrossRef](#)]
117. Bourassin, N.; Baaden, M.; Lojou, E.; Sacquin-Mora, S. Implicit Modeling of the Impact of Adsorption on Solid Surfaces for Protein Mechanics and Activity with a Coarse-Grained Representation. *J. Phys. Chem. B* **2020**, *124*, 8516–8523. [[CrossRef](#)] [[PubMed](#)]
118. Pankratov, D.; Sotres, J.; Barrantes, A.; Arnebrant, T.; Shleev, S. Interfacial Behavior and Activity of Laccase and Bilirubin Oxidase on Bare Gold Surfaces. *Langmuir* **2014**, *30*, 2943–2951. [[CrossRef](#)] [[PubMed](#)]
119. Kienle, D.F.; Falatach, R.M.; Kaar, J.L.; Schwartz, D.K. Correlating Structural and Functional Heterogeneity of Immobilized Enzymes. *ACS Nano* **2018**, *12*, 8091–8103. [[CrossRef](#)] [[PubMed](#)]
120. Zhang, Y.F.; Ge, J.; Liu, Z. Enhanced Activity of Immobilized or Chemically Modified Enzymes. *ACS Catal.* **2015**, *5*, 4503–4513. [[CrossRef](#)]
121. Garcia-Garcia, P.; Guisan, J.M.; Fernandez-Lorente, G. A mild intensity of the enzyme-support multi-point attachment promotes the optimal stabilization of mesophilic multimeric enzymes: Amine oxidase from *Pisum sativum*. *J. Biotechnol.* **2020**, *318*, 39–44. [[CrossRef](#)]

122. Weltz, J.S.; Kienle, D.F.; Schwartz, D.K.; Kaar, J.L. Reduced Enzyme Dynamics upon Multipoint Covalent Immobilization Leads to Stability-Activity Trade-off. *J. Am. Chem. Soc.* **2020**, *142*, 3463–3471. [[CrossRef](#)]
123. Mateo, C.; Palomo, J.M.; Fernandez-Lorente, G.; Guisan, J.M.; Fernandez-Lafuente, R. Improvement of enzyme activity, stability and selectivity via immobilization techniques. *Enzym. Microb. Technol.* **2007**, *40*, 1451–1463. [[CrossRef](#)]
124. Hitaishi, V.P.; Mazurenko, I.; Vengasseril Murali, A.; de Poulpiquet, A.; Coustillier, G.; Delaporte, P.; Lojou, E. Nanosecond Laser-Fabricated Monolayer of Gold Nanoparticles on ITO for Bioelectrocatalysis. *Front. Chem.* **2020**, *8*. [[CrossRef](#)] [[PubMed](#)]
125. Sigurdardottir, S.B.; Lehmann, J.; Grivel, J.C.; Zhang, W.J.; Kaiser, A.; Pinelo, M. Alcohol dehydrogenase on inorganic powders: Zeta potential and particle agglomeration as main factors determining activity during immobilization. *Colloids Surf. B-Biointerfaces* **2019**, *175*, 136–142. [[CrossRef](#)] [[PubMed](#)]
126. Johnson, B.J.; Algar, W.R.; Malanoski, A.P.; Ancona, M.G.; Medintz, I.L. Understanding enzymatic acceleration at nanoparticle interfaces: Approaches and challenges. *Nano Today* **2014**, *9*, 102–131. [[CrossRef](#)]
127. Sharifi, M.; Sohrabi, M.J.; Hosseinali, S.H.; Hasan, A.; Kani, P.H.; Talaie, A.J.; Karim, A.Y.; Nanakali, N.M.Q.; Salihi, A.; Aziz, F.M.; et al. Enzyme immobilization onto the nanomaterials: Application in enzyme stability and prodrug-activated cancer therapy. *Int. J. Biol. Macromol.* **2020**, *143*, 665–676. [[CrossRef](#)]
128. Zhang, Y.; Tang, Z.; Wang, J.; Wu, H.; Lin, C.-T.; Lin, Y. Apoferritin nanoparticle: A novel and biocompatible carrier for enzyme immobilization with enhanced activity and stability. *J. Mater. Chem.* **2011**, *21*, 17468–17475. [[CrossRef](#)]
129. Yang, Y.L.; Zhu, G.X.; Wang, G.C.; Li, Y.L.; Tang, R.K. Robust glucose oxidase with a Fe₃O₄@C-silica nanohybrid structure. *J. Mater. Chem. B* **2016**, *4*, 4726–4731. [[CrossRef](#)] [[PubMed](#)]
130. Suo, H.B.; Gao, Z.; Xu, L.L.; Xu, C.; Yu, D.H.; Xiang, X.R.; Huang, H.; Hu, Y. Synthesis of functional ionic liquid modified magnetic chitosan nanoparticles for porcine pancreatic lipase immobilization. *Mater. Sci. Eng. C Mater. Biol. Appl.* **2019**, *96*, 356–364. [[CrossRef](#)] [[PubMed](#)]
131. Ansari, S.A.; Husain, Q.; Qayyum, S.; Azam, A. Designing and surface modification of zinc oxide nanoparticles for biomedical applications. *Food Chem. Toxicol.* **2011**, *49*, 2107–2115. [[CrossRef](#)]
132. Grewal, J.; Ahmad, R.; Khare, S.K. Development of cellulase-nanoconjugates with enhanced ionic liquid and thermal stability for in situ lignocellulose saccharification. *Bioresour. Technol.* **2017**, *242*, 236–243. [[CrossRef](#)]
133. Shang, W.; Nuffer, J.H.; Dordick, J.S.; Siegel, R.W. Unfolding of ribonuclease A on silica nanoparticle surfaces. *Nano Lett.* **2007**, *7*, 1991–1995. [[CrossRef](#)]
134. Song, Y.; Zhong, D.; Luo, D.; Huang, M.; Huang, Z.; Tan, H.; Sun, L.; Wang, L. Effect of particle size on conformation and enzymatic activity of EcoRI adsorbed on CdS nanoparticles. *Colloids Surf. B-Biointerfaces* **2014**, *114*, 269–276. [[CrossRef](#)] [[PubMed](#)]
135. Asuri, P.; Karajanagi, S.S.; Yang, H.C.; Yim, T.J.; Kane, R.S.; Dordick, J.S. Increasing protein stability through control of the nanoscale environment. *Langmuir* **2006**, *22*, 5833–5836. [[CrossRef](#)] [[PubMed](#)]
136. Vertegel, A.A.; Siegel, R.W.; Dordick, J.S. Silica nanoparticle size influences the structure and enzymatic activity of adsorbed lysozyme. *Langmuir* **2004**, *20*, 6800–6807. [[CrossRef](#)] [[PubMed](#)]
137. Gagner, J.E.; Lopez, M.D.; Dordick, J.S.; Siegel, R.W. Effect of gold nanoparticle morphology on adsorbed protein structure and function. *Biomaterials* **2011**, *32*, 7241–7252. [[CrossRef](#)]
138. Bilal, M.; Asgher, M.; Cheng, H.R.; Yan, Y.J.; Iqbal, H.M.N. Multi-point enzyme immobilization, surface chemistry, and novel platforms: A paradigm shift in biocatalyst design. *Crit. Rev. Biotechnol.* **2019**, *39*, 202–219. [[CrossRef](#)]
139. Vila, N.; Andre, E.; Ciganda, R.; Ruiz, J.; Astruc, D.; Walcarius, A. Molecular Sieving with Vertically Aligned Mesoporous Silica Films and Electronic Wiring through Isolating Nanochannels. *Chem. Mater.* **2016**, *28*, 2511–2514. [[CrossRef](#)]
140. Abdelbar, M.F.; Shams, R.S.; Morsy, O.M.; Hady, M.A.; Shoueir, K.; Abdelmonem, R. Highly ordered functionalized mesoporous silicate nanoparticles reinforced poly (lactic acid) gatekeeper surface for infection treatment. *Int. J. Biol. Macromol.* **2020**, *156*, 858–868. [[CrossRef](#)]
141. Rodriguez-Abetxuko, A.; Sanchez-deAlcazar, D.; Munumer, P.; Beloqui, A. Tunable Polymeric Scaffolds for Enzyme Immobilization. *Front. Bioeng. Biotechnol.* **2020**, *8*. [[CrossRef](#)]
142. Inagaki, M.; Toyoda, M.; Soneda, Y.; Tsujimura, S.; Morishita, T. Templated mesoporous carbons: Synthesis and applications. *Carbon* **2016**, *107*, 448–473. [[CrossRef](#)]
143. Ruff, A.; Szczesny, J.; Markovic, N.; Conzuelo, F.; Zacarias, S.; Pereira, I.A.C.; Lubitz, W.; Schuhmann, W. A fully protected hydrogenase/polymer-based bioanode for high-performance hydrogen/glucose biofuel cells. *Nat. Commun.* **2018**, *9*. [[CrossRef](#)]
144. Stine, K.J. Enzyme Immobilization on Nanoporous Gold: A Review. *Biochem. Insights* **2017**, *10*. [[CrossRef](#)] [[PubMed](#)]
145. Baruch-Shpigler, Y.; Avnir, D. Enzymes in a golden cage. *Chem. Sci.* **2020**, *11*, 3965–3977. [[CrossRef](#)]
146. Ge, J.; Lei, J.D.; Zare, R.N. Protein-inorganic hybrid nanoflowers. *Nat. Nanotechnol.* **2012**, *7*, 428–432. [[CrossRef](#)] [[PubMed](#)]
147. Liang, W.; Wied, P.; Carraro, F.; Sumby, C.J.; Nidetzky, B.; Tsung, C.-K.; Falcaro, P.; Doonan, C.J. Metal-Organic Framework-Based Enzyme Biocomposites. *Chem. Rev.* **2021**. [[CrossRef](#)]
148. Lian, X.Z.; Fang, Y.; Joseph, E.; Wang, Q.; Li, J.L.; Banerjee, S.; Lollar, C.; Wang, X.; Zhou, H.C. Enzyme-MOF (metal-organic framework) composites. *Chem. Soc. Rev.* **2017**, *46*, 3386–3401. [[CrossRef](#)] [[PubMed](#)]
149. Li, P.; Moon, S.Y.; Guelta, M.A.; Harvey, S.P.; Hupp, J.T.; Farha, O.K. Encapsulation of a Nerve Agent Detoxifying Enzyme by a Mesoporous Zirconium Metal-Organic Framework Ensures Thermal and Long-Term Stability. *J. Am. Chem. Soc.* **2016**, *138*, 8052–8055. [[CrossRef](#)] [[PubMed](#)]

150. Feng, Y.X.; Zhong, L.; Hou, Y.; Jia, S.R.; Cui, J.D. Acid-resistant enzyme@MOF nanocomposites with mesoporous silica shells for enzymatic applications in acidic environments. *J. Biotechnol.* **2019**, *306*, 54–61. [[CrossRef](#)]
151. He, H.M.; Han, H.B.; Shi, H.; Tian, Y.Y.; Sun, F.X.; Song, Y.; Li, Q.S.; Zhu, G.S. Construction of Thermophilic Lipase-Embedded Metal Organic Frameworks via Biomimetic Mineralization: A Biocatalyst for Ester Hydrolysis and Kinetic Resolution. *ACS Appl. Mater. Interfaces* **2016**, *8*, 24517–24524. [[CrossRef](#)]
152. Wu, X.L.; Yang, C.; Ge, J.; Liu, Z. Polydopamine tethered enzyme/metal-organic framework composites with high stability and reusability. *Nanoscale* **2015**, *7*, 18883–18886. [[CrossRef](#)] [[PubMed](#)]
153. Wu, X.L.; Yang, C.; Ge, J. Green synthesis of enzyme/metal-organic framework composites with high stability in protein denaturing solvents. *Bioresour. Bioprocess.* **2017**, *4*. [[CrossRef](#)] [[PubMed](#)]
154. Knedel, T.O.; Ricklefs, E.; Schlusener, C.; Urlacher, V.B.; Janiak, A.C. Laccase Encapsulation in ZIF-8 Metal-Organic Framework Shows Stability Enhancement and Substrate Selectivity. *Chemistryopen* **2019**, *8*, 1337–1344. [[CrossRef](#)] [[PubMed](#)]
155. Song, J.Y.; He, W.T.; Shen, H.; Zhou, Z.X.; Li, M.Q.; Su, P.; Yang, Y. Construction of multiple enzyme metal-organic frameworks biocatalyst via DNA scaffold: A promising strategy for enzyme encapsulation. *Chem. Eng. J.* **2019**, *363*, 174–182. [[CrossRef](#)]
156. Gao, Y.; Doherty, C.M.; Mulet, X. A Systematic Study of the Stability of Enzyme/Zeoletic Imidazolate Framework-8 Composites in Various Biologically Relevant Solutions. *Chemistryselect* **2020**, *5*, 13766–13774. [[CrossRef](#)]
157. Nadar, S.S.; Rathod, V.K. Magnetic-metal organic framework (magnetic-MOF): A novel platform for enzyme immobilization and nanozyme applications. *Int. J. Biol. Macromol.* **2018**, *120*, 2293–2302. [[CrossRef](#)] [[PubMed](#)]
158. Gan, J.; Bagheri, A.R.; Aramesh, N.; Gul, I.; Franco, M.; Almulaiky, Y.Q.; Bilal, M. Covalent organic frameworks as emerging host platforms for enzyme immobilization and robust biocatalysis—A review. *Int. J. Biol. Macromol.* **2021**, *167*, 502–515. [[CrossRef](#)]
159. Chapman, R.; Stenzel, M.H. All Wrapped up: Stabilization of Enzymes within Single Enzyme Nanoparticles. *J. Am. Chem. Soc.* **2019**, *141*, 2754–2769. [[CrossRef](#)]
160. Chen, Y.Z.; Luo, Z.G.; Lu, X.X. Construction of Novel Enzyme-Graphene Oxide Catalytic Interface with Improved Enzymatic Performance and Its Assembly Mechanism. *ACS Appl. Mater. Interfaces* **2019**, *11*, 11349–11359. [[CrossRef](#)]
161. Wu, L.; Lu, X.; Niu, K.; Ma, D.; Chen, J. Tyrosinase nanocapsule based nano-biosensor for ultrasensitive and rapid detection of bisphenol A with excellent stability in different application scenarios. *Biosens. Bioelectron.* **2020**, *165*. [[CrossRef](#)]
162. Shen, X.T.; Yang, M.; Cui, C.X.; Cao, H. In situ immobilization of glucose oxidase and catalase in a hybrid interpenetrating polymer network by 3D bioprinting and its application. *Colloids Surf. A Physicochem. Eng. Asp.* **2019**, *568*, 411–418. [[CrossRef](#)]
163. Zhang, S.T.; Wu, Z.F.; Chen, G.; Wang, Z. An Improved Method to Encapsulate Laccase from *Trametes versicolor* with Enhanced Stability and Catalytic Activity. *Catalysts* **2018**, *8*, 286. [[CrossRef](#)]
164. Wan, L.; Chen, Q.S.; Liu, J.B.; Yang, X.H.; Huang, J.; Li, L.; Guo, X.; Zhang, J.; Wang, K.M. Programmable Self-Assembly of DNA-Protein Hybrid Hydrogel for Enzyme Encapsulation with Enhanced Biological Stability. *Biomacromolecules* **2016**, *17*, 1543–1550. [[CrossRef](#)]
165. Liang, H.; Jiang, S.H.; Yuan, Q.P.; Li, G.F.; Wang, F.; Zhang, Z.J.; Liu, J.W. Co-immobilization of multiple enzymes by metal coordinated nucleotide hydrogel nanofibers: Improved stability and an enzyme cascade for glucose detection. *Nanoscale* **2016**, *8*, 6071–6078. [[CrossRef](#)] [[PubMed](#)]
166. Yamaguchi, H.; Kiyota, Y.; Miyazaki, M. Techniques for Preparation of Cross-Linked Enzyme Aggregates and Their Applications in Bioconversions. *Catalysts* **2018**, *8*, 174. [[CrossRef](#)]
167. Sheldon, R.A.; van Pelt, S. Enzyme immobilisation in biocatalysis: Why, what and how. *Chem. Soci. Rev.* **2013**, *42*, 6223–6235. [[CrossRef](#)] [[PubMed](#)]
168. Sheldon, R.A.; van Pelt, S.; Kanbak-Aksu, S.; Rasmussen, J.A.; Janssen, M.H.A. Cross-Linked Enzyme Aggregates (CLEAs) in Organic Synthesis. *Aldrichimica Acta* **2013**, *46*, 81–93.
169. Qian, J.; Zhao, C.; Ding, J.; Chen, Y.; Guo, H. Preparation of nano-enzyme aggregates by crosslinking lipase with sodium tripolyphosphate. *Process Biochem.* **2020**, *97*, 19–26. [[CrossRef](#)]
170. Nadar, S.S.; Muley, A.B.; Ladole, M.R.; Joshi, P.U. Macromolecular cross-linked enzyme aggregates (M-CLEAs) of alpha-amylase. *Int. J. Biol. Macromol.* **2016**, *84*, 69–78. [[CrossRef](#)] [[PubMed](#)]
171. Wang, S.; Zheng, D.; Yin, L.; Wang, F. Preparation, activity and structure of cross-linked enzyme aggregates (CLEAs) with nanoparticle. *Enzym. Microb. Technol.* **2017**, *107*, 22–31. [[CrossRef](#)] [[PubMed](#)]
172. Ren, S.Z.; Li, C.H.; Jiao, X.B.; Jia, S.R.; Jiang, Y.J.; Bilal, M.; Cui, J.D. Recent progress in multienzymes co-immobilization and multienzyme system applications. *Chem. Eng. J.* **2019**, *373*, 1254–1278. [[CrossRef](#)]
173. Monteiro, R.R.C.; dos Santos, J.C.S.; Alcantara, A.R.; Fernandez-Lafuente, R. Enzyme-Coated Micro-Crystals: An Almost Forgotten but Very Simple and Elegant Immobilization Strategy. *Catalysts* **2020**, *10*, 891. [[CrossRef](#)]
174. Zerva, A.; Pentari, C.; Topakas, E. Crosslinked Enzyme Aggregates (CLEAs) of Laccases from *Pleurotus citrinopileatus* Induced in Olive Oil Mill Wastewater (OOMW). *Molecules* **2020**, *25*, 2221. [[CrossRef](#)]
175. Kopp, W.; da Costa, T.P.; Pereira, S.C.; Jafelicci, M., Jr.; Giordano, R.C.; Marques, R.F.C.; Araujo-Moreira, F.M.; Giordano, R.L.C. Easily handling penicillin G acylase magnetic cross-linked enzymes aggregates: Catalytic and morphological studies. *Process Biochem.* **2014**, *49*, 38–46. [[CrossRef](#)]
176. Cui, J.D.; Zhang, S.; Sun, L.M. Cross-Linked Enzyme Aggregates of Phenylalanine Ammonia Lyase: Novel Biocatalysts for Synthesis of L-Phenylalanine. *Appl. Biochem. Biotechnol.* **2012**, *167*, 835–844. [[CrossRef](#)] [[PubMed](#)]

177. Cui, J.D.; Jia, S.R. Optimization protocols and improved strategies of cross-linked enzyme aggregates technology: Current development and future challenges. *Crit. Rev. Biotechnol.* **2015**, *35*, 15–28. [[CrossRef](#)]
178. Tandjaoui, N.; Tassist, A.; Abouseoud, M.; Couvert, A.; Amrane, A. Preparation and characterization of cross-linked enzyme aggregates (CLEAs) of *Brassica rapa* peroxidase. *Biocatal. Agric. Biotechnol.* **2015**, *4*, 208–213. [[CrossRef](#)]
179. Dinh, T.H.; Jang, N.Y.; McDonald, K.A.; Won, K. Cross-linked aggregation of glutamate decarboxylase to extend its activity range toward alkaline pH. *J. Chem. Technol. Biotechnol.* **2015**, *90*, 2100–2105. [[CrossRef](#)]
180. Gupta, K.; Jana, A.K.; Kumar, S.; Jana, M.M. Solid state fermentation with recovery of Amyloglucosidase from extract by direct immobilization in cross linked enzyme aggregate for starch hydrolysis. *Agric. Biotechnol.* **2015**, *4*, 486–492. [[CrossRef](#)]
181. Lucena, G.N.; dos Santos, C.C.; Pinto, G.C.; Piazza, R.D.; Guedes, W.N.; Jafelicci Junior, M.; de Paula, A.V.; Marques, R.F.C. Synthesis and characterization of magnetic cross-linked enzyme aggregate and its evaluation of the alternating magnetic field (AMF) effects in the catalytic activity. *J. Magn. Magn. Mater.* **2020**, *516*. [[CrossRef](#)]
182. Primozic, M.; Kravanja, G.; Knez, Z.; Crnjac, A.; Leitgeb, M. Immobilized laccase in the form of (magnetic) cross-linked enzyme aggregates for sustainable diclofenac (bio) degradation. *J. Clean. Prod.* **2020**, *275*. [[CrossRef](#)]
183. Xu, M.Q.; Wang, S.S.; Li, L.N.; Gao, J.; Zhang, Y.W. Combined Cross-Linked Enzyme Aggregates as Biocatalysts. *Catalysts* **2018**, *8*, 460. [[CrossRef](#)]
184. Xu, M.Q.; Li, F.L.; Yu, W.Q.; Li, R.F.; Zhang, Y.W. Combined cross-linked enzyme aggregates of glycerol dehydrogenase and NADH oxidase for high efficiency in situ NAD(+) regeneration. *Int. J. Biol. Macromol.* **2020**, *144*, 1013–1021. [[CrossRef](#)] [[PubMed](#)]
185. Sellami, K.; Couvert, A.; Nasrallah, N.; Maachi, R.; Tandjaoui, N.; Abouseoud, M.; Amrane, A. Bio-based and cost effective method for phenolic compounds removal using cross-linked enzyme aggregates. *J. Hazard. Mater.* **2021**, *403*. [[CrossRef](#)] [[PubMed](#)]
186. Mai-Lan, P.; Polakovic, M. Microbial cell surface display of oxidoreductases: Concepts and applications. *Int. J. Biol. Macromol.* **2020**, *165*, 835–841. [[CrossRef](#)]
187. Ugwuodo, C.J.; Nwagu, T.N. Stabilizing enzymes by immobilization on bacterial spores: A review of literature. *Int. J. Biol. Macromol.* **2021**, *166*, 238–250. [[CrossRef](#)] [[PubMed](#)]
188. Hsieh, H.-Y.; Lin, C.-H.; Hsu, S.-Y.; Stewart, G.C. A *Bacillus* Spore-Based Display System for Bioremediation of Atrazine. *Appl. Environ. Microbiol.* **2020**, *86*. [[CrossRef](#)]
189. Tang, X.J.; Liang, B.; Yi, T.Y.; Manco, G.; Palchetti, I.; Liu, A.H. Cell surface display of organophosphorus hydrolase for sensitive spectrophotometric detection of p-nitrophenol substituted organophosphates. *Enzym. Microb. Technol.* **2014**, *55*, 107–112. [[CrossRef](#)]
190. Padkina, M.V.; Sambuk, E.V. Prospects for the Application of Yeast Display in Biotechnology and Cell Biology (Review). *Appl. Biochem. Microbiol.* **2018**, *54*, 337–351. [[CrossRef](#)]
191. Chen, H.; Chen, Z.; Ni, Z.; Tian, R.; Zhang, T.; Jia, J.; Chen, K.; Yang, S. Display of *Thermotoga maritima* MSB8 nitrilase on the spore surface of *Bacillus subtilis* using out coat protein CotG as the fusion partner. *J. Mol. Catal. B Enzym.* **2016**, *123*, 73–80. [[CrossRef](#)]
192. Lozancic, M.; Hossain, A.S.; Mrsa, V.; Teparic, R. Surface Display-An Alternative to Classic Enzyme Immobilization. *Catalysts* **2019**, *9*, 728. [[CrossRef](#)]
193. Marcus, R.A. On the theory of oxidation-reduction reactions involving electron transfer. 1. *J. Chem. Phys.* **1956**, *24*, 966–978. [[CrossRef](#)]
194. Richardson, D.J.; Butt, J.N.; Fredrickson, J.K.; Zachara, J.M.; Shi, L.; Edwards, M.J.; White, G.; Baiden, N.; Gates, A.J.; Marritt, S.J.; et al. The porin-cytochrome' model for microbe-to-mineral electron transfer. *Mol. Microbiol.* **2012**, *85*, 201–212. [[CrossRef](#)] [[PubMed](#)]
195. Hitaishi, V.P.; Clement, R.; Quattrocchi, L.; Parent, P.; Duche, D.; Zuily, L.; Ilbert, M.; Lojou, E.; Mazurenko, I. Interplay between Orientation at Electrodes and Copper Activation of *Thermus thermophilus* Laccase for O-2 Reduction. *J. Am. Chem. Soc.* **2020**, *142*, 1394–1405. [[CrossRef](#)] [[PubMed](#)]
196. Mazurenko, I.; Monsalve, K.; Rouhana, J.; Parent, P.; Laffon, C.; Le Goff, A.; Szunerits, S.; Boukherroub, R.; Giudici-Ortoni, M.T.; Mano, N.; et al. How the Intricate Interactions between Carbon Nanotubes and Two Bilirubin Oxidases Control Direct and Mediated O-2 Reduction. *ACS Appl. Mater. Interfaces* **2016**, *8*, 23074–23085. [[CrossRef](#)] [[PubMed](#)]
197. Oteri, F.; Ciaccafava, A.; de Poulpiquet, A.; Baaden, M.; Lojou, E.; Sacquin-Mora, S. The weak, fluctuating, dipole moment of membrane-bound hydrogenase from *Aquifex aeolicus* accounts for its adaptability to charged electrodes. *Phys. Chem. Chem. Phys.* **2014**, *16*, 11318–11322. [[CrossRef](#)]
198. Mazurenko, I.; Monsalve, K.; Infossi, P.; Giudici-Ortoni, M.T.; Topin, F.; Mano, N.; Lojou, E. Impact of substrate diffusion and enzyme distribution in 3D-porous electrodes: A combined electrochemical and modelling study of a thermostable H-2/O-2 enzymatic fuel cell. *Energy Environ. Sci.* **2017**, *10*, 1966–1982. [[CrossRef](#)]
199. Atalah, J.; Zhou, Y.; Espina, G.; Blamey, J.M.; Ramasamy, R.P. Improved stability of multicopper oxidase-carbon nanotube conjugates using a thermophilic laccase. *Catal. Sci. Technol.* **2018**, *8*, 1272–1276. [[CrossRef](#)]
200. Zafar, M.N.; Aslam, I.; Ludwig, R.; Xu, G.B.; Gorton, L. An efficient and versatile membraneless bioanode for biofuel cells based on *Corynascus thermophilus* cellobiose dehydrogenase. *Electrochim. Acta* **2019**, *295*, 316–324. [[CrossRef](#)]
201. Malinowski, S.; Wardak, C.; Jaroszynska-Wolinska, J.; Herbert, P.A.F.; Panek, R. Cold Plasma as an Innovative Construction Method of Voltammetric Biosensor Based on Laccase. *Sensors* **2018**, *18*, 4086. [[CrossRef](#)] [[PubMed](#)]

202. Bathinapatla, A.; Kanchi, S.; Sabela, M.I.; Ling, Y.C.; Bisetty, K.; Inamuddin. Experimental and Computational Studies of a Laccase Immobilized ZnONPs/GO-Based Electrochemical Enzymatic Biosensor for the Detection of Sucralose in Food Samples. *Food Anal. Methods* **2020**, *13*, 2014–2027. [[CrossRef](#)]
203. Aleksejeva, O.; Mateljak, I.; Ludwig, R.; Alcalde, M.; Shleev, S. Electrochemistry of a high redox potential laccase obtained by computer-guided mutagenesis combined with directed evolution. *Electrochem. Commun.* **2019**, *106*. [[CrossRef](#)]
204. Mohtar, L.G.; Aranda, P.; Messina, G.A.; Nazaren, M.A.; Pereira, S.V.; Raba, J.; Bertolino, F.A. Amperometric biosensor based on laccase immobilized onto a nanostructured screen-printed electrode for determination of polyphenols in propolis. *Microchem. J.* **2019**, *144*, 13–18. [[CrossRef](#)]
205. Chen, T.; Xu, Y.H.; Peng, Z.; Li, A.H.; Liu, J.Q. Simultaneous Enhancement of Bioactivity and Stability of Laccase by Cu²⁺/PAA/PPEGA Matrix for Efficient Biosensing and Recyclable Decontamination of Pyrocatechol. *Anal. Chem.* **2017**, *89*, 2065–2072. [[CrossRef](#)] [[PubMed](#)]
206. Palanisamy, S.; Ramaraj, S.K.; Chen, S.M.; Yang, T.C.K.; Yi-Fan, P.; Chen, T.W.; Velusamy, V.; Selvam, S. A novel Laccase Biosensor based on Laccase immobilized Graphene-Cellulose Microfiber Composite modified Screen-Printed Carbon Electrode for Sensitive Determination of Catechol. *Sci. Rep.* **2017**, *7*. [[CrossRef](#)]
207. Lee, J.Y.Y.; Elouarzaki, K.; Sabharwal, H.S.; Fisher, A.C.; Lee, J.-M. A hydrogen/oxygen hybrid biofuel cell comprising an electrocatalytically active nanoflower/laccase-based biocathode. *Catal. Sci. Technol.* **2020**, *10*, 6235–6243. [[CrossRef](#)]
208. Zhang, Y.N.; Li, X.; Li, D.W.; Wei, Q.F. A laccase based biosensor on AuNPs-MoS₂ modified glassy carbon electrode for catechol detection. *Colloids Surf. B Biointerfaces* **2020**, *186*. [[CrossRef](#)]
209. El Ichi-Ribault, S.; Zebda, A.; Tingry, S.; Petit, M.; Suherman, A.L.; Boualam, A.; Cinquin, P.; Martin, D.K. Performance and stability of chitosan-MWCNTs-laccase biocathode: Effect of MWCNTs surface charges and ionic strength. *J. Electroanal. Chem.* **2017**, *799*, 26–33. [[CrossRef](#)]
210. Yang, Y.; Zeng, H.; Huo, W.S.; Zhang, Y.H. Direct Electrochemistry and Catalytic Function on Oxygen Reduction Reaction of Electrodes Based on Two Kinds of Magnetic Nano-particles with Immobilized Laccase Molecules. *J. Inorg. Organomet. Polym. Mater.* **2017**, *27*, 201–214. [[CrossRef](#)]
211. Zappi, D.; Masci, G.; Sadun, C.; Tortolini, C.; Antonelli, M.L.; Bollella, P. Evaluation of new cholinium-amino acids based room temperature ionic liquids (RTILs) as immobilization matrix for electrochemical biosensor development: Proof-of-concept with *Trametes Versicolor* laccase. *Microchem. J.* **2018**, *141*, 346–352. [[CrossRef](#)]
212. Zhang, Y.; Lv, Z.Y.; Zhou, J.; Fang, Y.; Wu, H.; Xin, F.X.; Zhang, W.M.; Ma, J.F.; Xu, N.; He, A.Y.; et al. Amperometric Biosensors Based on Recombinant Bacterial Laccase CotA for Hydroquinone Determination. *Electroanalysis* **2020**, *32*, 142–148. [[CrossRef](#)]
213. Xu, R.; Cui, J.Y.; Tang, R.Z.; Li, F.T.; Zhang, B.R. Removal of 2,4,6-trichlorophenol by laccase immobilized on nano-copper incorporated electrospun fibrous membrane-high efficiency, stability and reusability. *Chem. Eng. J.* **2017**, *326*, 647–655. [[CrossRef](#)]
214. Wang, A.Q.; Ding, Y.P.; Li, L.; Duan, D.D.; Mei, Q.W.; Zhuang, Q.; Cui, S.Q.; He, X.Y. A novel electrochemical enzyme biosensor for detection of 17 beta-estradiol by mediated electron-transfer system. *Talanta* **2019**, *192*, 478–485. [[CrossRef](#)]
215. Yashas, S.R.; Sandeep, S.; Shivakumar, B.P.; Swamy, N.K. A matrix of perovskite micro-seeds and polypyrrole nanotubes tethered laccase/graphite biosensor for sensitive quantification of 2,4-dichlorophenol in wastewater. *Anal. Methods* **2019**, *11*, 4511–4519. [[CrossRef](#)]
216. Castrovilli, M.C.; Bolognesi, P.; Chiarinelli, J.; Avaldi, L.; Cartoni, A.; Calandra, P.; Tempesta, E.; Giardi, M.T.; Antonacci, A.; Arduini, F.; et al. Electrospray deposition as a smart technique for laccase immobilisation on carbon black-nanomodified screen-printed electrodes. *Biosens. Bioelectron.* **2020**, *163*. [[CrossRef](#)]
217. Lee, Y.G.; Liao, B.X.; Weng, Y.C. Ascorbic acid sensor using a PVA/laccase-Au-NPs/Pt electrode. *RSC Adv.* **2018**, *8*, 37872–37879. [[CrossRef](#)]
218. Lou, C.Q.; Jing, T.; Zhou, J.Y.; Tian, J.Z.; Zheng, Y.J.; Wang, C.; Zhao, Z.Y.; Lin, J.; Liu, H.; Zhao, C.Q.; et al. Laccase immobilized polyaniline/magnetic graphene composite electrode for detecting hydroquinone. *Int. J. Biol. Macromol.* **2020**, *149*, 1130–1138. [[CrossRef](#)] [[PubMed](#)]
219. Chen, T.; Xu, Y.H.; Wei, S.; Li, A.H.; Huang, L.; Liu, J.Q. A signal amplification system constructed by bi-enzymes and bi-nanospheres for sensitive detection of norepinephrine and miRNA. *Biosens. Bioelectron.* **2019**, *124*, 224–232. [[CrossRef](#)] [[PubMed](#)]
220. Mazlan, S.Z.; Lee, Y.H.; Abu Hanifah, S. A New Laccase Based Biosensor for Tartrazine. *Sensors* **2017**, *17*, 2859. [[CrossRef](#)] [[PubMed](#)]
221. Moraes, J.T.; Salamanca-Neto, C.A.R.; Svorc, L.; Schirmann, J.G.; Barbosa-Dekker, A.M.; Dekker, R.F.H.; Sartori, E.R. Laccase from *Botryosphaeria rhodina* MAMB-05 as a biological component in electrochemical biosensing devices. *Anal. Methods* **2019**, *11*, 717–720. [[CrossRef](#)]
222. Sedenho, G.C.; Hassan, A.; Macedo, L.J.A.; Crespilho, F.N. Stabilization of bilirubin oxidase in a biogel matrix for high-performance gas diffusion electrodes. *J. Power Sources* **2021**, *482*. [[CrossRef](#)]
223. Gentil, S.; Carriere, M.; Cosnier, S.; Gounel, S.; Mano, N.; Le Goff, A. Direct Electrochemistry of Bilirubin Oxidase from *Magnaporthe oryzae* on Covalently-Functionalized MWCNT for the Design of High-Performance Oxygen-Reducing Biocathodes. *Chem. A Eur. J.* **2018**, *24*, 8404–8408. [[CrossRef](#)]
224. Szczesny, J.; Markovic, N.; Conzuelo, F.; Zacarias, S.; Pereira, I.A.C.; Lubitz, W.; Plumere, N.; Schuhmann, W.; Ruff, A. A gas breathing hydrogen/air biofuel cell comprising a redox polymer/hydrogenase-based bioanode. *Nat. Commun.* **2018**, *9*. [[CrossRef](#)] [[PubMed](#)]

225. Markovic, N.; Conzuelo, F.; Szczesny, J.; Garcia, M.B.G.; Santos, D.H.; Ruff, A.; Schuhmann, W. An Air-breathing Carbon Cloth-based Screen-printed Electrode for Applications in Enzymatic Biofuel Cells. *Electroanalysis* **2019**, *31*, 217–221. [[CrossRef](#)]
226. Trifonov, A.; Stemmer, A.; Tel-Vered, R. Carbon-coated magnetic nanoparticles as a removable protection layer extending the operation lifetime of bilirubin oxidase-based bioelectrode. *Bioelectrochemistry* **2021**, *137*, 107640. [[CrossRef](#)] [[PubMed](#)]
227. Al-Lolage, F.A.; Bartlett, P.N.; Gounel, S.; Staigre, P.; Mano, N. Site-Directed Immobilization of Bilirubin Oxidase for Electrocatalytic Oxygen Reduction. *ACS Catal.* **2019**, *9*, 2068–2078. [[CrossRef](#)]
228. Takimoto, D.; Tsujimura, S. Oxygen Reduction Reaction Activity and Stability of Electrochemically Deposited Bilirubin Oxidase. *Chem. Lett.* **2018**, *47*, 1269–1271. [[CrossRef](#)]
229. Tsujimura, S.; Oyama, M.; Funabashi, H.; Ishii, S. Effects of pore size and surface properties of MgO-templated carbon on the performance of bilirubin oxidase-modified oxygen reduction reaction cathode. *Electrochim. Acta* **2019**, *322*. [[CrossRef](#)]
230. Tang, J.; Yan, X.M.; Huang, W.; Engelbrekt, C.; Duus, J.O.; Ulstrup, J.; Xiao, X.X.; Zhang, J.D. Bilirubin oxidase oriented on novel type three-dimensional biocathodes with reduced graphene aggregation for biocathode. *Biosens. Bioelectron.* **2020**, *167*. [[CrossRef](#)]
231. Walgama, C.; Pathiranaage, A.; Akinwale, M.; Montealegre, R.; Niroula, J.; Echeverria, E.; McLlroy, D.N.; Harriman, T.A.; Lucca, D.A.; Krishnan, S. Buckypaper–Bilirubin Oxidase Biointerface for Electrocatalytic Applications: Buckypaper Thickness. *ACS Appl. Bio Mater.* **2019**, *2*, 2229–2236. [[CrossRef](#)]
232. Zhang, L.; Carucci, C.; Reculosa, S.; Goudeau, B.; Lefrancois, P.; Gounel, S.; Mano, N.; Kuhn, A. Rational Design of Enzyme-Modified Electrodes for Optimized Bioelectrocatalytic Activity. *Chemelectrochem* **2019**, *6*, 4980–4984. [[CrossRef](#)]
233. Mukha, D.; Cohen, Y.; Yehezkeili, O. Bismuth Vanadate/Bilirubin Oxidase Photo(bio)electrochemical Cells for Unbiased, Light-Triggered Electrical Power Generation. *ChemSuschem* **2020**, *13*, 2684–2692. [[CrossRef](#)]
234. Wang, Y.; Song, Y.; Ma, C.; Kang, Z.; Zhu, Z. A heterologously-expressed thermostable *Pyrococcus furiosus* cytoplasmic [NiFe]-hydrogenase I used as the catalyst of H₂/air biofuel cells. *Int. J. Hydrogen Energy* **2021**, *46*, 3035–3044. [[CrossRef](#)]
235. Gentil, S.; Mansor, S.M.C.; Jamet, H.; Cosnier, S.; Cavazza, C.; Le Goff, A. Oriented Immobilization of NiFeSe Hydrogenases on Covalently and Noncovalently Functionalized Carbon Nanotubes for H₂/Air Enzymatic Fuel Cells. *ACS Catal.* **2018**, *8*, 3957–3964. [[CrossRef](#)]
236. Szczesny, J.; Birrell, J.A.; Conzuelo, F.; Lubitz, W.; Ruff, A.; Schuhmann, W. Redox-Polymer-Based High-Current-Density Gas-Diffusion H₂-Oxidation Bioanode Using FeFe Hydrogenase from *Desulfovibrio desulfuricans* in a Membrane-free Biofuel Cell. *Angew. Chem. Int. Ed.* **2020**, *59*, 16506–16510. [[CrossRef](#)]
237. Ruff, A.; Szczesny, J.; Vega, M.; Zacarias, S.; Matias, P.M.; Gounel, S.; Mano, N.; Pereira, I.A.C.; Schuhmann, W. Redox-Polymer-Wired NiFeSe Hydrogenase Variants with Enhanced O₂ Stability for Triple-Protected High-Current-Density H₂-Oxidation Bioanodes. *ChemSuschem* **2020**, *13*, 3627–3635. [[CrossRef](#)] [[PubMed](#)]
238. Adachi, T.; Kitazumi, Y.; Shirai, O.; Kano, K. Direct Electron Transfer-Type Bioelectrocatalysis of Redox Enzymes at Nanostructured Electrodes. *Catalysts* **2020**, *10*, 236. [[CrossRef](#)]
239. Pereira, A.R.; Luz, R.A.S.; Lima, F.; Crespilho, F.N. Protein Oligomerization Based on Bronsted Acid Reaction. *ACS Catal.* **2017**, *7*, 3082–3088. [[CrossRef](#)]
240. Bulutoglu, B.; Macazo, F.C.; Bale, J.; King, N.; Baker, D.; Minter, S.D.; Banta, S. Multimerization of an Alcohol Dehydrogenase by Fusion to a Designed Self-Assembling Protein Results in Enhanced Bioelectrocatalytic Operational Stability. *ACS Appl. Mater. Interfaces* **2019**, *11*, 20022–20028. [[CrossRef](#)] [[PubMed](#)]
241. Barbosa, C.; Silveira, C.M.; Silva, D.; Brissos, V.; Hildebrandt, P.; Martins, L.O.; Todorovic, S. Immobilized dye-decolorizing peroxidase (DyP) and directed evolution variants for hydrogen peroxide biosensing. *Biosens. Bioelectron.* **2020**, *153*. [[CrossRef](#)] [[PubMed](#)]
242. Mate, D.M.; Alcalde, M. Laccase engineering: From rational design to directed evolution. *Biotechnol. Adv.* **2015**, *33*, 25–40. [[CrossRef](#)]
243. Matelj, I.; Monza, E.; Lucas, M.F.; Guallar, V.; Aleksejeva, O.; Ludwig, R.; Leech, D.; Shleev, S.; Alcalde, M. Increasing Redox Potential, Redox Mediator Activity, and Stability in a Fungal Laccase by Computer-Guided Mutagenesis and Directed Evolution. *ACS Catal.* **2019**, *9*, 4561–4572. [[CrossRef](#)]
244. Lopes, P.; Koschorreck, K.; Pedersen, J.N.; Ferapontov, A.; Lorcher, S.; Pedersen, J.S.; Urlacher, V.B.; Ferapontova, E.E. *Bacillus licheniformis* CotA Laccase Mutant: Electrocatalytic Reduction of O₂ from 0.6 V (SHE) at pH 8 and in Seawater. *Chemelectrochem* **2019**, *6*, 2043–2049. [[CrossRef](#)]
245. Al-Lolage, F.A.; Meneghello, M.; Ma, S.; Ludwig, R.; Bartlett, P.N. A Flexible Method for the Stable, Covalent Immobilization of Enzymes at Electrode Surfaces. *Chemelectrochem* **2017**, *4*, 1528–1534. [[CrossRef](#)]
246. Meneghello, M.; Al-Lolage, F.A.; Ma, S.; Ludwig, R.; Bartlett, P.N. Studying Direct Electron Transfer by Site-Directed Immobilization of Cellobiose Dehydrogenase. *Chemelectrochem* **2019**, *6*, 700–713. [[CrossRef](#)] [[PubMed](#)]
247. Li, X.; Li, D.W.; Zhang, Y.N.; Lv, P.F.; Feng, Q.; Wei, Q.F. Encapsulation of enzyme by metal-organic framework for single-enzymatic biofuel cell-based self-powered biosensor. *Nano Energy* **2020**, *68*. [[CrossRef](#)]
248. Itoh, T.; Shibuya, Y.; Yamaguchi, A.; Hoshikawa, Y.; Tanaike, O.; Tsunoda, T.; Hanaoka, T.A.; Hamakawa, S.; Mizukami, F.; Hayashi, A.; et al. High-performance bioelectrocatalysts created by immobilization of an enzyme into carbon-coated composite membranes with nano-tailored structures. *J. Mater. Chem. A* **2017**, *5*, 20244–20251. [[CrossRef](#)]
249. Funabashi, H.; Murata, K.; Tsujimura, S. Effect of Pore Size of MgO-templated Carbon on the Direct Electrochemistry of D-fructose Dehydrogenase. *Electrochemistry* **2015**, *83*, 372–375. [[CrossRef](#)]

250. Mazurenko, I.; Clement, R.; Byrne-Kodjabachian, D.; de Poulpiquet, A.; Tsujimura, S.; Lojou, E. Pore size effect of MgO-templated carbon on enzymatic H₂ oxidation by the hyperthermophilic hydrogenase from *Aquifex aeolicus*. *J. Electroanal. Chem.* **2018**, *812*, 221–226. [[CrossRef](#)]
251. Wanibuchi, M.; Kitazumi, Y.; Shirai, O.; Kano, K. Enhancement of the Direct Electron Transfer-type Bioelectrocatalysis of Bilirubin Oxidase at the Interface between Carbon Particles. *Electrochemistry* **2021**, *89*, 43–48. [[CrossRef](#)]
252. Takahashi, Y.; Wanibuchi, M.; Kitazumi, Y.; Shirai, O.; Kano, K. Improved direct electron transfer-type bioelectrocatalysis of bilirubin oxidase using porous gold electrodes. *J. Electroanal. Chem.* **2019**, *843*, 47–53. [[CrossRef](#)]
253. Wu, F.; Su, L.; Yu, P.; Mao, L.Q. Role of Organic Solvents in Immobilizing Fungus Laccase on Single Walled Carbon Nanotubes for Improved Current Response in Direct Bioelectrocatalysis. *J. Am. Chem. Soc.* **2017**, *139*, 1565–1574. [[CrossRef](#)] [[PubMed](#)]
254. Hickey, D.P.; Lim, K.; Cai, R.; Patterson, A.R.; Yuan, M.W.; Sahin, S.; Abdellaoui, S.; Minteer, S.D. Pyrene hydrogel for promoting direct bioelectrochemistry: ATP-independent electroenzymatic reduction of N₂. *Chem. Sci.* **2018**, *9*, 5172–5177. [[CrossRef](#)] [[PubMed](#)]
255. Kuk, S.K.; Gopinath, K.; Singh, R.K.; Kim, T.D.; Lee, Y.; Choi, W.S.; Lee, J.K.; Park, C.B. NADH-Free Electroenzymatic Reduction of CO₂ by Conductive Hydrogel-Conjugated Formate Dehydrogenase. *ACS Catal.* **2019**, *9*, 5584–5589. [[CrossRef](#)]
256. El Ichi, S.; Zebda, A.; Laaroussi, A.; Reverdy-Bruas, N.; Chaussy, D.; Belgacem, M.N.; Cinquin, P.; Martin, D.K. Chitosan improves stability of carbon nanotube biocathodes for glucose biofuel cells. *Chem. Commun.* **2014**, *50*, 14535–14538. [[CrossRef](#)]
257. El Ichi, S.; Zebda, A.; Alcaraz, J.P.; Laaroussi, A.; Boucher, F.; Boutonnat, J.; Reverdy-Bruas, N.; Chaussy, D.; Belgacem, M.N.; Cinquin, P.; et al. Bioelectrodes modified with chitosan for long-term energy supply from the body. *Energy Environ. Sci.* **2015**, *8*, 1017–1026. [[CrossRef](#)]
258. Matsumoto, T.; Isogawa, Y.; Tanaka, T.; Kondo, A. Streptavidin-hydrogel prepared by sortase A-assisted click chemistry for enzyme immobilization on an electrode. *Biosens. Bioelectron.* **2018**, *99*, 56–61. [[CrossRef](#)]
259. Ghimire, A.; Pattamrattel, A.; Maher, C.E.; Kasi, R.M.; Kumar, C.V. Three-Dimensional, Enzyme Biohydrogel Electrode for Improved Bioelectrocatalysis. *ACS Appl. Mater. Interfaces* **2017**, *9*, 42556–42565. [[CrossRef](#)]
260. Heller, A. Electrical connection of enzyme redox centers to electrodes. *J. Phys. Chem.* **1992**, *96*, 3579–3587. [[CrossRef](#)]
261. Cadoux, C.; Milton, R.D. Recent Enzymatic Electrochemistry for Reductive Reactions. *Chemelectrochem* **2020**, *7*, 1974–1986. [[CrossRef](#)]
262. Ruth, J.C.; Milton, R.D.; Gu, W.Y.; Spormann, A.M. Enhanced Electrosynthetic Hydrogen Evolution by Hydrogenases Embedded in a Redox-Active Hydrogel. *Chem. A Eur. J.* **2020**, *26*, 7323–7329. [[CrossRef](#)]
263. Xiao, X.X.; Conghaile, P.O.; Leech, D.; Magner, E. Use of Polymer Coatings to Enhance the Response of Redox-Polymer-Mediated Electrodes. *Chemelectrochem* **2019**, *6*, 1344–1349. [[CrossRef](#)]
264. Diaz-Gonzalez, J.C.M.; Escalona-Villalpando, R.A.; Arriaga, L.G.; Minteer, S.D.; Casanova-Moreno, J.R. Effects of the cross-linker on the performance and stability of enzymatic electrocatalytic films of glucose oxidase and dimethylferrocene-modified linear poly(ethyleneimine). *Electrochim. Acta* **2020**, *337*. [[CrossRef](#)]
265. Tsujimura, S.; Takeuchi, S. Toward an ideal platform structure based on MgO-templated carbon for flavin adenine dinucleotide-dependent glucose dehydrogenase-Os polymer-hydrogel electrodes. *Electrochim. Acta* **2020**, *343*. [[CrossRef](#)]
266. Huang, X.C.; Zhang, L.L.; Zhang, Z.; Guo, S.; Shang, H.; Li, Y.B.; Liu, J. Wearable biofuel cells based on the classification of enzyme for high power outputs and lifetimes. *Biosens. Bioelectron.* **2019**, *124*, 40–52. [[CrossRef](#)]
267. Kim, J.H.; Hong, S.G.; Wee, Y.; Hu, S.; Kwon, Y.; Ha, S.; Kim, J. Enzyme precipitate coating of pyranose oxidase on carbon nanotubes and their electrochemical applications. *Biosens. Bioelectron.* **2017**, *87*, 365–372. [[CrossRef](#)]
268. Garcia, K.E.; Babanova, S.; Scheffler, W.; Hans, M.; Baker, D.; Atanassov, P.; Banta, S. Designed Protein Aggregates Entrapping Carbon Nanotubes for Bioelectrochemical Oxygen Reduction. *Biotechnol. Bioeng.* **2016**, *113*, 2321–2327. [[CrossRef](#)]
269. Caserta, G.; Lorent, C.; Ciaccafava, A.; Keck, M.; Breglia, R.; Greco, C.; Limberg, C.; Hildebrandt, P.; Cramer, S.P.; Zebger, I.; et al. The large subunit of the regulatory NiFe₂-hydrogenase from *Ralstonia eutropha*—A minimal hydrogenase? *Chem. Sci.* **2020**, *11*, 5453–5465. [[CrossRef](#)]
270. Rodriguez-Padron, D.; Puente-Santiago, A.R.; Caballero, A.; Balu, A.M.; Romero, A.A.; Luque, R. Highly efficient direct oxygen electro-reduction by partially unfolded laccases immobilized on waste-derived magnetically separable nanoparticles. *Nanoscale* **2018**, *10*, 3961–3968. [[CrossRef](#)] [[PubMed](#)]
271. Gutierrez-Sanchez, C.; Ciaccafava, A.; Blanchard, P.Y.; Monsalve, K.; Giudici-Orticoni, M.T.; Lecomte, S.; Lojou, E. Efficiency of Enzymatic O₂ Reduction by *Myrothecium verrucaria* Bilirubin Oxidase Probed by Surface Plasmon Resonance, PMIRRAS, and Electrochemistry. *ACS Catal.* **2016**, *6*, 5482–5492. [[CrossRef](#)]
272. Singh, K.; McArdle, T.; Sullivan, P.R.; Blanford, C.F. Sources of activity loss in the fuel cell enzyme bilirubin oxidase. *Energy Environ. Sci.* **2013**, *6*, 2460–2464. [[CrossRef](#)]
273. Zelechowska, K.; Stolarczyk, K.; Lyp, D.; Rogalski, J.; Roberts, K.P.; Bilewicz, R.; Biernat, J.F. Aryl and N-arylamide carbon nanotubes for electrical coupling of laccase to electrodes in biofuel cells and biobatteries. *Biocybern. Biomed. Eng.* **2013**, *33*, 235–245. [[CrossRef](#)]
274. Yahata, N.; Saitoh, T.; Takayama, Y.; Ozawa, K.; Ogata, H.; Higuchi, Y.; Akutsu, H. Redox interaction of cytochrome c(3) with NiFe hydrogenase from *Desulfovibrio vulgaris* Miyazaki F. *Biochemistry* **2006**, *45*, 1653–1662. [[CrossRef](#)]

275. Sugimoto, Y.; Kitazumi, Y.; Shirai, O.; Nishikawa, K.; Higuchi, Y.; Yamamoto, M.; Kano, K. Electrostatic roles in electron transfer from NiFe hydrogenase to cytochrome c(3) from *Desulfovibrio vulgaris* Miyazaki F. *Biochim. Et Biophys. Acta Proteins Proteom.* **2017**, *1865*, 481–487. [[CrossRef](#)]
276. McArdle, T.; McNamara, T.P.; Fei, F.; Singh, K.; Blanford, C.F. Optimizing the Mass-Specific Activity of Bilirubin Oxidase Adlayers through Combined Electrochemical Quartz Crystal Microbalance and Dual Polarization Interferometry Analyses. *ACS Appl. Mater. Interfaces* **2015**, *7*, 25270–25280. [[CrossRef](#)] [[PubMed](#)]
277. Kitazumi, Y.; Shirai, O.; Yamamoto, M.; Kano, K. Numerical simulation of diffuse double layer around microporous electrodes based on the Poisson-Boltzmann equation. *Electrochim. Acta* **2013**, *112*, 171–175. [[CrossRef](#)]
278. Olloqui-Sariego, J.L.; Calvente, J.J.; Andreu, R. Immobilizing redox enzymes at mesoporous and nanostructured electrodes. *Curr. Opin. Electrochem.* **2021**, *26*, 100658. [[CrossRef](#)]
279. Sakai, K.; Xia, H.-Q.; Kitazumi, Y.; Shirai, O.; Kano, K. Assembly of direct-electron-transfer-type bioelectrodes with high performance. *Electrochim. Acta* **2018**, *271*, 305–311. [[CrossRef](#)]
280. Sakai, K.; Kitazumi, Y.; Shirai, O.; Kano, K. Nanostructured Porous Electrodes by the Anodization of Gold for an Application as Scaffolds in Direct-electron-transfer-type Bioelectrocatalysis. *Electrochim. Acta* **2018**, *34*, 1317–1322. [[CrossRef](#)]
281. Armstrong, F.A.; Bond, A.M.; Hill, H.A.O.; Oliver, B.N.; Psalti, I.S.M. Electrochemistry of cytochrome-c, plastocyanin, and ferredoxin at edge-plane and basal-plane graphite-electrodes interpreted via a model based on electron-transfer at electroactive sites of microscopic dimensions in size. *J. Am. Chem. Soc.* **1989**, *111*, 9185–9189. [[CrossRef](#)]
282. Komori, K.; Huang, J.; Mizushima, N.; Ko, S.; Tatsuma, T.; Sakai, Y. Controlled direct electron transfer kinetics of fructose dehydrogenase at cup-stacked carbon nanofibers. *Phys. Chem. Chem. Phys.* **2017**, *19*, 27795–27800. [[CrossRef](#)] [[PubMed](#)]
283. Kavetskiy, T.; Smutok, O.; Demkiv, O.; Mat'ko, I.; Svajdlenkova, H.; Sausa, O.; Novak, I.; Berek, D.; Cechova, K.; Pecz, M.; et al. Microporous carbon fibers as electroconductive immobilization matrixes: Effect of their structure on operational parameters of laccase-based amperometric biosensor. *Mater. Sci. Eng. C Mater. Biol. Appl.* **2020**, *109*. [[CrossRef](#)] [[PubMed](#)]
284. de Poulpiquet, A.; Marques-Knopf, H.; Wernert, V.; Giudici-Ortoni, M.T.; Gadiou, R.; Lojou, E. Carbon nanofiber mesoporous films: Efficient platforms for bio-hydrogen oxidation in biofuel cells. *Phys. Chem. Chem. Phys.* **2014**, *16*, 1366–1378. [[CrossRef](#)] [[PubMed](#)]
285. Pandelia, M.E.; Fourmond, V.; Tron-Infossi, P.; Lojou, E.; Bertrand, P.; Leger, C.; Giudici-Ortoni, M.T.; Lubitz, W. Membrane-Bound Hydrogenase I from the Hyperthermophilic Bacterium *Aquifex aeolicus*: Enzyme Activation, Redox Intermediates and Oxygen Tolerance. *J. Am. Chem. Soc.* **2010**, *132*, 6991–7004. [[CrossRef](#)]
286. Ciaccafava, A.; De Poulpiquet, A.; Techer, V.; Giudici-Ortoni, M.T.; Tingry, S.; Innocent, C.; Lojou, E. An innovative powerful and mediatorless H₂/O₂ biofuel cell based on an outstanding bioanode. *Electrochem. Commun.* **2012**, *23*, 25–28. [[CrossRef](#)]
287. Oughli, A.A.; Velez, M.; Birrell, J.A.; Schuhmann, W.; Lubitz, W.; Plumere, N.; Rudiger, O. Viologen-modified electrodes for protection of hydrogenases from high potential inactivation while performing H₂ oxidation at low overpotential. *Dalton Trans.* **2018**, *47*, 10685–10691. [[CrossRef](#)]
288. Plumere, N.; Rudiger, O.; Oughli, A.A.; Williams, R.; Vivekananthan, J.; Poller, S.; Schuhmann, W.; Lubitz, W. A redox hydrogel protects hydrogenase from high-potential deactivation and oxygen damage. *Nat. Chem.* **2014**, *6*, 822–827. [[CrossRef](#)]
289. Ruff, A.; Szczesny, J.; Zacarias, S.; Pereira, I.A.C.; Plumere, N.; Schuhmann, W. Protection and Reactivation of the NiFeSe Hydrogenase from *Desulfovibrio vulgaris* Hildenborough under Oxidative Conditions. *ACS Energy Lett.* **2017**, *2*, 964–968. [[CrossRef](#)]
290. Mano, N. Engineering glucose oxidase for bioelectrochemical applications. *Bioelectrochemistry* **2019**, *128*, 218–240. [[CrossRef](#)]
291. Elouarzaki, K.; Bourourou, M.; Holzinger, M.; Le Goff, A.; Marks, R.S.; Cosnier, S. Freestanding HRP-GOx redox buckypaper as an oxygen-reducing biocathode for biofuel cell applications. *Energy Environ. Sci.* **2015**, *8*, 2069–2074. [[CrossRef](#)]
292. Lopez, F.; Zeria, S.; Ruff, A.; Schuhmann, W. An O₂ Tolerant Polymer/Glucose Oxidase Based Bioanode as Basis for a Self-powered Glucose Sensor. *Electroanalysis* **2018**, *30*, 1311–1318. [[CrossRef](#)]
293. Sahin, S.; Wongnate, T.; Chuaboon, L.; Chaiyen, P.; Yu, E.H. Enzymatic fuel cells with an oxygen resistant variant of pyranose-2-oxidase as anode biocatalyst. *Biosens. Bioelectron.* **2018**, *107*, 17–25. [[CrossRef](#)]
294. Tremey, E.; Stines-Chaumeil, C.; Gounel, S.; Mano, N. Designing an O₂-Insensitive Glucose Oxidase for Improved Electrochemical Applications. *Chemelectrochem* **2017**, *4*, 2520–2526. [[CrossRef](#)]
295. Li, H.; Münchberg, U.; Oughli, A.A.; Buesen, D.; Lubitz, W.; Freier, E.; Plumeré, N. Suppressing hydrogen peroxide generation to achieve oxygen-insensitivity of a [NiFe] hydrogenase in redox active films. *Nat. Commun.* **2020**, *11*, 920. [[CrossRef](#)]
296. Zebda, A.; Alcaraz, J.P.; Vadgama, P.; Shleev, S.; Minteer, S.D.; Boucher, F.; Cinquin, P.; Martin, D.K. Challenges for successful implantation of biofuel cells. *Bioelectrochemistry* **2018**, *124*, 57–72. [[CrossRef](#)] [[PubMed](#)]
297. Xu, Z.H.; Liu, Y.C.; Williams, I.; Li, Y.; Qian, F.Y.; Wang, L.; Lei, Y.; Li, B.K. Flat enzyme-based lactate biofuel cell integrated with power management system: Towards long term in situ power supply for wearable sensors. *Appl. Energy* **2017**, *194*, 71–80. [[CrossRef](#)]
298. Lv, J.; Jeerapan, I.; Tehrani, F.; Yin, L.; Silva-Lopez, C.A.; Jang, J.H.; Joshua, D.; Shah, R.; Liang, Y.Y.; Xie, L.Y.; et al. Sweat-based wearable energy harvesting-storage hybrid textile devices. *Energy Environ. Sci.* **2018**, *11*, 3431–3442. [[CrossRef](#)]
299. Ruff, A.; Conzuelo, F.; Schuhmann, W. Bioelectrocatalysis as the basis for the design of enzyme-based biofuel cells and semi-artificial biophotoelectrodes. *Nat. Catal.* **2020**, *3*, 214–224. [[CrossRef](#)]

300. Clement, R.; Wang, X.; Biaso, F.; Ilbert, M.; Mazurenko, I.; Lojou, E. Mutations in the coordination spheres of T1 Cu affect Cu²⁺-activation of the laccase from *Thermus thermophilus*. *Biochimie* **2021**. [\[CrossRef\]](#)
301. Zhang, L.L.; Cui, H.Y.; Zou, Z.; Garakani, T.M.; Novoa-Henriquez, C.; Jooyeh, B.; Schwaneberg, U. Directed Evolution of a Bacterial Laccase (CueO) for Enzymatic Biofuel Cells. *Angew. Chem. Int. Ed.* **2019**, *58*, 4562–4565. [\[CrossRef\]](#)
302. Herkendell, K.; Stemmer, A.; Tel-Vered, R. Extending the operational lifetimes of all-direct electron transfer enzymatic biofuel cells by magnetically assembling and exchanging the active biocatalyst layers on stationary electrodes. *Nano Res.* **2019**, *12*, 767–775. [\[CrossRef\]](#)
303. Hammond, J.L.; Gross, A.J.; Giroud, F.; Travelet, C.; Borsali, R.; Cosnier, S. Solubilized Enzymatic Fuel Cell (SEFC) for Quasi-Continuous Operation Exploiting Carbohydrate Block Copolymer Glyconanoparticle Mediators. *ACS Energy Lett.* **2019**, *4*, 142–148. [\[CrossRef\]](#)
304. Wang, D.D.; Jana, D.L.; Zhao, Y.L. Metal-Organic Framework Derived Nanozymes in Biomedicine. *Acc. Chem. Res.* **2020**, *53*, 1389–1400. [\[CrossRef\]](#)
305. Navyatha, B.; Singh, S.; Nara, S. AuPeroxidase nanozymes: Promises and applications in biosensing. *Biosens. Bioelectron.* **2021**, *175*, 112882. [\[CrossRef\]](#) [\[PubMed\]](#)
306. Ahmed, M.E.; Dey, A. Recent developments in bioinspired modelling of NiFe- and FeFe-hydrogenases. *Curr. Opin. Electrochem.* **2019**, *15*, 155–164. [\[CrossRef\]](#)
307. Laureanti, J.A.; O'Hagan, M.; Shaw, W.J. Chicken fat for catalysis: A scaffold is as important for molecular complexes for energy transformations as it is for enzymes in catalytic function. *Sustain. Energy Fuels* **2019**, *3*, 3260–3278. [\[CrossRef\]](#)
308. Yang, Y.; Xiong, Y.; Zeng, R.; Lu, X.; Krumov, M.; Huang, X.; Xu, W.; Wang, H.; DiSalvo, F.J.; Brock, J.D.; et al. Operando Methods in Electrocatalysis. *ACS Catal.* **2021**, *11*, 1136–1178. [\[CrossRef\]](#)
309. de Souza, J.C.P.; Macedo, L.J.A.; Hassan, A.; Sedenho, G.C.; Modenez, I.A.; Crespilho, F.N. In Situ and Operando Techniques for Investigating Electron Transfer in Biological Systems. *Chemelectrochem* **2020**. [\[CrossRef\]](#)
310. Kornienko, N.; Ly, K.H.; Robinson, W.E.; Heidary, N.; Zhang, J.Z.; Reisner, E. Advancing Techniques for Investigating the Enzyme-Electrode Interface. *Acc. Chem. Res.* **2019**, *52*, 1439–1448. [\[CrossRef\]](#)
311. Singh, K.; Blanford, C.F. Electrochemical Quartz Crystal Microbalance with Dissipation Monitoring: A Technique to Optimize Enzyme Use in Bioelectrocatalysis. *Chemcatchem* **2014**, *6*, 921–929. [\[CrossRef\]](#)
312. Sezer, M.; Kielb, P.; Kuhlmann, U.; Mohrmann, H.; Schulz, C.; Heinrich, D.; Schlesinger, R.; Heberle, J.; Weidinger, I.M. Surface Enhanced Resonance Raman Spectroscopy Reveals Potential Induced Redox and Conformational Changes of Cytochrome c Oxidase on Electrodes. *J. Phys. Chem. B* **2015**, *119*, 9586–9591. [\[CrossRef\]](#) [\[PubMed\]](#)
313. Dagys, M.; Laurynenas, A.; Ratautas, D.; Kulys, J.; Vidziunaite, R.; Talaikis, M.; Niaura, G.; Marcinkeviciene, L.; Meskys, R.; Shleev, S. Oxygen electroreduction catalysed by laccase wired to gold nanoparticles via the trinuclear copper cluster. *Energy Environ. Sci.* **2017**, *10*, 498–502. [\[CrossRef\]](#)
314. Olejnik, P.; Pawlowska, A.; Palys, B. Application of Polarization Modulated Infrared Reflection Absorption Spectroscopy for electrocatalytic activity studies of laccase adsorbed on modified gold electrodes. *Electrochim. Acta* **2013**, *110*, 105–111. [\[CrossRef\]](#)
315. Macedo, L.J.A.; Hassan, A.; Sedenho, G.C.; Crespilho, F.N. Assessing electron transfer reactions and catalysis in multicopper oxidases with operando X-ray absorption spectroscopy. *Nat. Commun.* **2020**, *11*. [\[CrossRef\]](#) [\[PubMed\]](#)
316. Abdiaziz, K.; Salvadori, E.; Sokol, K.P.; Reisner, E.; Roessler, M.M. Protein film electrochemical EPR spectroscopy as a technique to investigate redox reactions in biomolecules. *Chem. Commun.* **2019**, *55*, 8840–8843. [\[CrossRef\]](#)
317. Harris, T.; Heidary, N.; Kozuch, J.; Frielingsdorf, S.; Lenz, O.; Mroginski, M.A.; Hildebrandt, P.; Zebger, I.; Fischer, A. In Situ Spectroelectrochemical Studies into the Formation and Stability of Robust Diazonium-Derived Interfaces on Gold Electrodes for the Immobilization of an Oxygen-Tolerant Hydrogenase. *ACS Appl. Mater. Interfaces* **2018**, *10*, 23380–23391. [\[CrossRef\]](#)
318. Abad, J.M.; Tesio, A.Y.; Martinez-Perinan, E.; Pariente, F.; Lorenzo, E. Imaging resolution of biocatalytic activity using nanoscale scanning electrochemical microscopy. *Nano Res.* **2018**, *11*, 4232–4244. [\[CrossRef\]](#)
319. Tassy, B.; Dauphin, A.L.; Man, H.M.; Le Guenno, H.; Lojou, E.; Bouffier, L.; de Poulpiquet, A. In Situ Fluorescence Tomography Enables a 3D Mapping of Enzymatic O-2 Reduction at the Electrochemical Interface. *Anal. Chem.* **2020**, *92*, 7249–7256. [\[CrossRef\]](#) [\[PubMed\]](#)
320. Zigah, D.; Lojou, E.; de Poulpiquet, A. Micro- and Nanoscopic Imaging of Enzymatic Electrodes: A Review. *Chemelectrochem* **2019**, *6*, 5524–5546. [\[CrossRef\]](#)
321. Barrozo, A.; Orio, M. Molecular Electrocatalysts for the Hydrogen Evolution Reaction: Input from Quantum Chemistry. *ChemSuschem* **2019**, *12*, 4905–4915. [\[CrossRef\]](#) [\[PubMed\]](#)
322. Qiu, S.Y.; Li, Q.Y.; Xu, Y.J.; Shen, S.H.; Sun, C.H. Learning from nature: Understanding hydrogenase enzyme using computational approach. *Wiley Interdiscip. Rev. Comput. Mol. Sci.* **2020**, *10*. [\[CrossRef\]](#)
323. Yang, S.J.; Liu, J.; Quan, X.B.; Zhou, J. Bilirubin Oxidase Adsorption onto Charged Self-Assembled Monolayers: Insights from Multiscale Simulations. *Langmuir* **2018**, *34*, 9818–9828. [\[CrossRef\]](#) [\[PubMed\]](#)